GloFouling
PARTNERSHIPS
Global Industry Alliance

Analysing the Impact of Marine Biofouling on the Energy Efficiency of Ships and the GHG Abatement Potential of Biofouling Management Measures

gef

UNDP
Empowered lives.
Resilient nations.

IMO INTERNATIONAL MARITIME ORGANIZATION

Analysing the Impact of Marine Biofouling on the Energy Efficiency of Ships and the GHG Abatement Potential of Biofouling Management Measures

gef

UNDP
Empowered lives.
Resilient nations.

IMO INTERNATIONAL MARITIME ORGANIZATION

GloFouling PARTNERSHIPS
Global Industry Alliance

Published* in 2022 by the
GloFouling Partnerships Project Coordination Unit
International Maritime Organization
4 Albert Embankment
London SE1 7SR
United Kingdom

Cover Design by Tina Davidian

Photo and Infographic credits: ©Eric Gao, Adel Kacimi and shutterstock (cover); ©shutterstock (page 3); ©piqsels (page 5); ©shutterstock (page 8); ©GEF-UNDP-IMO GloFouling Partnerships, Lena Granhag and Sergio Russo (Flickr) (page 10); ©Biofouling Solutions PTY Ltd (photo 1); ©Biofouling Solutions PTY Ltd (photo 2); ©Sonihull (photo 3); ©Mini Pamper (photo 4); ©EcoSubSea (photo 5); ©Gabuchan (WikiCommons) (page 16) ©adobe stock (page 18); ©adobe stock (page 47).

Please cite this document as: GEF-UNDP-IMO GloFouling Partnerships Project and GIA for Marine Biosafety, 2022, Analysing the Impact of Marine Biofouling on the Energy Efficiency of Ships and the GHG Abatement Potential of Biofouling Management Measures.

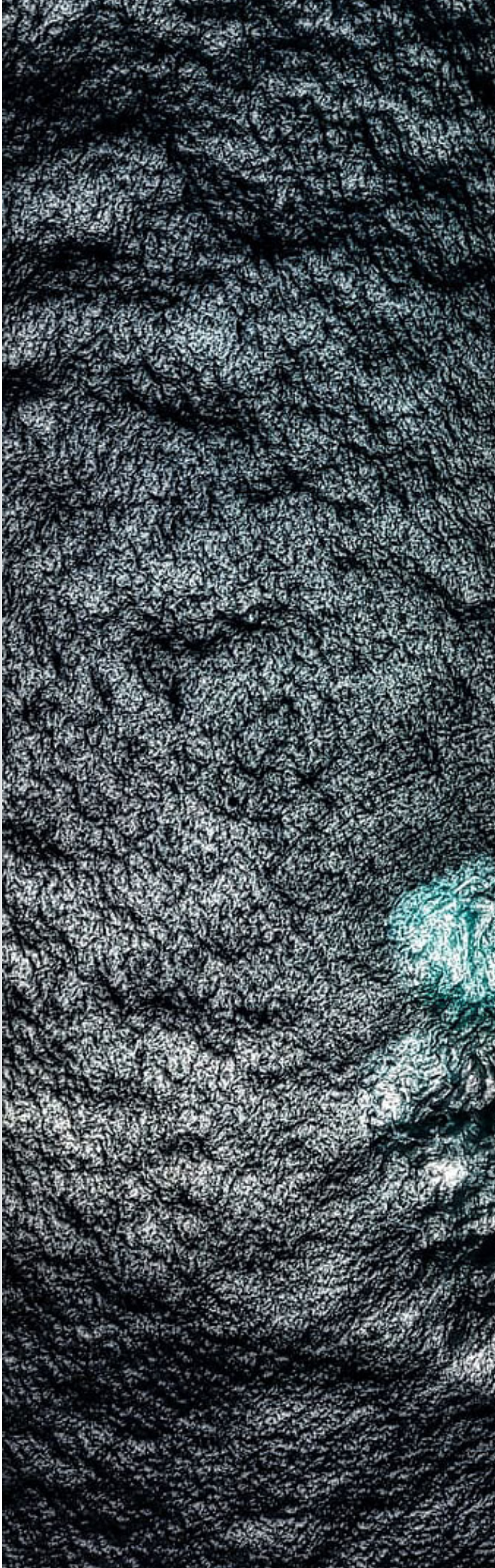

*Electronic version available for download at https://www.glofouling.imo.org/publications-menu

GLOFOULING PARTNERSHIPS

Building Partnerships to Assist Developing Countries to Minimize the Impacts from Aquatic Biofouling (GloFouling Partnerships) is a collaboration between the Global Environment Facility (GEF), the United Nations Development Programme (UNDP) and the International Maritime Organization (IMO). The project aims to develop tools and solutions to help developing countries to reduce the transfer of aquatic invasive species through the implementation of the IMO Guidelines for the control and management of ships' biofouling.
www.glofouling.imo.org

FUNDING AGENCY

GEF - the Global Environment Facility - was established on the eve of the 1992 Rio Earth Summit to help tackle our planet's most pressing environmental problems. Since then, the GEF has provided over USD 21.1 billion in grants and mobilized an additional USD 114 billion in co-financing for more than 5000 projects in 170 countries. Today, the GEF is an international partnership of 184 countries, international institutions, civil society organizations and the private sector that addresses global environmental issues.
www.thegef.org

IMPLEMENTING AGENCY

UNDP – the United Nations Development Programme – partners with people at all levels of society to help build nations that can withstand crisis, drive and sustain the kind of growth that improves the quality of life for everyone. On the ground in nearly 170 countries and territories, we offer global perspective and local insight to help empower lives and build resilient nations.
www.undp.org

EXECUTING AGENCY

IMO - the International Maritime Organization – is the United Nations specialized agency with responsibility for the safety and security of shipping and the prevention of marine pollution by ships.
www.imo.org

TABLE OF CONTENTS

LIST OF TABLES

LIST OF FIGURES

ACKNOWLEDGMENTS

THIS GUIDE IS THE PRODUCT OF THE GEF-UNDP-IMO GLOFOULING PARTNERSHIPS PROJECT.

The report Analysing the Impact of Marine Biofouling on the Energy Efficiency of Ships and the GHG Abatement Potential of Biofouling Management Measures was written by Yigit Kemal Demirel and Soonseok Song, independent consultants with contribution, editorial review, comments and input, from Lilia Khodjet El Khil, Project Technical Manager; John Alonso, Project Technical Analyst, GloFouling Partnerships Project, the Department of Partnerships and Projects, IMO; Roel Hoenders, Head, Air Pollution and Energy Efficiency; Camille Bourgeon and John Calleya, Technical Officers, from Sub-Division for Protective Measures, Marine Environment Division, IMO.

Great thanks are also due to Violeta Luque, Senior Project Assistant; and Jurga Shaule, Project Assistant, GloFouling Partnerships project, the Department of Partnerships and Projects, IMO, who provided coordination and editing support to produce this report.

The GloFouling Partnerships Project Coordination Unit (PCU) would like to acknowledge contributions of the members of the Global Industry Alliance (GIA) for Marine Biosafety, who commissioned and financed the study and provided contacts, information and industry insights. Special thanks are given to Professors Michael Schultz, Nicholas Hutchins, Jason Monty and Inwon Lee, and Dr. Bagus Nugroho. All gave substantial comments during the early stages and contributed valuable insights. An acknowledgement is also due to many stakeholders from the shipping, in-water cleaning and coatings industries around the world who contributed by providing their comments. We truly appreciate their time, effort, expertise, and cooperation.

At the time of printing this report, the members of the GIA for Marine Biosafety were: AkzoNobel, CleanSubSea, ECOsubsea, Tas Global, Hapag-Lloyd, HullWiper, KCC Marine Coatings, SLM Global and Sonihull.

For further information please contact:

GloFouling Partnerships Project Coordination Unit
Department of Partnerships and Projects
International Maritime Organization
4 Albert Embankment
London SE1 7SR
United Kingdom

Web: www.glofouling.imo.org

ACRONYMS AND ABBREVIATIONS

AFS Convention – International Convention on the Control of Harmful Anti-fouling Systems on Ships (Anti-fouling Convention)

AF coating – Anti-fouling coating

AFS – Anti-fouling system

AHR – Average hull roughness

CDP – Controlled depletion polymer

CFD – Computational fluid dynamics

CO_2e – CO_2 equivalent

EEDI – Energy Efficiency Design Index

EEXI – Energy Efficiency Existing Ship Index

FR – Fouling rating

FRC – Fouling-release coatings

GEF – Global Environment Facility

GHG – Greenhouse gases

GIA – Global Industry Alliance for Marine Biosafety

IAS – Invasive Aquatic Species

IMO – International Maritime Organization

ITTC – International Towing Tank Conference

IWC – In-water cleaning

MHR – Mean hull roughness

NSTM – US Navy Naval Ships' Technical Manual

SEEMP – Ship Energy Efficiency Management Plan

SPC – Self-polishing copolymer

TBT – Tributyltin

TEU – Twenty-foot container unit

UNDP – United Nations Development Programme

EXECUTIVE SUMMARY

GHG EMISSIONS CAUSED BY BIOFOULING ON SHIPS

Maritime trade is critical for the movement of goods and people around the globe. Whilst shipping is one of the most economical and environmentally friendly modes of transport available, it currently contributes to roughly 3% of the global greenhouse gas (GHG) emissions every year due to the size of the sector.[1]

In order to reduce the GHG emissions from international shipping, the International Maritime Organization (IMO) has adopted a series of legally binding ship design and operational performance indices that must be achieved by individual vessels. Following the adoption in 2011 of the Energy Efficiency Design Index (EEDI) and the Ship Energy Efficiency Management Plan (SEEMP), IMO's Marine Environment Protection Committee (MEPC), at its 76th session, adopted a combination of technical and operational measures, referred to as short term carbon intensity measures. The new measures, adopted as amendments to the International Convention for the Prevention of Pollution from Ships (MARPOL) Annex VI, will require all ships to calculate their Energy Efficiency Existing Ship Index (EEXI) and to establish their annual operational carbon intensity indicator (CII) and CII rating. The aim of these measures is to ensure that ship operators consider options to improve the efficiency of their vessels throughout their life cycle and in doing so to help reach the levels of ambition of the Initial IMO GHG Strategy, adopted in 2018, which aims to reduce carbon intensity of international shipping by 40% by 2030, compared to 2008.

One of the most significant factors impacting the efficiency of all ships in service is associated with the resistance generated by the friction of water on the ship's hull. Resistance increases when the hull is fouled. Therefore, maintaining a smooth and clean hull free from biofouling is of paramount importance to optimise the energy efficiency of ships..

The ship hull biofouling penalty

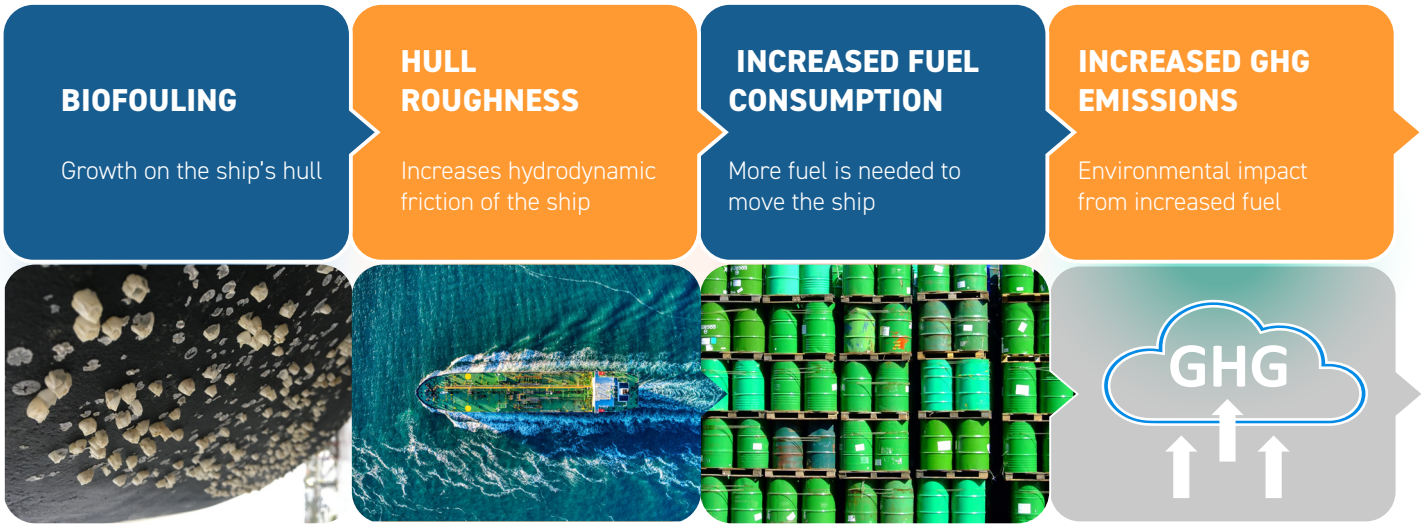

[1] *Fourth IMO Greenhouse Gas Study 2020. International Maritime Organization, 2021.*

Biofouling, which is the build-up of microorganisms, plants, algae or small animals, is known to increase the roughness of the colonized surfaces. When biofouling species colonize the underwater parts of a ship's hull, the increased roughness will increase a ship's hydrodynamic drag. The immediate effect is a loss in ship speed at a constant power – or a power increase to maintain a constant speed. Both have negative economic and environmental impacts through increased fuel consumption and atmospheric emissions, including GHG.

This report on the impact of ships' biofouling on greenhouse gas emissions responds to a decision in 2020 by the Global Industry Alliance for Marine Biosafety[2] to increase understanding within the shipping industry of the relationship between ships' biofouling and fuel consumption and resulting GHG emissions. The focus is twofold:

- Analyse the impact of biofouling accumulation on the energy efficiency of ships, and
- Analyse the sustainable solutions currently available to shipowners to effectively reduce GHG emissions through the minimization of biofouling.

The results of the report are based on an updated assessment of the current state of knowledge, complemented by newly developed research.

SHIPS' BIOFOULING: QUANTIFYING THE POTENTIAL IMPACT IF UNMANAGED

The measurement of ship performance can be challenging due to the wide variety of ship types and the conditions under which they operate. In the case of biofouling, there are plenty of studies in the scientific literature demonstrating its drastic impact on ship resistance and propulsion performance, and Chapter 1 of this report includes an historic overview. However, estimating the impact of biofouling is not straightforward from such findings in the literature, as quantification is done using different ship performance parameters such as increased frictional resistance, effective power or shaft power. These parameters are not easy to understand from the perspective of non-specialists in ship hydrodynamics.

The biofouling process

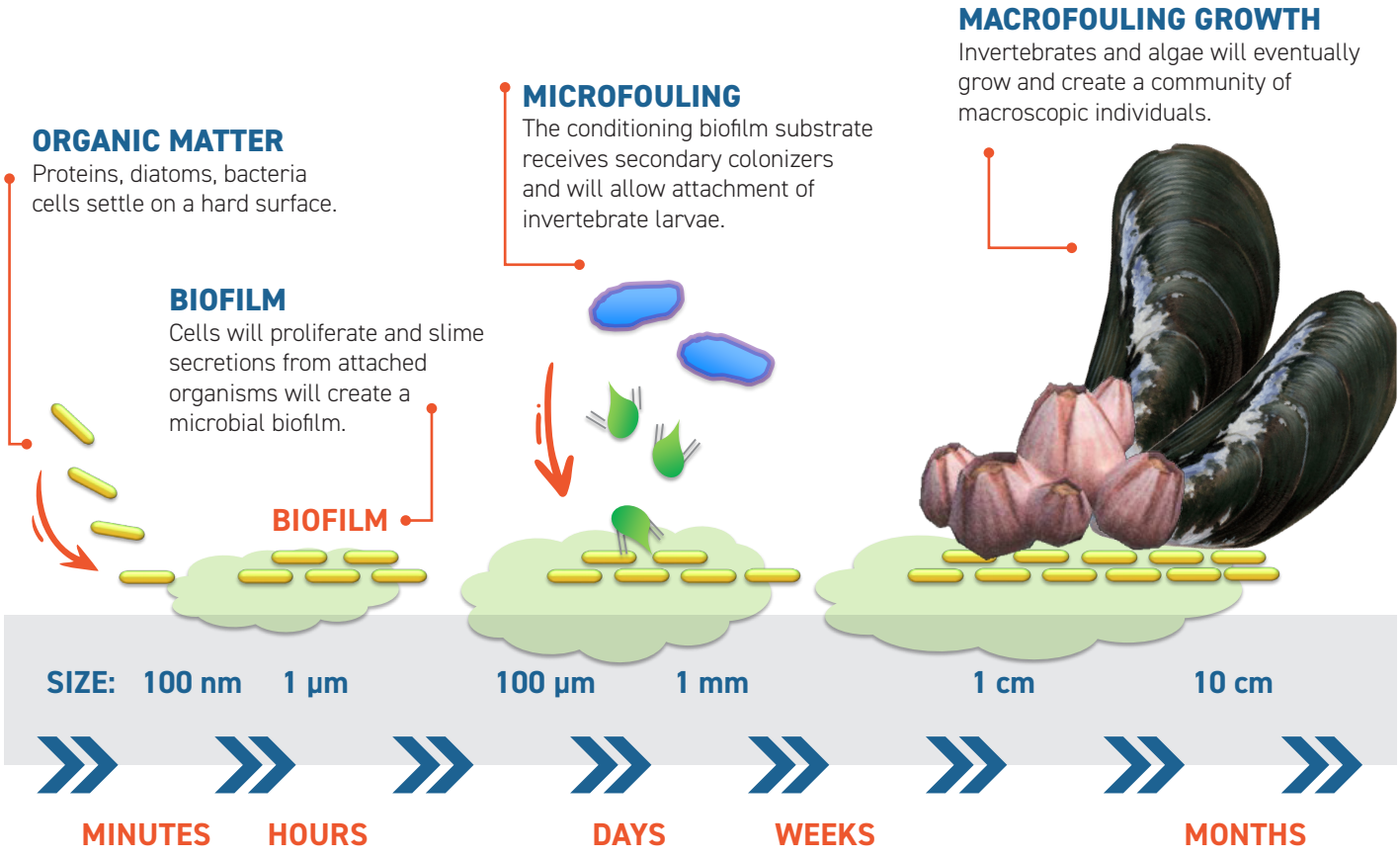

[2] *The Global Industry Alliance for Marine Biosafety is an alliance that brings together committed leaders from maritime-based industries to support two key IMO pressing environmental objectives via improved biofouling management: protect marine biodiversity and decarbonize shipping. The GIA is formed by members from the maritime industry and entities with an observer status.*

Table 1 Approximate equivalency of commonly used classifications for hull biofouling and surface roughness levels

Description of condition	NSTM rating	Schultz (k_s)	IMO *(in development)*[3]
Typical as applied AF coating	0	30	0
Deteriorated coating or light slime	10-20	100	1
Heavy slime	30	300	2
Small calcareous fouling or weed	40-60	1,000	3
Medium calcareous fouling	70-80	3,000	4
Heavy calcareous fouling	90-100	10,000	5

Additionally, there are several classification systems for quantifying the level of roughness and/or biofouling on a hull. The most commonly shared being one published by the US Navy in its Naval Ships' Technical Manual (NSTM) in 2002, and a widely referenced paper by Schultz (2007). Some of these qualitative classifications of biofouling are linked to surface roughness levels (represented by the roughness coefficient symbol k_s), as seen in Table 1.

To give a better picture of the impact of biofouling on ships, the first part of this report has compiled and summarized all kinds of results found in the scientific literature published to date. Figure 1 (See next page) illustrates the outcome of this work in the form of increase in GHG emissions from ships for different categories of biofouling. To achieve these findings, all parameters were converted into an equivalent unit[4] that allowed categorization into several fouling categories as per the classification in Table 1 above. The authors then compared how surface roughness relates to the energy (fuel) requirements of ships and the equivalent estimated GHG emissions

At the lower end, studies compiled in Figure 1 (See next page) consistently highlight the inherent ability of biofilms and slime to induce an effective roughness that is well in excess of what its physical appearance would traditionally suggest. For example, a layer of slime as thin as 0.5 mm covering up to 50% of a hull surface could trigger

A SLIME LAYER COULD TRIGGER UP TO

25% INCREASE IN GHG EMISSIONS

an increase of GHG emissions in the range of 25 to 30%, depending on ship characteristics, its speed and other prevailing conditions.

For more severe biofouling conditions, such as a light layer of small calcareous growth (barnacles or tubeworms), an average-length container ship could see an increase in GHG emissions of up to 60%, dependent on ship characteristics and speed. For the medium calcareous fouling surfaces, the increase in GHG emissions could be as high as 90%.

The results of this review reflect the impact at a specific moment in time for the different biofouling levels or categories. However, the lack of public data, as well as the number and variety of ship types, operational profiles and hull conditions of the global fleet, make it very difficult to extrapolate these results to calculate the exact overall contribution of biofouling to GHG emissions from ships.

[3] *As proposed in the draft revised Guidelines for the control and management of ships' biofouling to minimize the transfer of Invasive Aquatic Species (IMO document PPR 9/7), being further developed at the time of publishing this report.*

[4] *It should be noted that some studies in the literature use other roughness parameters and not necessarily sand-grain roughness height values (k_s). For the purpose of this graphic representation, all roughness parameters were converted by the authors to the same unit (k_s) to allow better comparability. In addition to this, they were categorized for the sake of uniformity, even though they were not originally categorized by the authors of each source.*

Photo 1: Light slime layer

Photo 2: Barnacles – medium calcareous fouling

Figure 1 Impact of ship hull fouling on GHG emissions. Summary of results from published research studies.

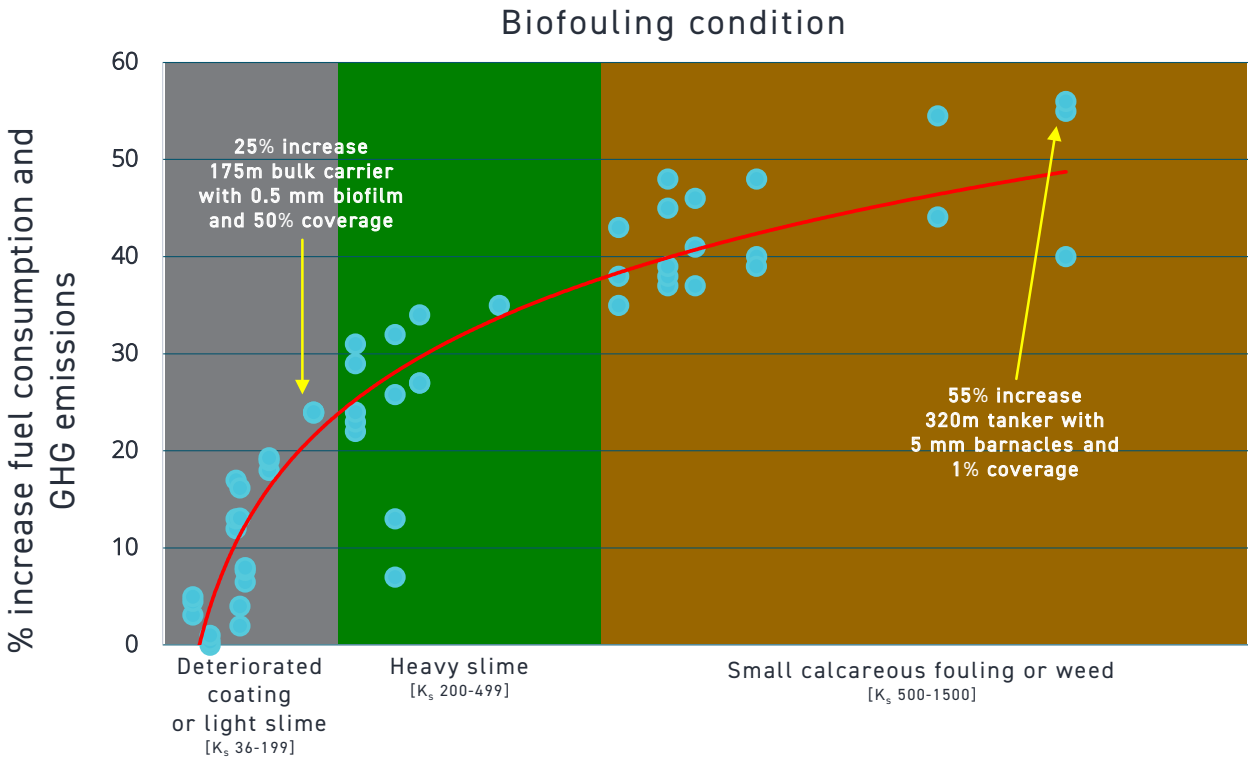

Recently published studies have given some insight into existing levels of biofouling accumulated on ships hulls. A survey of 249 ships in Northern Europe conducted by the Safinah Group (2020) found that 40% of ships had more than 20% hard macrofouling on their flat bottoms and approximately 10% of sampled ships had more than 40% of their underwater areas covered by hard macrofouling (although these results did not take into account their operational profile or the prevailing environmental conditions).

In addition to the outcome of this compilation of scientific studies and despite the difficulty of extrapolating figures to the global fleet without more data, some studies have tried to estimate the potential savings that could be achieved through improved biofouling prevention and management. Swain et al. (2022) roughly calculated that if all international ships maintained a smooth condition, free from biofouling, global GHG emissions from ships could be reduced by at least 19% per year (or 198 million tons of CO_2e). This result was based solely on the global estimations published by IMO in its Fourth Greenhouse Gas Study. Including domestic fleets in this equation could notably increase this result.

ASSESSING THE IMPACT OF BIOFOULING MANAGEMENT SOLUTIONS

There are a range of commercially available options for biofouling prevention and management today that can significantly reduce the impact of biofouling on the energy efficiency of ships and thereby enhance their performance. These include using optimized anti-fouling coatings, marine growth prevention systems (such as ultrasonic systems) and technologies for grooming or cleaning the hull while in-water. All these solutions can form part of a holistic hull management approach for the ship operator. While it is common practice for some shipowners and ship operators to manage biofouling using the latest technologies or resources, there is an opportunity to extend the use of best management practices to the entire industry.

Anti-fouling coatings are the first and foremost tool that is used across the industry to prevent biofouling. Choosing an adequate anti-fouling coating is essential to prevent the accumulation of biofouling. There are many of anti-fouling coatings in the market and leading paint manufacturers develop tools and recommendations to aid end users in the selection process based on their product ranges and

Photo 3: An ultrasonics transducer fixed to a ships' hull

the specific operational profile of a ship. Despite these resources, product selection or performance is not always adequate due to the changing scenarios in the operation of ships, such as unplanned lengthy idle periods or operating in different geographical areas and water conditions. The correct application of the coatings is another often overlooked and important aspect that could determine their future performance. Another important challenge is just the breadth, number and biology of biofouling organisms that exist out there.

When the performance of anti-fouling coatings over time may fail to provide full protection from biofouling (for some of the reasons stated in the previous paragraph), new technologies have been developed to prevent or manage any growth that may accumulate on the surface of a ship. The most common technologies currently in use for biofouling mitigation are ultrasonics and hull and propeller cleaning.

Ultrasonic treatment is becoming increasingly common as a marine growth prevention system. The way this technology works is through the use of transducers such as the one in Photo 3. The transducers are attached at various points along the vessel hull and emit frequency waves into the water column, in this case directed towards a box cooler or a sea chest unit on a vessel, with the idea that at specific frequencies certain biofouling organisms are deterred from wanting to settle or grow within the range of those frequencies.

Another preventive measures for biofouling establishment is proactive measure. This differs from conventional in-water hull cleaning, which is primarily referred to as reactive cleaning. Reactive cleaning is when a vessel or some structure has heavy amounts of biofouling on it which is then cleaned off in order to return it to an "original state". Proactive cleaning on the other hand is intended to clean underwater surfaces before any hard or well-established biofouling has a chance to develop. For that reason, it is sometimes referred to as "hull grooming" because the surface is groomed to maintain it at a rather pristine level before there is a chance for any complex biofouling to establish. Devices can be typically operated either manually by divers, such as the one shown in Photo 4, or as remotely operated vehicles – or ROV in Photo 5. Guidance and/or standards on how these technologies should be assessed and operated have been developed by some organizations and, most recently, by the industry (BIMCO, 2021).

Photo 4: Diver-operated cleaning cart.

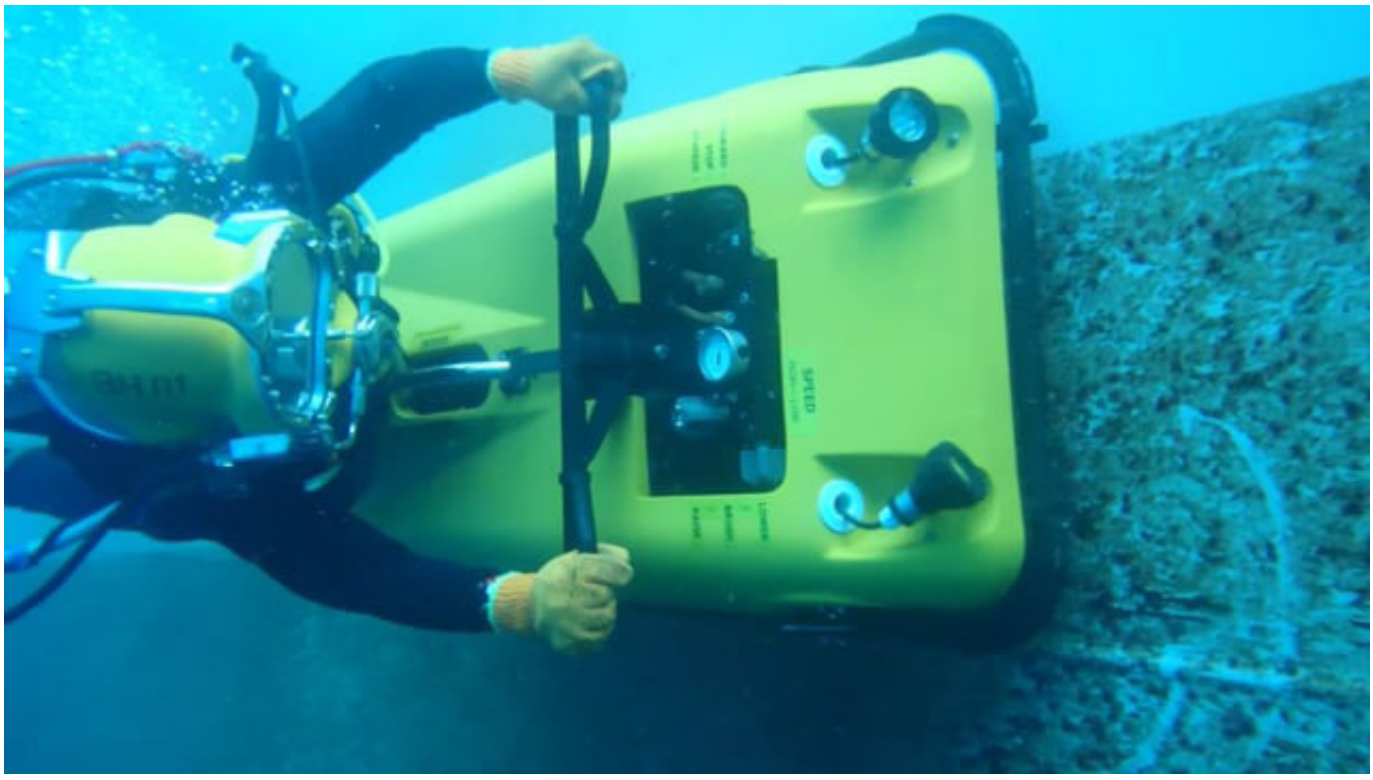

Photo 5: A remotely operated vehicle (ROV) in action against a ship hull.

The second part of this report focuses on newly developed research to analyse the effect of some solutions for biofouling management. To achieve this, the predictions of the impacts of biofouling on ships' energy efficiency found in the scientific literature were converted into the impacts of the hull and/or propeller cleanings. Additionally, a life cycle approach was used to assess the impacts of different biofouling management solutions between drydocking periods from the economic and environmental perspectives.

To simplify this assessment, the performance of anti-fouling coatings was not part of the analysis conducted in this report, which focused solely on calculating the potential benefits of hull cleaning, propeller cleaning and ultrasonic anti-fouling systems. The performance of a bulk carrier was predicted under different combinations of these solutions. The increase in the engine power of the ship was predicted based on two biofouling growth scenarios, allowing the estimation of daily and cumulative fuel consumptions and GHG emissions. Figure 2 illustrates the biofouling growth on a ship with no cleaning in two different regions: one based on the prevailing conditions in the Mediterranean and the other based on an Equatorial region.

Figure 2 Biofouling growth on the hull under the No cleaning scenario in two different regions

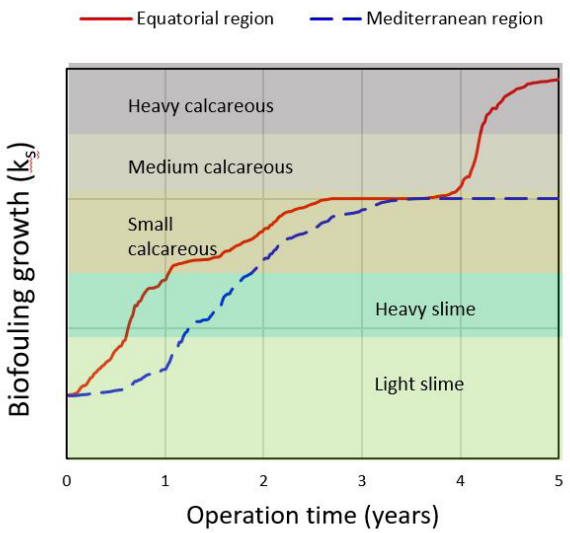

Figure 3 shows the power increase that would be required if no cleaning is undertaken over the 5-year period between drydocking and then compares it with the performance of two different biofouling management strategies:

- Reactive cleaning for the hull and use of ultrasonics for the propeller (which are assumed to keep the propeller free from fouling for the full 5 years), and
- Proactive cleaning for hull and propeller.

As shown in the graph, hull maintenance would not be conducted before reaching certain thresholds linked to increased engine power needs. In the case of proactive cleaning, the first clean would be conducted when the biofouling penalty reaches a 20% increase in power needs (in the model this happened 1.5 years after a new coating was applied, and is reflected by the grey line returning back to the 0% line), and then repeated every half year. For reactive hull cleaning, the first clean would be triggered when the power penalty reaches 40% (in the model this happened 3 years after a new coating was applied), and then repeated every year.

Table 2 (see page 17) summarizes the differences in total fuel cost and GHG emissions with three different biofouling management scenarios explained in the previous section: no cleaning; reactive hull cleaning with ultrasonic protection of the propeller; and proactive cleaning of the hull and the propeller. For the purpose of estimating cost, a fuel price of $572.5 per metric ton of FO fuel was used for the calculation. Chapter 2 of this report includes full details of these calculations, plus the results for four other biofouling management combinations for a ship operating in Mediterranean waters and a ship operating in an Equatorial region.

Figure 3 Required engine power increase of the bulk carrier at the design speed with different anti-fouling strategies over the 5-year operation (Equatorial region)

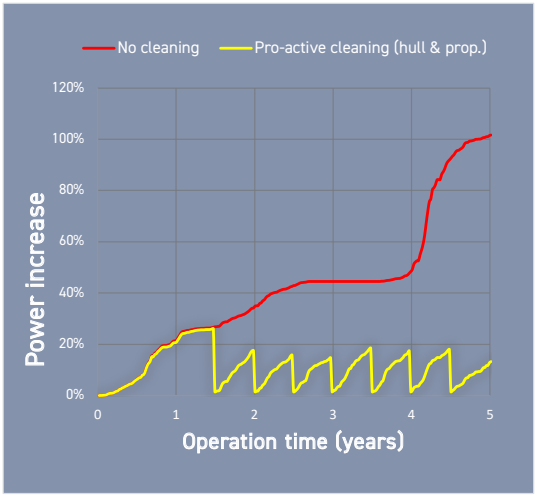

Table 2 Difference in the total fuel cost and GHG emissions with different biofouling management scenarios (operating in an Equatorial region)

	Total fuel cost	Savings compared to *"No cleaning"*	%	CO_2e emissions reduction	Assumptions
No cleaning	$29.65 mil.	N/A	N/A	N/A	N/A
Reactive hull cleaning + Ultrasonic anti-fouling for propeller	$25.27 mil.	-$4.39 mil.	-15%	-23,825 t	Hull cleaning only years 3 & 4
Proactive cleaning (hull & propeller)	$23.07 mil.	-$6.58 mil.	-22%	-35,760 t	Cleaning after 2 ½, 3, 3 ½, 4, 4 ½ years.

Under the conservative scenario illustrated by this example, biofouling growth in the absence of cleaning would remain at the small calcareous fouling (level 3) until year 4. Conducting proactive cleaning could entail approximately 22% savings in fuel consumption and GHG emissions, whereas reactive cleaning undertaken during years 3 and 4 before entering dry dock could result in 15% savings. This is not a comparison between these two approaches, but the result of the analysis of options for biofouling management conducted under specific assumptions.

CONCLUSIONS

Overall, the results presented in this report clearly indicate how the perceived impact of biofouling is likely to have been historically underestimated by the shipping community. While anti-fouling coatings remain the first and foremost option for preventing biofouling growth, this study highlights the notable potential of biofouling management measures to support the performance of anti-fouling coatings and to reduce fuel consumption of ships.

Combined with recent surveys on the true level of biofouling prevalent within the shipping fleet, the outcome of this report clearly underscores the importance of biofouling management as an essential component in the toolbox for GHG emissions reduction by the shipping industry. This is especially true in the short to medium term, where biofouling management may be used as a means of compliance with IMO carbon intensity requirements, while the development and deployment of other GHG reduction strategies based on new low carbon and zero-carbon fuels or technologies come to fruition.

Future work may focus on analysis based on ships' operation data without involving any prediction methods. Such data accumulation would establish the prevailing biofouling levels in the shipping sector and may help to define a useful formulation to correlate the ship resistance characteristics and different hull/propeller fouling conditions, which will enable users to estimate ship performance easily and robustly under different biofouling conditions. Another area not yet well understood that needs more data is that of biofouling in niche areas or internal seawater systems and the impact of mitigation options.

Besides securing data to determine the prevailing levels of biofouling within the shipping sector, the development of knowledge and awareness materials aimed at ship operations and ports are essential to promote understanding of biofouling and increase the adoption of good biofouling prevention and management tools. Incorporating direct and indirect economic components is likely to provide compelling evidence to improve alignment between the industry and environmental priorities of the shipping industry.

HULL IN-WATER CLEANING

UP TO

22%

SAVINGS IN FUEL CONSUMPTION, AND REDUCTION OF GHG EMISSIONS.

Over a 5-year period for a 179m bulk carrier

CHAPTER 1

IMPACT OF BIOFOULING ON SHIPS

1.1 REPORTED IMPACTS OF BIOFOULING

The penalty for hull and propeller roughness is either the loss of speed for a ship using the same level of power (constant power) or the need to increase power to maintain the same speed level (constant speed). Both options will result in economic and environmental penalties. This section presents a historical overview of the impact of biofouling on ship propulsion and energy efficiency.

One of the first comprehensive investigations into the biofouling penalty is the full-scale measurement of Davis (1930), who recorded the delivered shaft powers of a destroyer and a battleship to develop various speeds over different operational times. The result showed that the required shaft power of the destroyer (named Putnam) at the speed of 28 knots increased by 32% after 8 months of operation, while the required shaft power of the battleship (named Tennessee) at 28 knots was increased by 37% after 10 months of operation. Hiraga (1934) investigated the effect of biofouling on the resistance of a brass plate coated with anti-fouling paint. After 24 days of immersion, barnacles and slime grew on the surface and resulted in a 20% increase in the total drag. Interestingly, the resistance with the fouled surface showed initial decreases during the testing and eventually converged to a constant value and this was attributed to the washing-off of existing slime by the force of the water current. Izubuchi (1934) performed a full-scale towing test using an old Japanese destroyer to determine the increase in the ship resistance due to hull biofouling. The vessel was docked, painted, and had the propeller removed, and was immediately subjected to towing test. The towing test was repeated at intervals to show the effect of hull biofouling over time. They obtained the resistance constants in Froude's formula, $R_f=fSV^n$ with different exposure times. Redfield et al. (1952) used these constants to estimate the resistance increase and speed loss of the same Japanese destroyer after various periods at anchor. For example, at 16 knots, the total resistance was doubled after 375 days of exposure, and the ship speed produced by a towing force of 10 tons was reduced from 20 knots to 15.4 knots. Unfortunately, no information is reported about the biofouling levels of the destroyer during the test periods.

Kempf (1937) investigated the effect of biofouling on the frictional resistance of a 77-metre-long pontoon with various rough surfaces. The result showed that the frictional resistance increased more than 100% with 3 to 4 mm barnacles covering 25% of the surface. Denny (1951) reported that the frictional resistance of a 58 m passenger vessel was increased by 5% due to a thin coat of slime and deterioration of the bituminous aluminium paint on the hull after being moored for 40 days.

Lewthwaite et al. (1985) conducted an experiment to measure the local skin friction of a 23 m fleet tender. After 240 days of operation, a 25% increase in the local frictional resistance was measured with a thin slime coverage. After 2 years of operation, a 1 mm-thick dense slime film and extensive weed had developed on the hull, which resulted in an 80% increase in the local skin friction. Haslbeck et al. (1992) conducted a full-scale trial on a Knox class frigate that had an organotin and cuprous oxide anti-fouling coating. After 22 months out of the dock, the vessel showed an 18% increase in the delivered power with a small amount of calcareous biofouling and a mature slime film.

Hundley et al. (1991) presented the changes in power requirements of a 96 m destroyer due to hull and propeller fouling as well as hull and propeller cleanings. After a 795-day (2 years and 2 months) operation, the fouled hull and fouled propeller led to a 115% increase in the required shaft power at 17.4 knots. Then the penalty was relieved to a 70% increase after a diver-cleaning of the propeller. After the 900-day operation, the hull and propeller were diver-cleaned and the increase in the shaft power was reduced to 9%.

Ballegooijen et al. (2016) measured the in-service resistance and propulsion performance of a 13,000 TEU containership. After 1.5 years of operation, the container vessel showed a 9.2% increase (6.4% per year) in the total resistance while the propeller efficiency decreased by 3.7% (2.6% per year). Unfortunately, the hull condition during the measurement

period is not reported. Murrant et al. (2019) compared the performance of a 62 m long offshore patrol ship before and after hull and propeller cleanings. Before the cleanings, as a result of 2 years of operation, the hull was covered with soft biofouling and the divers determined the fouling rating (*FR*) of most of the hull regions as *FR* 20, while the propeller blades were covered in light to moderate slime. The sea trial results showed the required power was reduced by 5% after the hull cleaning, between 13.5 and 16 knots. Unexpectedly, no additional power reduction was identified after the propeller cleaning.

Relatively few studies have been devoted to investigating propeller fouling, although its impact has been recognized since the early days of naval architecture. Bengough et al. (1943) reasoned that the failure of a Shoreham-class sloop reaching the design speed is due to her fouled propeller. When subsequently docked, the propellers were found to be colonized by calcareous tubeworms. The target speed could be eventually achieved after a propeller cleaning. Taylor (1943) claimed that even the ships operating with a propeller in moderately good condition can suffer a power loss of the order of 10%. One of the common conclusions of studies is that propeller fouling can be as destructive as hull fouling, or even worse considering the impact per unit area, but the remedy is much cheaper (ICCT, 2011; Mosaad, 1986; Townsin et al., 1981). Table 3 shows a summary of the reported impacts of biofouling on ship hydrodynamic performances.

Table 3 Reported impacts of biofouling on ship resistance and powering

Authors	Ship	Speed	Exposure time	Surface condition	Findings ΔC_T: increase in total resistance ΔC_F: increase in friction resistance ΔP_D: increase in delivered power
Izubuchi (1934)	111 m destroyer	10-20 knots	12 months	Unknown	ΔC_T=100%
Kempf (1937)	77 m pontoon	Unknown	Unknown	Barnacles and slime	ΔC_F=100%
Redfield et al. (1952)	a. 120 m cargo vessel b. 96 m destroyer	a. 9 knots b. 24 knots	Unknown	Barnacles and slime	*a.* ΔC_F=330% *b.* ΔC_F=280%
Davis (1930)	a. 115 m destroyer b. 183 m battleship	a. 28 knots b. 21 knots	1. 8 months 2. 300 days	Unknown	*a.* ΔP_D=32% *b.* ΔP_D=37%
Denny (1951)	58 m passenger carrier	5-15 knots	40 days	Slime	ΔC_F=5%

Table 3 Reported impacts of biofouling on ship resistance and powering continued

Authors	Ship	Speed	Exposure time	Surface condition	Findings ΔC_T: increase in total resistance ΔC_F: increase in friction resistance ΔP_D: increase in delivered power
Lewthwaite et al. (1985)	23 m fleet tender	Unknown	1. 240 days 2. 500 days	1. thin slime (too thin to measure) 2. thick slime (1 mm) and extensive weed	*1.* ΔC_F*=25%* *2.* ΔC_F*=80%*
Hundley et al. (1991)	96 m destroyer	17.4 knots	1. 651 days 2. 795 days 3. 796 days 4. 900 days 5. 1,165 days	1. Fouled hull and propeller 2. Fouled hull and propeller 3. Fouled hull and diver-cleaned propeller 4. Diver-cleaned hull and propeller 5. Re-fouled hull and propeller	*1.* ΔP_D*=79%* *2.* ΔP_D*=115%* *3.* ΔP_D*=70%* *4.* ΔP_D*=9%* *5.* ΔP_D*=125%*
Ballegooijen et al. (2016)	13,000 TEU container ship	Unknown	1.5 years		ΔC_T*=9.2%*
Murrant et al. (2019)	62 m offshore patrol ship	13.5-16 knots	2 years	Light slime	ΔP_D*=5%*

1.2 BIOFOULING IN NICHE AREAS

While the impact of hull and propeller fouling is well established, less focus has been given to biofouling in niche areas (i.e. sea chests, bow/stern thrusters, propeller shafts, inlet gratings, dry-dock support strips, etc.). The presence of biofouling in niche areas and internal seawater systems may not directly affect the ship's resistance and propulsion performances, but the performance reduction of such devices can disrupt water flow, compromise the structural integrity, degrade the operational health of the ship and also threaten the marine ecosystem by transporting the Invasive Aquatic Species. Surface and flow impacts change the work rate required to pump water through the system, increasing the energy use and emissions of the ship. Cooling systems directly affect engine efficiency and fuel costs.

Niche areas are often blind spots for maintenance and, at the same time, hot spots for biofouling accumulation. There are several factors driving niche areas to be more prone to biofouling accumulation. Some niche areas (e.g. bow/stern tunnels) experience a much smaller amount of flow than other areas and therefore act as a shelter for biofouling communities. Coatings in some niche areas (e.g. bilge keel) are more prone to damages due to the shape and protrusions, which diminishes anti-fouling coating effectiveness and thus accelerates colonization by biofouling species. Additionally, the complex nature of niche areas not only impairs the effective application of anti-fouling coatings but also makes them more difficult to maintain and more likely to sustain damage during operations.

According to Hoffmann (2021), a data set obtained from a 249-ship sample showed that 95% of the vessels have animal biofouling organisms in their niche areas, while only 44% of them had unacceptable levels of hard biofouling (>10%) on the hulls. These differences imply that the hull anti-fouling solutions might not be the best solution for niche areas, and therefore, developments of different biofouling control solutions dedicated to niche areas with different hydrodynamic conditions are encouraged.

1.3 PREDICTING THE IMPACT OF BIOFOULING

1.3.1 REVIEW OF REPRESENTATIVE BIOFOULING CONDITIONS FOR PENALTY PREDICTION

Schultz (2004) conducted a series of towing tests of flat plates coated with different anti-fouling paints under unfouled, fouled (after 287 days of marine exposure) and cleaned conditions. From the test results, the study determined the roughness functions (see **ANNEX D**) of the fouled coating surfaces and found that the roughness functions follow the Colebrook-type roughness function model of Grigson (1992). Accordingly, the roughness length scales (equivalent Grigson roughness height, k_G) were determined and correlated with the biofouling quantities of the surfaces. Further details about the equivalent Grigson roughness height can be found in **ANNEX E**. For example, the k_G of the surfaces with barnacle biofouling can be calculated as $k_G=0.059_{barnnacle}\sqrt{}\%SC_{barnacle}$ and $\%SC_{barnacle}$ are the height of the largest barnacles and the percentage coverage of the barnacle biofouling, given in Table 4. And k_G of the SPC TBT surface can be calculated as $k_G=0.11\ h_{slime}$, in which h_{slime} is the thickness of the slime film, given in Table 4. The result of this study was used to determine the typical representative hull conditions in his later study (Schultz, 2007).

Table 4 Anti-fouling surfaces with biofouling accumulation after 287 days of marine exposure Schultz (2004)

Test surface (fouled)	Total biofouling coverage (%)	Slime (%)	Hydroids (%)	Barnacles (%)	Biofouling description	k_G (µm)
Silicone 1	75	10	5	60	Uniform coverage of barnacles (~6 mm in height)	2,742
Silicone 2	95	15	5	75	Uniform coverage of barnacles (~7 mm in height)	3,577
Ablative copper	76	75	0	1	Dense layer of diatomaceous and bacterial slime with very isolated barnacles (~5 mm in height)	295
SPC copper	73	65	3	4	Moderate layer of diatomaceous and bacterial slime with isolated barnacles (~5 mm in height)	590
SPC TBT	70	70	0	0	Light layer of diatomaceous and bacterial slime (~1 mm in height)	110

Table 5 Representative coating and biofouling conditions and the corresponding *FR*, k_s, and Rt_{50} values determined by Schultz (2007)

Representative surface condition	*NSTM fouling rating*	k_s (µm)	*AHR* (µm)
Hydraulically smooth surface	0	0	0
Typical as applied AF coating	0	30	150
Deteriorated coating or light slime	10-20	100	300
Heavy slime	30	300	600
Small calcareous fouling or weed	40-60	1,000	1,000
Medium calcareous fouling	70-80	3,000	3,000
Heavy calcareous fouling	90-100	10,000	10,000

Table 6 Representative biofilm conditions of Schultz et al. (2015) and their k_s values

Test surface	Average biofilm thickness (μm)	Coverage (%)	k_s (μm)
FRC A (3 months exposure)	545	19.6	132.7
FRC B (3 months exposure)	443	11.8	83.7
FRC C (3 months exposure)	574	6.4	93.8
Acrylic control (3 months exposure)	527	18.1	123.3
FRC A (6 months exposure)	520	14.2	107.8
FRC B (6 months exposure)	443	13.7	90.2
FRC C (6 months exposure)	98	49.2	37.8
Acrylic control (3 months exposure)	392	27.8	113.7

Schultz (2007) presented typical hull surface conditions for anti-fouling coatings with and without the presence of biofouling and determined their corresponding hull roughness parameters (i.e. NSTM *FR*, k_s, and *AHR* (average Rt_{50}) values). Further details about the NSTM fouling rating and hull roughness parameters can be found in appendices A7 and A4. Table 5 (see page 22) shows the representative surface conditions of Schultz (2007).

Schultz et al. (2015) tested the frictional drag of the test panels coated with foul release coatings after 3 and 6 months of immersions in the USNA dynamic biofilm exposure facility. The frictional drag values of the test plates were measured using a fully developed turbulent channel flow facility. Based on the test data, they concluded that the equivalent sand-grain roughness height, k_s, of the biofilm surfaces can be calculated as k_s=0.055 $k_{biofilm}$ $\sqrt{\%SC_{biofilm}}$, where $k_{biofilm}$ and $\%SC_{biofilm}$ are the thickness and the coverage of the biofilm. Table 6 shows the representative biofilm conditions of Schultz et al. (2015) and the corresponding k_s values.

Demirel et al. (2017b) conducted a series of towing tests using a flat plate covered with 3D printed barnacle patches to investigate the impact of barnacles with varying sizes and coverages. The roughness functions of the barnacles showed a good collapse on top of the Colebrook-type roughness function model of Grigson (1992), and corresponding k_G were determined, as shown in Table 7 (see next page). Furthermore, an equation was proposed to calculate the k_G of the barnacle surfaces using the heights and the surface coverages of the barnacle surfaces, as

$$k_G = -17.53 - 8.128\,\%SC + 0.6957\,h + 0.4501\,\%SC^2 + 0.4165\,\%SCh - 14.81h^2 - 0.00548\,\%SC^3 + 0.000456\,\%SC^2\,h + 0.937\,\%SCh^2 \quad (4)$$

where, h and $\%SC$ are the height and surface coverage (%) of the barnacles.

Monty et al. (2016) scanned light calcareous tubeworm fouling, scaled and reproduced for wind-tunnel testing to determine the equivalent sand-grain roughness, k_s. Table 8 (see next page) shows the key surface parameters from the scanned surface data and the equivalent sand-grain roughness height, k_s.

1.3.2 REVIEW OF PREDICTION METHODS

Townsin et al. (1990) found that the added resistance due to hull roughness is correlated well enough with the Rt_{50} of the rough surfaces and proposed a simple formula for the added resistance in terms of average hull roughness (*AHR*) as,

$$\Delta C_F \times 10^3 = 44\left\{\left(\frac{AHR}{L}\right)^{\frac{1}{3}} - 10\,Re_L^{-\frac{1}{3}}\right\} + 0.125 \quad (5)$$

where, ΔC_F is the added resistance coefficient due to the hull roughness, L is the ship length and Re_L is the Reynolds number based on the ship length and speed defined as $Re_L = VL/\nu$, in which V and ν are the ship speed and kinematic viscosity of water, respectively. This formula has been adopted by the International Towing Tank Conference (ITTC) as a roughness allowance, with standard value of *AHR* = 150 μm. Further details about the average hull roughness can be found in **ANNEX C**.

However, the formula of Townsin et al. (1990) was proposed to be used for coating surfaces of ship hulls without biofouling and the experimental data used to develop the

Table 7 Representative barnacle surfaces of Demirel et al. (2017b) and their k_G values

Test surface	Description	k_G (μm)	k_G (μm) (from Eq. 4)
S10%	1.25 mm barnacles with 10% coverage	24	24
S20%	1.25 mm barnacles with 20% coverage	63	60
S40%	1.25 mm barnacles with 40% coverage	149	171
S50%	1.25 mm barnacles with 50% coverage	194	181
M10%	2.5 mm barnacles with 10% coverage	84	91
M20%	2.5 mm barnacles with 20% coverage	165	176
M40%	2.5 mm barnacles with 40% coverage	388	386
M50%	2.5 mm barnacles with 50% coverage	460	445

Table 8 Key surface parameters from the scanned light calcareous tubeworm fouling surface, and equivalent sand-grain roughness height, k_s

Roughness parameter	Value
Mean roughness height, k_a (Ra)	94 μm
Equivalent sand-grain roughness height, k_s	325 μm

formula were restricted to Rt_{50} < 230 μm. Therefore, the validity of the formula for a fouled hull has been questioned and the ITTC recommends the researchers to develop new formulae or methods. However, there exists no simple method predicting the added resistance due to the fact that the roughness effect cannot be fully represented by only one parameter. In other words, although different surfaces have the same roughness height (e.g. *AHR*), the roughness effect may vary owing to other surface properties such as frontal solidity, effective slope, plan solidity and skewness. (Chung et al., 2021).

1.3.2.1 SIMILARITY LAW SCALING

Once the roughness function (see ANNEX D) of the surface of interest is known, the roughness effect on the boundary layer can be predicted based on the assumption that the smooth and rough wall turbulence behave similarly away from the wall (Raupach et al., 1991; Townsend, 1956). Based on this assumption, the frictional resistance of a flat plate with an arbitrary length and speed can be predicted once the roughness function, ΔU^+, of the surface is given. The prediction procedures have been developed by Prandtl et al. (1934) and Granville (1958), while the latter has been mostly used by many researchers. Monty et al. (2016) revisited these approaches and proposed a similar (but simpler) approach that can cope with varying roughness heights along with the flat plate. Similarly, Song et al. (2021b) proposed a procedure to predict the added resistance due to a heterogenous hull roughness based on the similarity law scaling of Granville (1958).

However, these similarity-law-based prediction methods have several limitations due to the "flat plate" assumption. In other words, the frictional resistance of the rough hull is assumed to be equal to that of an equivalent flat plate with the same length. Therefore, the three-dimensional (3D) effects (i.e. hull form effects) are discarded and thus this method can predict the roughness effect on the frictional resistance only. However, recent studies claim that the hull roughness also affects other pressure-related resistance components (e.g. residuary resistance, viscous pressure resistance, wave-making resistance), and therefore the

Figure 4 Smooth and rough wall-functions used for the smooth and wall boundary conditions

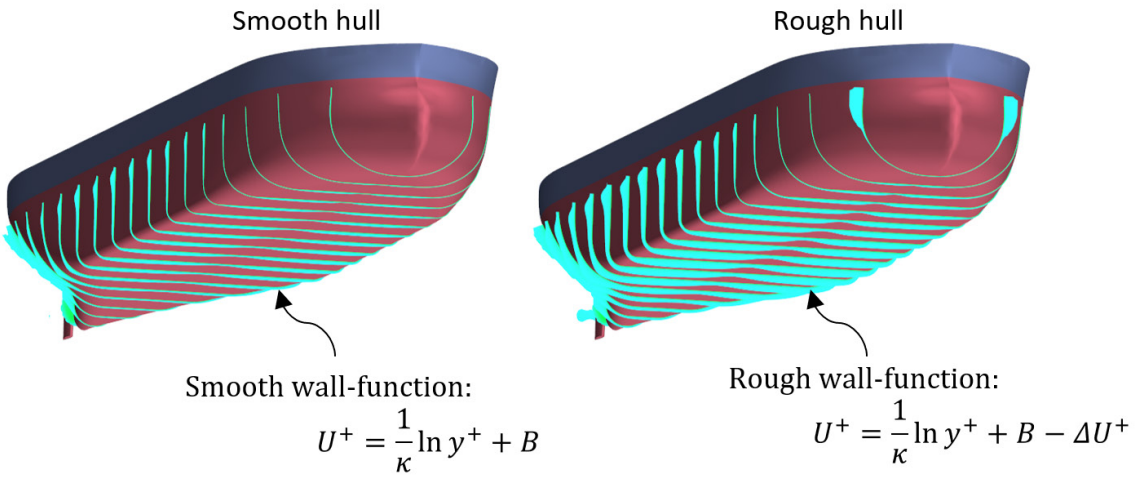

validity of the similarity law scaling method is being questioned in recent studies (Farkas et al., 2019; Song et al., 2019; Song et al., 2020e).

1.3.2.2 COMPUTATIONAL FLUID DYNAMICS

Computational fluid dynamics (CFD) have been considered in recent times as an effective alternative to predict the effect of biofouling on full-scale ship performances. The most prevalently used technique is using modified wall-functions by employing the roughness function, such that the wall boundary condition can represent the effect of rougher surface, as illustrated in Figure 4. These CFD simulations can avoid the aforementioned shortcomings of the similarity law scaling. The merit of CFD simulations taking into account 3D effects is that it not only improves the accuracy of the resistance prediction, but also enables the prediction of the roughness effect on the propeller performance, as it can also predict the roughness effect on the pressure field around the propeller blades.

1.3.3 REVIEW OF PREDICTION STUDIES

As discussed in section 1.3.2, the merit of the boundary layer similarity law scaling methods is that the frictional resistance of a ship with any length and speed can be predicted once the roughness function, ΔU^+, of the surface is given.

Schultz (2004, 2007) and Schultz et al. (2011) used the similarity law scaling procedure of Granville (1958) to predict the impact of biofouling on ship resistance and powering, with different representative hull conditions. Schultz (2004) predicted the impacts of biofouling on the frictional resistance of a 150 m flat plate, which represents midsized merchant and naval ships. The equivalent Grigson roughness heights, k_G, representing barnacle and slime surfaces were used with the similarity law scaling. The results showed that the frictional resistance of the 150 m flat plate can increase by 205% due to 7 mm barnacles covering 75% of the hull. Schultz (2007) predicted the impacts of biofouling on the total resistance of a 124 m Oliver Perry-class frigate (FFG-7). Equivalent sand-grain roughness heights, k_s, of representative coating and biofouling conditions were used for the similarity law scaling. The results showed up to an 80% increase in the total resistance with the heavy calcareous fouling condition. Furthermore, the increase in the shaft power values at constant speed was estimated considering the changes in the operational condition of the propeller (e.g. change in the propeller rotational speed). The result showed that the Oliver Perry-class frigate requires 86% more shaft power to maintain 15 knots under the heavy calcareous fouling condition. Schultz et al. (2011) predicted the effect of biofouling on a 142 m Arleigh Burke-class destroyer using the same representative coating and fouling conditions of Schultz (2007). The similarity law analysis showed that the total resistance and shaft power of the vessel increase by 69% and 76%, respectively, with heavy calcareous fouling formed on the hull.

Monty et al. (2016) predicted the effect of tubeworm fouling on the resistance of a 124 m Oliver Perry-class frigate using a newly proposed prediction method based on the boundary layer similarity law. The equivalent sand-grain roughness height of the tubeworm surface was used

with the new prediction method. It was found that the total resistance and the effective power of the vessel can increase by 23% due to the tubeworm fouling.

Demirel et al. (2017b) employed the similarity law scaling of Granville (1958) to predict the effect of barnacle fouling on ship resistance and powering. The equivalent Grigson roughness heights, k_G, of barnacle surfaces with different sizes and coverages were determined and used in the similarity law scaling. The prediction suggested that the total resistance and effective power of a 230 m container ship can increase up to 66% due to 5 mm barnacles covering 20% of the hull. Demirel et al. (2019) generated added resistance diagrams to be used for predicting the biofouling impact on ship resistance. The representative coating and fouling conditions of Schultz (2007) were employed with the similarity law scaling of Granville (1958) to predict the impact of different surfaces on the frictional resistance of flat plates with different lengths (10-400 m) and speeds (8-50 knots). Using the generated added resistance diagrams, the resistance and powering penalties of different ship types were predicted.

On the other hand, computational fluid dynamics (CFD) simulations have been widely used in recent years to predict the biofouling penalties on ship resistance and propulsion performances. Most of the CFD studies used the modified wall-function approach that employs the roughness functions into the wall-function of the CFD model such that the wall boundary conditions of the simulation represent different surface conditions.

Demirel et al. (2017a) conducted CFD simulations of a 230 m containership to predict the added resistance with different hull conditions. A roughness function model was employed in the simulations with the equivalent sand grain roughness height, k_s, to simulate the representative coating and fouling conditions of Schultz (2007). The simulations showed that the total resistance and effective power of the ship can increase by 107.5% with heavy calcareous fouling on the hull.

Farkas et al. (2018, 2019) predicted the impact of biofilm on a 230 m containership and a 175 m bulk carrier using CFD simulations. Several representative biofilm surfaces were determined based on the findings of Schultz (2004) and Schultz et al. (2015). The corresponding roughness function models with different equivalent sand grain roughness height values, k_s, were employed in the simulations. The results showed up to 28.9% and 29% increases in the total resistance of the containership and bulk carrier, respectively, with a 500 μm biofilm covering 50% of the surface.

Song et al. (2019; 2020e) employed the representative barnacle surface conditions of Demirel et al. (2017b) in the CFD models of a 230 m containership and a 320 m tanker. The roughness function model of Grigson (1992) was embedded in the CFD model with the equivalent Grigson roughness height values, k_G, to simulate the effect of barnacles with different sizes and coverages. The simulations showed up to 66% and 78% increases in the total resistance values of the containership and the tanker, respectively, due to the 5 mm barnacles with 20% coverage.

Farkas et al. (2020a) determined hard fouling conditions based on the findings of Schultz (2004) and employed these conditions in the CFD simulations of a 230 m containership and a 320 m tanker. The simulations suggested that, due to 7 mm barnacles with 25% coverage, the total resistance of the containership and the tanker increase by 86% and 117%, respectively.

As mentioned in Section 1.3.2.2, one of the advantages of such CFD methods is that the impact of propeller fouling can also be predicted as the roughness effect on the pressure field can be effectively predicted in the CFD simulations.

Song et al. (2020d) conducted CFD simulations to predict the penalty of barnacle fouling on the blades of a 7.9 m propeller, which is designed for a 230 m containership. The representative barnacle surfaces of Demirel et al. (2017b) were employed in the CFD model to simulate the fouled blade surfaces of the propeller. The simulations showed that the propeller open water efficiency, η_0, decreases by 14% due to the 5 mm barnacles with 20% coverage. In addition, the increase in the delivered power due to the propeller fouling was estimated using the predicted propeller performances. The result suggests that the 230 m containership requires 20% more delivered power, to maintain the design speed, due to the propeller fouling only (5 mm barnacles with 20% coverage) while the hull remains clean.

Farkas et al. (2021) developed CFD models of three different propellers, i.e. 6.2 m, 7.9 m, and 9.9 m propellers designed for a 175 m bulk carrier, 230 m containership, and a 320 m tanker, respectively. Representative biofilm and hard fouling conditions were employed in the CFD simulations to predict the impact of biofouling on propeller performances. It was observed that the open water efficiencies of the 6.2 m, 7.9 m and 9.9 m propellers decreased by 29%, 28%, and 32%, respectively, due to 7 mm barnacles with 25% coverage.

The CFD method has also been used for predicting the effect of biofouling on ship self-propulsion performances. Song et al. (2020c) conducted simulations of self-propelled a 230 m containership with different hull and/or propeller fouling scenarios, using the representative barnacle

fouling conditions of Demirel et al. (2017b). The result showed that the increases in the delivered power of the ship increases by 58%, 19%, and 82%, respectively for the *fouled-hull/clean-propeller*, *clean-hull/fouled-propeller*, *fouled-hull/fouled-propeller* scenarios (5 mm barnacles with 20% coverage). Furthermore, the effects of the hull and/or propeller fouling on the propulsion efficiencies were investigated using the simulation results.

Farkas et al. (2020b) investigated the effect of biofilms on ship self-propulsion performance of a 230 m containership. Different representative biofilm surface conditions were used to simulate the fouled hull and propeller surfaces. The simulation showed that a 500 μm biofilm with 50% coverage increases the delivered power by 25.8%.

A summary of the results of the studies in the literature that used the prediction methods discussed in section 1.3.3 can be found in **ANNEX H**.

1.4 SUMMARIZING THE FINDINGS OF PREDICTION STUDIES

The studies reviewed in sections 1.1 and 1.3.3 show the drastic impacts of biofouling on ship resistance and propulsion performances. However, estimating the economic and environmental consequences of biofouling is not straightforward from findings in the literature, as the impacts were represented by different ship performance parameters (e.g. C_T, C_F, P_E, P_D, P_S, η_0). Therefore, this section aims to summarize and translate the impact to recognizable parameters such as increase in fuel consumption and GHG emissions.

The relative increases of fuel consumption (ΔFC) and GHG emission (ΔGE) values were estimated based on several simplifications. For example, it was assumed that GHG emissions are proportional to the fuel consumption (therefore, $\%\Delta FC=\%\Delta GE$). Also, the fuel consumption was assumed to be proportional to the effective power, shaft power or delivered power (whichever is available). For the results where only the impacts on the frictional resistance is presented, the impact on the total resistance was estimated with the aid of the ship resistance approximation method of Holtrop et al. (1982).

ANNEX I includes a table showing the economic and environmental impacts of biofouling (i.e. ΔFC and ΔGE) interpretated from the studies reviewed in sections 1.1 and 1.3.3. Figure 5 below, plots the results of this analysis in a graphic representation that clearly demonstrates the notable impacts of biofouling (understood as surface roughness levels k_s) on the GHG emissions of a ship.

Figure 5 Percentage increase in the GHG emission from ships due to hull fouling (based on compendium of results from published research studies

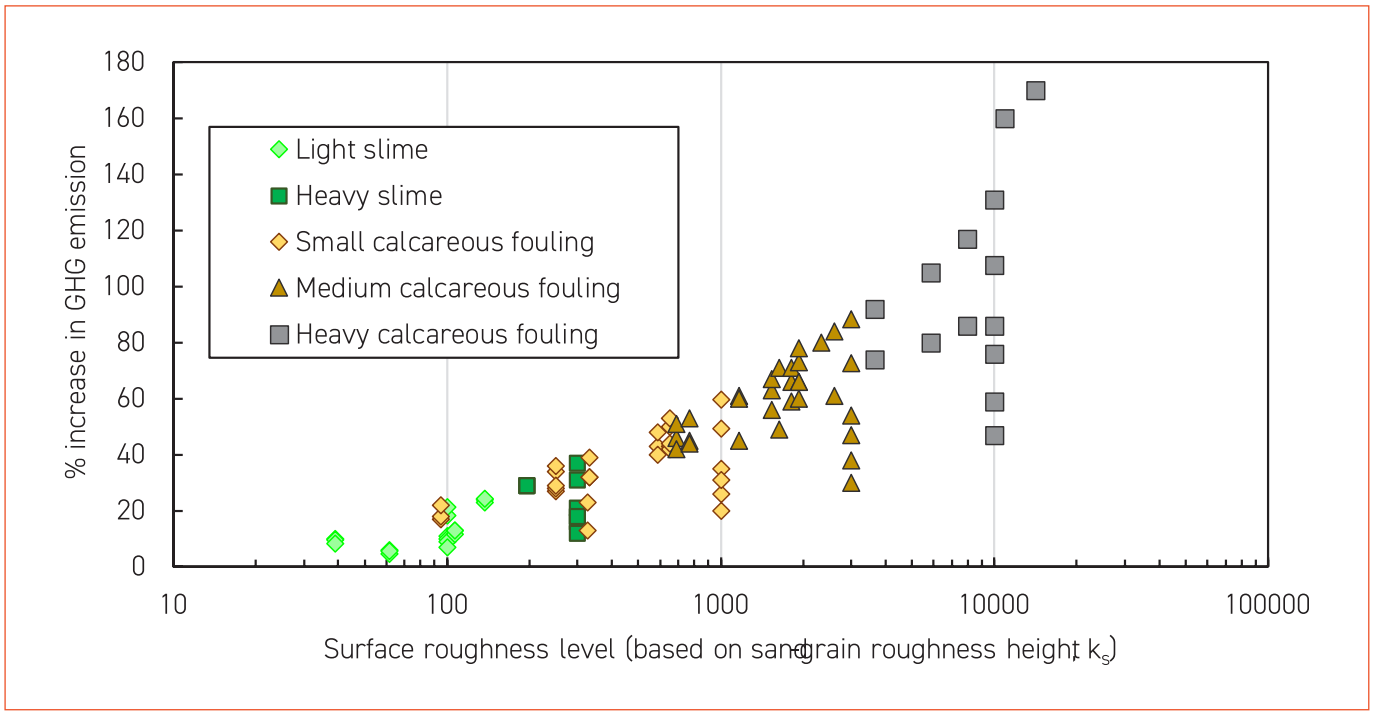

CHAPTER 2

BIOFOULING PREVENTION AND MANAGEMENT MEASURES

2.1 REVIEW OF CURRENT INDUSTRY PRACTICES FOR BIOFOULING PREVENTION AND MANAGEMENT AND THEIR IMPACT

2.1.1 BIOFOULING PREVENTION, MITIGATION AND MANAGEMENT OPTIONS

2.1.1.1 ANTI-FOULING COATINGS

Although many non-traditional methods have been proposed, such as ultrasonics, electric currents, magnetic fields and optical methods, coatings (paints), in particular biocidal coatings, have been the most popular anti fouling method owing to their excellent anti-fouling performance and low cost. Biocidal anti-fouling coatings are recognized as the most cost-effective over the other anti-fouling methods. Their advantages include ease of manufacture, high speed and low-cost application, durability, and applicability to a variety of structural forms and compositions. Biocidal anti-fouling coatings contain toxins (i.e. biocide). Biocide in the paint surface is gradually released into water and a toxic layer is formed around the surface. This layer prevents biofouling species from attaching to the surface, either by killing the biofouling organisms or deterring their settlement.

Coatings must maintain a certain level of biocide release (also known as "leach rate"). Once the leach rate falls below this level, whether through biocide depletion in the coating or by the formation of insoluble precipitates on the coating surface, the anti-fouling action will cease and marine organisms will start to settle on the surface. As a result, the effective life of typical copper-based insoluble matrix biocidal coatings rarely exceeds 18 months.

In the early 1970s the traditional copper-based anti-fouling paints were replaced by organotin compounds, due to their unbeatable anti-fouling ability and numerous other advantages, such as an effective life of 5 years or more, controllable biocide release rate, and ability to overcoat without loss of activity. Tributyltin (TBT) was the most used organotin compound together with triphenyltin (TPT).

These organotin compounds were thought to be environmentally safe when they were first introduced, because they degraded rapidly to harmless inorganic forms of tin. Unfortunately, research revealed that the TBT exposure causes severe impacts on marine ecosystems including the malformation of oyster shells and imposex of gastropod molluscs. Stirred by this information, the global community, through IMO's International Convention on the Control of Harmful Anti-fouling Systems on Ships (AFS Convention), banned the application of anti-fouling coatings with TBT in 2003 and banned the operation of ships coated with TBT paints in 2008. In 2021, IMO expanded these controls to the biocide cybutryne. The amendments to the AFS Convention will enter into force on 1 January 2023.

Modern biofouling control coatings can be classified into either "biocidal" or "non-biocidal" coatings by their composition. Biocidal coatings include controlled depletion polymer (CDP), self-polishing copolymer (SPC), and hybrid SPC. Non-biocidal coatings include fouling-release coatings (FRC), which are also termed as non-stick coatings.

The rosin-based CDP uses the hydration process to release biocides into the seawater. Seawater migrates into the CDP paint film which in turn dissolves rosin and biocides. However, the exponential release rate is the problem. Initially, the rate of release is wastefully high, then falls rapidly towards a point at which insufficient biocide is released to prevent the settlement of the biofouling species. The leached layers can become thick and increase the hull roughness. In general, the performance of CDP is considered as poor but, due to its low cost, they are still preferred for vessels which have short dry-dock intervals and those operating in low-biofouling regions.

The banning of TBT led to the development of tin-free self-polishing copolymers (SPC). SPCs have good initial hydrodynamic performance due to their smooth surface and the self-polishing action as the name suggests. The dissolution rate of biocides is controlled via

interaction with seawater, resulting in better anti-fouling performances. SPCs can remain effective for up to 5 years and therefore these coatings are preferred for vessels which have longer dry-dock intervals.

The biocide release mechanism of hybrid SPCs may be regarded as a hybrid of self-polishing and hydration, combining SPC acrylic polymers with a certain amount of rosin. The performance and price of hybrid SPCs, therefore, are midway between the CDP (rosin-based) and SPC (acrylic-based).

The main alternatives to biocidal anti-fouling coatings are widely known as fouling-release coatings (FRC). These were initially developed in the 1970s and rely on a physical mechanism to deter and release biofouling. They do this by producing a coating whose surface has been designed to produce low surface energy which in turn, reduces the adhesion properties of any biofouling which has been able to settle. Due to the mode of action of these coatings, they are most suitable for use on vessels which reach higher speeds and have higher levels of activity.

2.1.1.2 HULL AND PROPELLER CLEANING

The most straightforward biofouling mitigation method is hull and/or propeller cleaning.

Song et al. (2020 a) reviewed available ship hull cleaning technologies including cleaning methods and devices for dry-dock cleaning and underwater cleaning. Murrant et al. (2019) compared the performance of a 62 m long offshore patrol ship before and after hull cleaning. After the 2-year operation, the hull was covered with soft biofouling and the divers determined the fouling rating of most of the hull regions as *FR* 20. The operation data showed that the engine power at the speed of 13.5-16 knots was reduced by 5% after the hull cleaning. Bengough et al. (1943) reasoned that the failure of a Shoreham-class sloop reaching the design speed is due to her fouled propeller. When subsequently docked, the propellers were found to be colonized by calcareous tubeworms. The target speed could be eventually achieved after a propeller cleaning.

2.1.1.3 PROACTIVE CLEANING

While conventional biofouling mitigation and management methods are often of a reactive nature, proactive biofouling control methods have been recently highlighted due to their economic and environmental advantages over more conventional reactive methods.

The recent progress in the robotics and automation technology has accelerated the development of proactive in-water hull and propeller cleaning devices. The basic idea of a proactive cleaning approach (i.e. grooming) is keeping the hull and propeller clean with mild and frequent cleanings before hard growth settles down and the biofouling process accelerates. Proactive hull and propeller cleaning has the potential for economic and environmental benefits, not only because it can proactively eliminate the possible penalties of biofouling, but also it can save the cost associated with intensive hull cleaning in dry dock. Proactive cleaning is less aggressive and thus causes less damage to the anti-fouling coating, while reducing the risk of transporting invasive alien species.

2.1.1.4 ULTRASONIC ANTI-FOULING SYSTEMS

Ultrasonic technology has been widely used for various applications (e.g. medical equipment, jewellery), and also adopted in the shipping industry as a biofouling mitigating method. Ultrasonic anti-fouling systems emit low powered ultrasonic pulses via transducers that are in direct contact with the inside of the hull. The movement of water molecules over the entire underwater profile of the hull prevents the growth of microorganisms. One of the biggest advantages of ultrasonic anti-fouling system is the effectiveness in niche areas. As discussed in section 1.2, niche areas often experience a much smaller amount of flow than other areas and thus the performance of FRC can be greatly degraded. Furthermore, the complex nature of niche areas disturbs the hull cleaning and coating applications. Ultrasonic anti-fouling systems can avoid such difficulties as they use a different anti-fouling mechanism.

2.1.2 REPORTED IMPACTS OF BIOFOULING MITIGATION MEASURES

There have been studies assessing the anti-fouling performances of different marine coatings through either static or dynamic exposure to biofouling accumulations as shown in Table 9 (see next page).

Schultz (2004) compared the biofouling growth of different anti-fouling surfaces after 287 days exposure. The silicone anti-fouling coatings showed the most severe biofouling accumulations showing heavy barnacle coverages up to 75% of the immersed surface. The ablative copper surface was fouled with a dense layer of slime (75%) with very isolated barnacles (1%). The SPC copper anti-fouling coating surface showed a moderate layer of slime (65%) with isolated barnacles (4%). The best anti-fouling performance was shown by the SPC TBT surface only with a light layer of slime (70%). Cassé et al. (2006) conducted static and dynamic seawater immersion tests to assess the anti-fouling performances of four commercial anti-fouling coatings, of which three

Table 9 Studies comparing anti-fouling performances of different coatings

Author	Coating	Method	Note
Schultz (2004)	2 Silicone FRs Ablative copper SPC copper SPC TBT	Marine exposure / 287 days	Hydrodynamic test and full-scale extrapolation
Cassé et al. (2006)	TBT SPC Copper SPC Copper ablative Silicone FR	Static and dynamic immersion / 60 and 15 days	
Hunsucker et al. (2014)	Copper SPC Silicone FR	in-service condition (two cruise ships) / 31 and 14 months	
Schultz et al. (2015)	3 Silicone FRs	Dynamic laboratory exposure	Hydrodynamic test and full-scale extrapolation
Yeginbayeva et al. (2019)	9 FRs 4 SPCs	Marine exposure / 1 month	Hydrodynamic test

were biocide based (tributyltin self-polishing, copper self-polishing, copper ablative) and one was biocide-free (silicone foul release). After static immersion for 60 days, all coatings showed similar anti-fouling performances, while a few tubeworms settled only on the fouling-release coating. After the static immersion, the same panels (without any cleaning) were directly placed in dynamic immersion for 15 days in a polyethylene tank. After the dynamic immersion, there was a reduction in diatom numbers for all coatings, while the largest reduction of biofouling organisms was found on the fouling-release coating. Hunsucker et al. (2014) compared the anti-fouling performances of a copper-based SPC coating and an FRC, by applying them on two in-service cruise ships with the same cruise cycles. Greater richness of diatom species was found on the ship hull coated with the FRC system compared to the copper-based SPC coating. Schultz et al. (2015) compared the skin friction of three different FRC and an acrylic control surface after dynamic exposure to diatomaceous biofilms under a laboratory condition for 3 and 6 months. All surfaces showed significant increase in the skin friction after the dynamic exposure, while the extent differed among the different coatings. Yeginbayeva et al. (2019) investigated the biofouling growth on biocidal anti-fouling coatings and FRC. The FRC were applied on discs and deployed in the Saltholmen Marina, Sweden for one month. The classical fouling-release and reinforced silicone coating showed the same performance while the hybrid coating was found to be more hydrodynamically efficient (less drag increase). The biocidal coatings were exposed statically for four months. Interestingly, the biocidal coating surfaces with rough application showed smaller species richness and diversity compared to the biocidal coating surfaces with standard procedures.

2.2 PREDICTING THE IMPACT OF BIOFOULING MITIGATION MEASURES

2.2.1 REVIEW OF PREDICTION STUDIES FOR THE EFFECT OF BIOFOULING MITIGATION MEASURES

The prediction studies reviewed in Section 1.3 show the impacts of biofouling on the energy efficiency of ships and also provide insights into the effects of biofouling mitigation measures. For example, in the study of Song et al. (2020c), the differences between the delivered power

of different hull and propeller conditions (i.e. *clean/hull-clean/propeller*, *fouled-hull/clean-propeller*, *clean-hull/fouled-propeller* and *fouled-hull/fouled-propeller* conditions) can be used to estimate the economic and environmental impacts of hull and propeller cleaning.

Table 10 shows how the findings of Song et al. (2020c) can be used to estimate the effect of hull and propeller cleaning on a 230 m containership's delivered power (P_D) and thus its fuel consumption and GHG emissions.

Table 10 Effects of hull and propeller cleanings for a 230 m containership interpretated from the findings of Song et al. (2020c)

Condition before	Mitigation measure	Condition after	Effect of mitigation (%savings) ΔP_D: change in delivered power ΔFC: change in fuel consumption ΔGE: change in GHG emission
fouled-propeller	Hull cleaning	*fouled-propeller*	
*fouled surface with		*fouled surface with	
1. 1.25 mm barnacles with 10% coverage		1. 1.25 mm barnacles with 10% coverage	1. $\Delta P_D = \Delta FC = \Delta GE$ = -14%
2. 1.25 mm barnacles with 20% coverage		2. 1.25 mm barnacles with 20% coverage	2. $\Delta P_D = \Delta FC = \Delta GE$ = -21%
3. 1.25 mm barnacles with 40% coverage		3. 1.25 mm barnacles with 40% coverage	3. $\Delta P_D = \Delta FC = \Delta GE$ = -27%
4. 1.25 mm barnacles with 50% coverage		4. 1.25 mm barnacles with 50% coverage	4. $\Delta P_D = \Delta FC = \Delta GE$ = -29%
5. 2.5 mm barnacles with 10% coverage		5. 2.5 mm barnacles with 10% coverage	5. $\Delta P_D = \Delta FC = \Delta GE$ = -22%
6. 2.5 mm barnacles with 20% coverage		6. 2.5 mm barnacles with 20% coverage	6. $\Delta P_D = \Delta FC = \Delta GE$ = -23%
7. 2.5 mm barnacles with 40% coverage		7. 2.5 mm barnacles with 40% coverage	7. $\Delta P_D = \Delta FC = \Delta GE$ = -35%
8. 2.5 mm barnacles with 50% coverage		8. 2.5 mm barnacles with 50% coverage	8. $\Delta P_D = \Delta FC = \Delta GE$ = -36%
9. 5 mm barnacles with 10% coverage		9. 5 mm barnacles with 10% coverage	9. $\Delta P_D = \Delta FC = \Delta GE$ = -29%
10. 5 mm barnacles with 20% coverage		10. 5 mm barnacles with 20% coverage	10. $\Delta P_D = \Delta FC = \Delta GE$ = -37%
Fouled-hull/fouled-propeller	Propeller cleaning	*Fouled-hull/clean-propeller*	
*fouled surface with		*fouled surface with	
1. 1.25 mm barnacles with 10% coverage		1. 1.25 mm barnacles with 10% coverage	1. $\Delta PD = \Delta FC = \Delta GE$ = -6%
2. 1.25 mm barnacles with 20% coverage		2. 1.25 mm barnacles with 20% coverage	2. $\Delta PD = \Delta FC = \Delta GE$ = -7%
3. 1.25 mm barnacles with 40% coverage		3. 1.25 mm barnacles with 40% coverage	3. $\Delta PD = \Delta FC = \Delta GE$ = -10%
4. 1.25 mm barnacles with 50% coverage		4. 1.25 mm barnacles with 50% coverage	4. $\Delta PD = \Delta FC = \Delta GE$ = -10%
5. 2.5 mm barnacles with 10% coverage		5. 2.5 mm barnacles with 10% coverage	5. $\Delta PD = \Delta FC = \Delta GE$ = -9%
6. 2.5 mm barnacles with 20% coverage		6. 2.5 mm barnacles with 20% coverage	6. $\Delta PD = \Delta FC = \Delta GE$ = -10%
7. 2.5 mm barnacles with 40% coverage		7. 2.5 mm barnacles with 40% coverage	7. $\Delta PD = \Delta FC = \Delta GE$ = -13%
8. 2.5 mm barnacles with 50% coverage		8. 2.5 mm barnacles with 50% coverage	8. $\Delta PD = \Delta FC = \Delta GE$ = -13%
9. 5 mm barnacles with 10% coverage		9. 5 mm barnacles with 10% coverage	9. $\Delta PD = \Delta FC = \Delta GE$ = -10%
10. 5 mm barnacles with 20% coverage		10. 5 mm barnacles with 20% coverage	10. $\Delta PD = \Delta FC = \Delta GE$ = -13%

Table 10 Effects of hull and propeller cleanings for a 230 m containership interpretated from the findings of Song et al. (2020c) - continued

Condition before	Mitigation measure	Condition after	Effect of mitigation (%savings) ΔP_D: change in delivered power ΔFC: change in fuel consumption ΔGE: change in GHG emission
Fouled-hull/fouled-propeller	Hull cleaning and propeller cleaning	Clean-hull/clean-propeller	
*fouled surface with			
1. 1.25 mm barnacles with 10% coverage			1. $\Delta PD = \Delta FC = \Delta GE$ = -19%
2. 1.25 mm barnacles with 20% coverage			2. $\Delta PD = \Delta FC = \Delta GE$ = -26%
3. 1.25 mm barnacles with 40% coverage			3. $\Delta PD = \Delta FC = \Delta GE$ = -34%
4. 1.25 mm barnacles with 50% coverage			4. $\Delta PD = \Delta FC = \Delta GE$ = -36%
5. 2.5 mm barnacles with 10% coverage			5. $\Delta PD = \Delta FC = \Delta GE$ = -29%
6. 2.5 mm barnacles with 20% coverage			6. ΔPD= ΔFC= ΔGE = -35%
7. 2.5 mm barnacles with 40% coverage			7. $\Delta PD = \Delta FC = \Delta GE$ = -43%
8. 2.5 mm barnacles with 50% coverage			8. $\Delta PD = \Delta FC = \Delta GE$ = -44%
9. 5 mm barnacles with 10% coverage			9. $\Delta PD = \Delta FC = \Delta GE$ = -35%
10. 5 mm barnacles with 20% coverage			10. $\Delta PD = \Delta FC = \Delta GE$ = -45%
Fouled-hull/clean-propeller	Hull cleaning	Clean-hull/clean-propeller	
*fouled surface with			
1. 1.25 mm barnacles with 10% coverage			1. $\Delta PD = \Delta FC = \Delta GE$ = -14%
2. 1.25 mm barnacles with 20% coverage			2. $\Delta PD = \Delta FC = \Delta GE$ = -21%
3. 1.25 mm barnacles with 40% coverage			3. $\Delta PD = \Delta FC = \Delta GE$ = -27%
4. 1.25 mm barnacles with 50% coverage			4. $\Delta PD = \Delta FC = \Delta GE$ = -29%
5. 2.5 mm barnacles with 10% coverage			5. $\Delta PD = \Delta FC = \Delta GE$ = -22%
6. 2.5 mm barnacles with 20% coverage			6. $\Delta PD = \Delta FC = \Delta GE$ = -28%
7. 2.5 mm barnacles with 40% coverage			7. $\Delta PD = \Delta FC = \Delta GE$ = -35%
8. 2.5 mm barnacles with 50% coverage			8. $\Delta PD = \Delta FC = \Delta GE$ = -36%
9. 5 mm barnacles with 10% coverage			9. $\Delta PD = \Delta FC = \Delta GE$ = -29%
10. 5 mm barnacles with 20% coverage			10. $\Delta PD = \Delta FC = \Delta GE$ = -37%
Clean-hull/fouled-propeller	Propeller cleaning	Clean-hull/clean-propeller	
*fouled surface with			
1. 1.25 mm barnacles with 10% coverage			1. $\Delta PD = \Delta FC = \Delta GE$ = -6%
2. 1.25 mm barnacles with 20% coverage			2. $\Delta PD = \Delta FC = \Delta GE$ = -8%
3. 1.25 mm barnacles with 40% coverage			3. $\Delta PD = \Delta FC = \Delta GE$ = -12%
4. 1.25 mm barnacles with 50% coverage			4. $\Delta PD = \Delta FC = \Delta GE$ = -12%
5. 2.5 mm barnacles with 10% coverage			5. ΔPD= ΔFC= ΔGE = -9%
6. 2.5 mm barnacles with 20% coverage			6. $\Delta PD = \Delta FC = \Delta GE$ = -12%
7. 2.5 mm barnacles with 40% coverage			7. $\Delta PD = \Delta FC = \Delta GE$ = -15%
8. 2.5 mm barnacles with 50% coverage			8. $\Delta PD = \Delta FC = \Delta GE$ = -16%
9. 5 mm barnacles with 10% coverage			9. $\Delta PD = \Delta FC = \Delta GE$ = -12%
10. 5 mm barnacles with 20% coverage			10. $\Delta PD = \Delta FC = \Delta GE$ = -16%

As shown in Table 10 (see page 31), predicting the impact of biofouling on ships' hydrodynamic performance provides insights of the effects of partial and full hull cleanings. However, evaluating the economic and environmental impacts of different anti-fouling strategies may not be accurate unless the time-dependent aspects are considered throughout the ships' operation between dry-dock intervals.

Uzun et al. (2019b) developed a representative time-dependent biofouling growth model which can predict the biofouling accumulation of slime, non-shell and calcareous type biofouling organisms on a typical SPC-type anti-fouling coating. This model considers the cumulative idle time of a ship, including port stays, as well as the seawater temperature. Using this model, Uzun et al. (2019b) predicted the biofouling growth on a 176 m tanker during a one-year long operation and the impact on the ship's energy efficiency was estimated using the similarity law scaling method of Granville (1958).

2.2.2 ADDITIONAL RESEARCH

The time-based method enables the assessment of the impacts of different anti-fouling strategies for a ship between drydocking periods. This section employs the time-based approach to investigate the economic and environmental impacts of different anti-fouling scenarios applied to a commercial vessel over an operation period of 5 years.

Table 11 shows the principal characteristics and anti-fouling scenarios of the target vessel used for the time based assessment. The principal particulars of a 179 m bulk carrier were adopted as used by Uzun et al. (2019 a), while a virtual operational profile of the bulk carrier was created for a 5-year operation period in two different regions: Equatorial and Mediterranean. Figure 6 (see next page) shows the cumulative idle time of the vessel during the 5-year operation. The time-dependent biofouling growth model of Uzun et al. (2019b) was adopted to predict the biofouling growth on the bulk carrier with different anti-fouling scenarios over the 5-year operation in the two operational regions. It is of note that the method of Uzun et al. (2019b) takes into account the seawater temperature of the operating regions to calculate the growth rate of biofouling accumulation, and temperatures of 25°C and 17°C were used for the Equatorial and Mediterranean regions, respectively.

Table 11 Principal particulars and operational profile of the target vessel

Vessel type	Bulk carrier
Deadweight	40,000 t
Length	179 m
Breadth	28 m
Design draft	10.6 m
Wetted surface area	7,350 m^2
Coating	self-polishing copolymer (SPC)
Speed	14 knots
Engine power	6.6 kW
Fuel type	Bunker C oil
Fuel consumption (without biofouling)	20.4 ton/day
Operating region (average seawater temp.)	Equatorial region (25°C) and Mediterranean region (17°C)
Operation period	5 years
Idle time including port stays in 5-year operation	556 days
Operating days in 5-year operation	1,271 days

Figure 6 Cumulative idle time (including port stays) of the bulk carrier during the 5-year operation

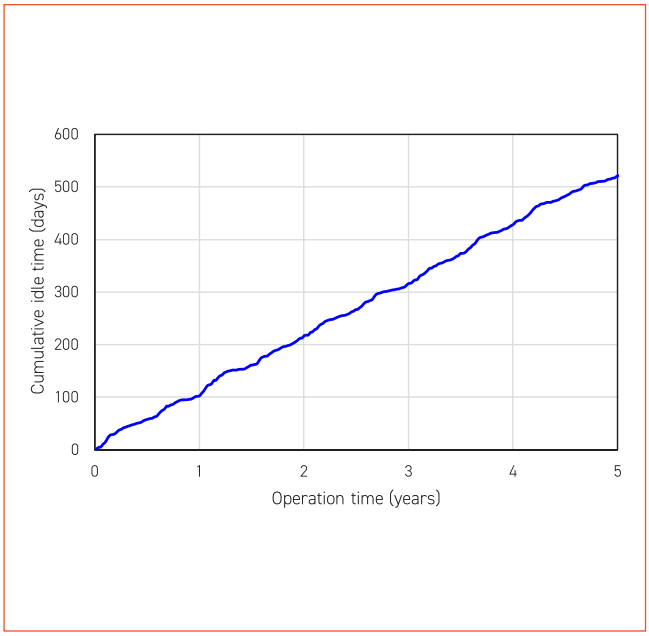

Figure 7 Growth of values on the hull under the No cleaning scenario

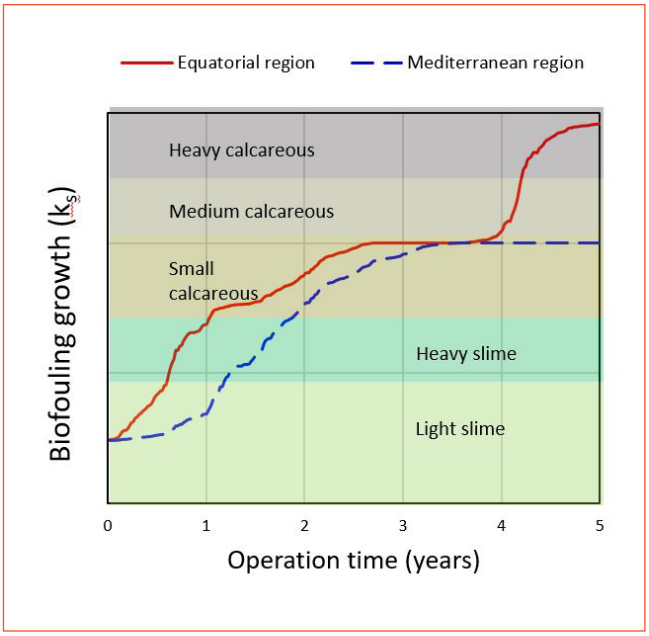

Figure 7 shows the biofouling growth on the hull of the bulk carrier over the 5-year operation in the two different operational regions, which is represented by the k_s values calculated using the time-dependent biofouling growth model of Uzun et al. (2019b) together with the operation profile of the bulk carrier. It is of note that no anti-fouling activity is considered in this example apart from the use of SPC anti-fouling coating.

In the case of the Equatorial region, biofouling on the hull reaches the heavy slime level at the end of the first year of operation, and reaches the *small calcareous fouling* level during the second year of operation. Biofouling growth accelerates after 4 years of operation and enters the *medium calcareous fouling* level, eventually reaching *heavy calcareous fouling* for the rest of the operational period. On the other hand, biofouling growth is relatively slow for the Mediterranean case. Biofouling growth enters the *Heavy slime* level during the second year of operation and increases to *small calcareous fouling* after two years of operation, when growth is relatively interrupted and remains at that level for the rest of the operational period.

It is of note that these results only represent the biofouling growth of these specific examples of the bulk carrier and can change significantly depending on the operational profile, operating region, the type of anti-fouling coatings, etc.

Table 12 (see next page) shows the seven anti-fouling scenarios, while the assumptions used for the scenarios are described in Table 13 (see page 36). It is of note that the hull is assumed to be coated with a typical SPC coating in all scenarios. Under the *No cleaning* scenario, neither hull nor propeller cleaning is performed. Under the *Hull cleaning* scenario, the hull is cleaned at year 3 and year 4 and the propeller is not cleaned, whereas both the hull and propeller are cleaned under the *Hull & propeller cleaning* scenario at year 3 and year 4. Under the Ultrasonic anti-fouling for propeller scenario, the ultrasonic anti-fouling system is used for the propeller, while hull cleanings are used together at year 3 and year 4 with the ultrasonic anti-fouling system under the *Hull cleaning + Ultrasonic anti-fouling for propeller* scenario. Under these scenarios, the propeller is assumed to be kept as always clean owing to the anti-fouling performance of the ultrasonic system. The *Proactive cleaning (hull & propeller)* scenario involves frequent hull and propeller cleanings before the fouling level moves to the macrofouling stage. It is of note that the practice of proactive cleaning (e.g. timing of first cleaning, frequency) can be altered based on the needs of individual ships. Furthermore, an ideal but unrealistic condition, *Always* clean scenario, was added to give a reference where it is assumed the hull and propeller are always kept clean without any biofouling accumulation throughout the entire period of operation.

Table 12 Anti-fouling scenarios used for the time-based assessment

Anti-fouling scenario	Hull coating	Hull related measures	Propeller related measures	Assumptions used (see Table 14, page 40)
No cleaning	SPC AF coating	No	No	Assumption 1 Assumption 2 Assumption 4
Hull cleaning	SPC AF coating	Hull cleaning after 3 & 4 years	No	Assumption 1 Assumption 2 Assumption 3 Assumption 4
Propeller cleaning	SPC AF coating	No	Propeller cleaning after 3 & 4 years	Assumption 1 Assumption 2 Assumption 4 Assumption 5
Hull & propeller cleaning	SPC AF coating	Hull cleaning after 3 & 4 years	Propeller cleaning after 3 & 4 years	Assumption 1 Assumption 2 Assumption 3 Assumption 4 Assumption 5
Ultrasonic anti-fouling for propeller	SPC AF coating	No	Ultrasonic anti-fouling system for propeller	Assumption 1 Assumption 2 Assumption 6
Hull cleaning + Ultrasonic anti-fouling for propeller	SPC AF coating	Hull cleaning after 3 & 4 years	Ultrasonic anti-fouling system for propeller	Assumption 1 Assumption 2 Assumption 6
Proactive cleaning (hull & propeller)	SPC AF coating	Hull cleaning after 1 ½, 2, 2 ½, 3, 3 ½, 4, 4 ½ years	Propeller cleaning after 1 ½, 2, 2 ½, 3, 3 ½, 4, 4 ½ years	Assumption 1 Assumption 2 Assumption 3 Assumption 4 Assumption 6
Always clean	SPC AF coating	Always kept clean	Always kept clean	Assumption 1 Assumption 7

For the prediction of time-dependent biofouling growth of these anti-fouling scenarios, several assumptions were made as shown in Table 13 (see next page). For all scenarios (except Always clean), it was assumed that the biofouling growth on the hull/propeller follows the time-dependent biofouling growth model, and the surfaces come back to slightly damaged hull/propeller surfaces after a cleaning. When the ultrasonic anti-fouling system is used for the propeller, the surface was assumed to be free of biofouling. The resistance of the ship with no hull fouling was estimated based on the empirical method of Holtrop et al. (1982). The added resistance, ΔC_F, due to hull fouling was predicted based on the similarity law scaling method of Granville (1958), while the propeller efficiency loss due to the propeller fouling was estimated based on the CFD simulation results of Farkas et al. (2021).

Table 13 Assumptions made for the anti-fouling scenarios in the time-based approach

Assumptions	Description
Assumption 1	1. Ship resistance coefficients can be calculated following the method of Holtrop et al. (1982). 2. Total resistance of a fouled hull can be calculated as, $C_{T,r}=C_{Ts}+\Delta C_F$, where ΔC_F is the added resistance due to hull fouling calculated from Granville's extrapolation method.
Assumption 2	1. The biofouling growths on the hull follow the time-dependent biofouling growth model of Uzun et al. (2019b). 2. The entire hull is fouled homogeneously. 3. The hull surface for the unfouled (clean) hull is a typical as applied AF coating surface
Assumption 3	1. After a hull cleaning, the hull surface becomes a slightly deteriorated AF coating (i.e. k_s=40 μm).
Assumption 4	1. The biofouling growths on the propeller follow the time-dependent biofouling growth model of Uzun et al. (2019b). 2. The entire propeller is fouled homogeneously. 3. Propeller efficiency loss due to propeller fouling can be estimated following the results of Farkas et al. (2021).
Assumption 5	1. After a propeller cleaning, the propeller surface becomes a slightly damaged propeller surface (i.e. k_s=40 μm).
Assumption 6	1. Ultrasonic anti-fouling system prevents biofouling growth on the propeller (i.e. propeller is always clean). 2. Ultrasonic anti-fouling system is continuously active for the lifetime.
Assumption 7	1. *Always clean* scenario is an ideal and unrealistic condition added as a reference. 2. Under this scenario, the hull and propeller are assumed to be always clean with no biofouling.

2.2.3 RESULT: EQUATORIAL REGION

Figure 8 (see page 37) shows the added frictional resistance coefficients, ΔC_F, of the bulk carrier with different anti-fouling strategies over the 5-year operation in the Equatorial region. The ΔC_F values were calculated using the similarity law scaling method of Granville (1958) based on the biofouling growth prediction with different anti-fouling strategies. As expected, the *No cleaning, Propeller cleaning and Ultrasonic anti-fouling for propeller* scenarios showed the largest ΔC_F values, while the *Hull cleaning, Hull & propeller cleaning, Hull cleaning + Ultrasonic anti-fouling for propeller, and Proactive cleaning (hull & propeller)* scenarios showed significant reductions in the ΔC_F after the hull cleanings compared to the No cleaning scenario. The ΔC_F values of the Proactive cleaning scenario showed smaller increases compared to other hull cleaning scenarios owing to the frequent cleanings. It is of note that although there is no increase in the ΔC_F of the *Always clean* scenario, there is small and constant ΔC_F due to the hull roughness of the applied AF coating.

Figure 9 (see page 37) shows the propeller efficiency loss of the bulk carrier with different anti-fouling strategies over the 5 year operation. The efficiency loss was estimated based on the time-based biofouling growth prediction and the findings of the CFD prediction study of Farkas et al. (2021). When no mitigating measure is used for the propeller, the efficiencies drop by 13%. The propeller efficiency recovers after a propeller cleaning is applied. The efficiencies under the *Propeller cleaning* and *Hull & Propeller cleaning* scenarios drop by 8% before the first cleaning is conducted and remained within 6% for the rest of the operation time. The propeller efficiency of the *Proactive cleaning (hull & propeller)* scenario drops by 3% before the first cleaning and the efficiency loss remained within 2.5% for the rest of the operation time owing to the frequent cleanings. On the other hand, the *Ultrasonic anti-fouling for propeller and Hull cleaning + Ultrasonic anti-fouling for propeller* scenarios showed no efficiency drop with the ultrasonic anti-fouling system activated for the 5-year operation time

Figure 8 added frictional resistance of the bulk carrier with different anti-fouling strategies over the 5-year operation (Equatorial region)

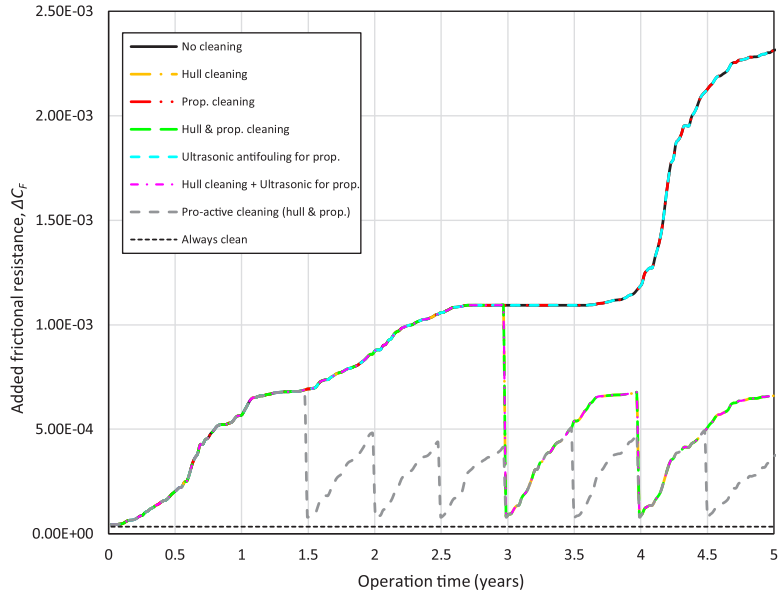

Figure 9 Propeller efficiency loss of the bulk carrier with different anti-fouling strategies over the 5-year operation (Equatorial region)

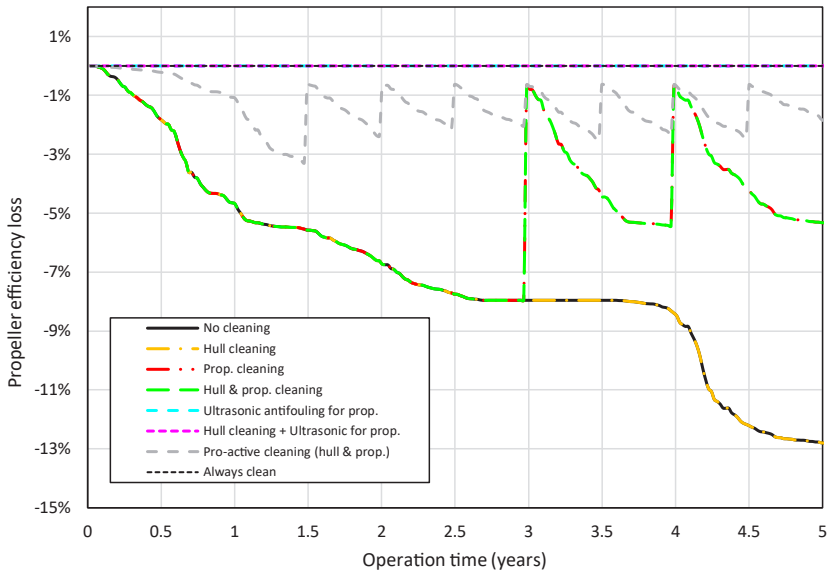

Figure 10 Required engine power increase of the bulk carrier at the design speed with different anti-fouling strategies over the 5-year operation (Equatorial region)

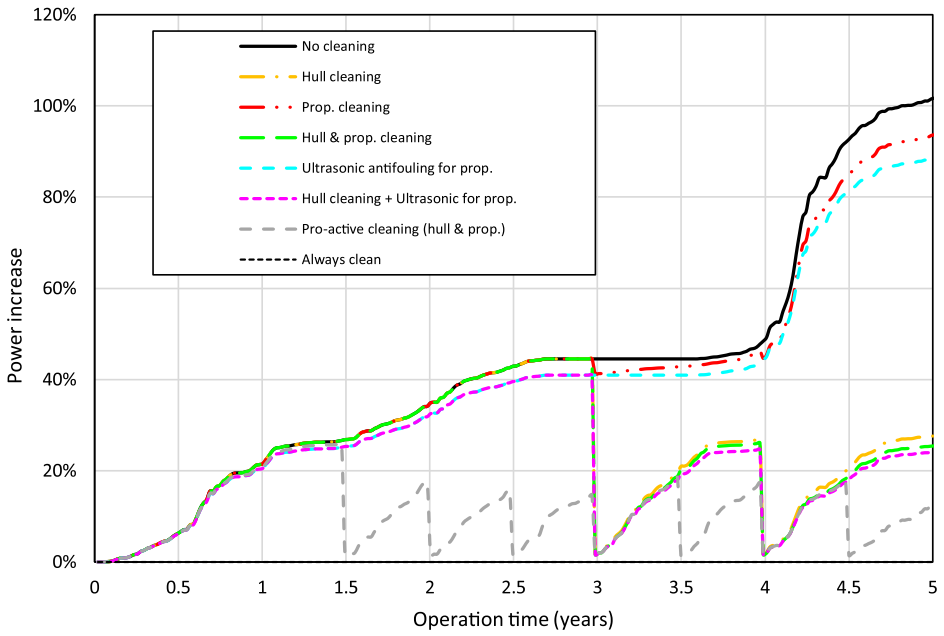

Figure 10 shows the % increases in the required engine power of the bulk carrier to maintain the design speed. As expected, the No cleaning scenario shows the most severe increase in the engine power up to more than 100%, while the *Propeller cleaning and Ultrasonic anti-fouling for propeller* scenarios show slightly lower increases. The *Hull cleaning, Hull & propeller cleaning and hull Cleaning + Ultrasonic anti-fouling for propeller* scenarios showed similar trends with the power increases up to around 40%. The *Proactive cleaning (hull & propeller)* scenario showed the best performances owing to the frequent hull and propeller cleanings.

Based on the predictions of the engine power, the daily fuel consumption of the bulk carrier was estimated as well as the cumulative fuel consumption over the 5-year operation. Figure 11 (see page 39) compares the cumulative fuel consumption of the bulk carrier with different anti-fouling scenarios. The differences in the cumulative fuel consumption between the different anti-fouling scenarios become more pronounced as the operation time is prolonged. The no *cleaning* scenario shows more than 51,000 tonnes of total fuel consumption over the 5-year operation. The fuel consumption can be reduced to below 45,000 tonnes if the hull is cleaned after 3 and 5 years of operations, while it can be further reduced to 40,000 tonnes with the proactive cleaning strategy.

Based on the predicted fuel consumption of the bulk carrier for the 5-year operation, the total fuel costs with different scenarios were estimated. Figure 12 (see page 39) shows the total fuel cost of the bulk carrier under the different anti-fouling scenarios. Note that fuel price of $572.5 per metric ton of FO fuel was used for the calculation.

The result shows that the total fuel cost of the bulk carrier over the 5-year operation can be up to $29.65 million under the no cleaning scenario, and it is reduced to $25.64 million, $29.27 million and $25.55 million under the *hull cleaning, propeller cleaning, and hull & propeller cleaning scenarios*, respectively. On the other hand, the *Ultrasonic anti-fouling for propeller and Hull cleaning + Ultrasonic anti-fouling for propeller* scenarios showed total fuel costs of $28.85 million and $25.27 million, respectively. Finally, the total fuel cost can be reduced to $23.07 million under the *Proactive cleaning* (*hull & propeller*) scenario. Table 14 (see page 40) compares the differences in the total fuel cost between different anti-fouling scenarios.

Figure 11 Cumulative fuel consumption of the bulk carrier at the design speed with different anti-fouling strategies over the 5-year operation (Equatorial region)

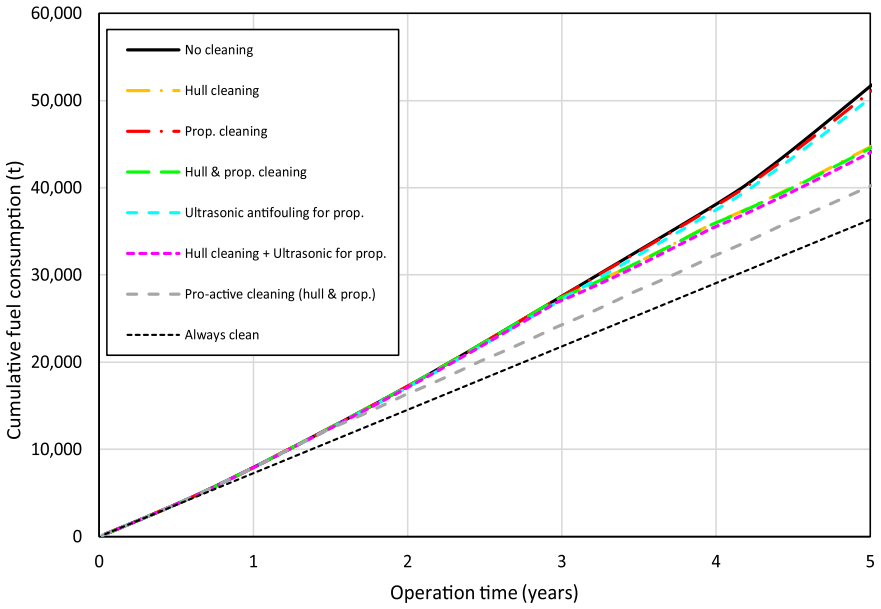

Figure 12 Total fuel cost of the bulk carrier over the 5-year operation with different anti-fouling strategies (Equatorial region)

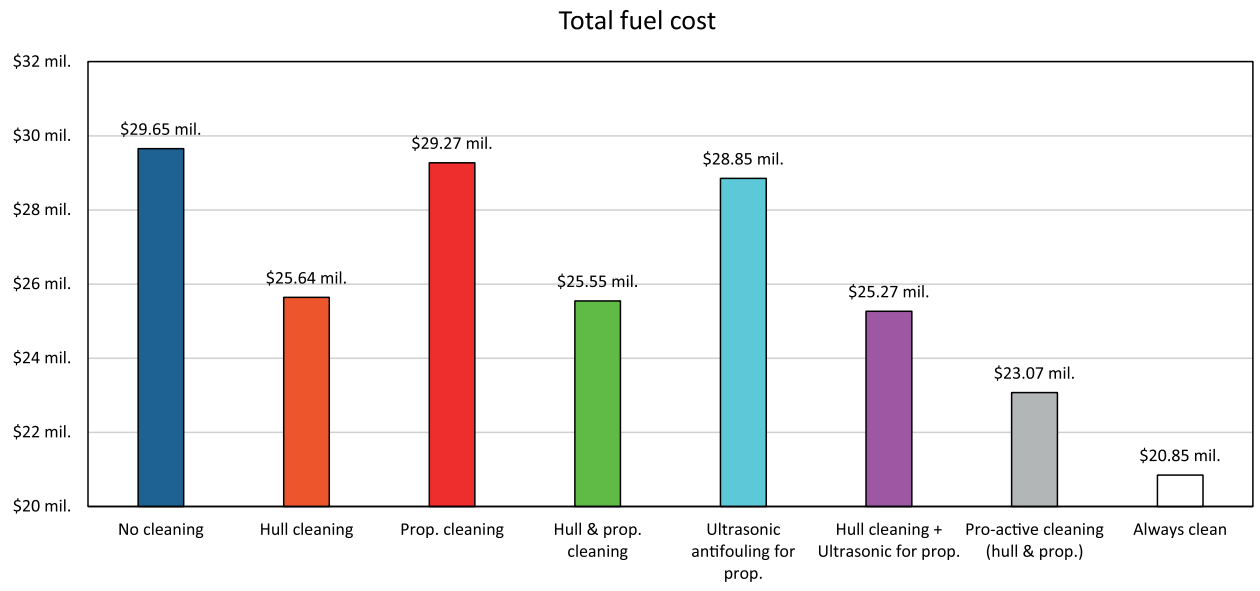

Table 14 Difference in the total fuel cost with different anti-fouling scenarios (Equatorial region)

	Total fuel cost	Difference compared to *"No cleaning"*	%	Difference compared to *"Always clean"*	%
No cleaning	$29.65 mil.	N/A	N/A	$8.81 mil.	42%
Hull cleaning	$25.64 mil.	-$4.01 mil.	-14%	$4.79 mil.	23%
Propeller cleaning	$29.27 mil.	-$0.38 mil.	-1%	$8.43 mil.	40%
Hull & propeller cleaning	$25.55 mil.	-$4.11 mil.	-14%	$4.70 mil.	23%
Ultrasonic anti-fouling for propeller	$28.85 mil.	-$0.80 mil.	-3%	$8.00 mil.	38%
Hull cleaning + Ultrasonic anti-fouling for propeller	$25.27 mil.	-$4.39 mil.	-15%	$4.42 mil.	21%
Proactive cleaning (hull & propeller)	$23.07 mil.	-$6.58 mil.	-22%	$2.22 mil.	11%
Always clean	$20.85 mil.	-$8.81 mil.	-30%	N/A	N/A

Figure 13 Total CO_2 emission from the bulk carrier over the 5-year operation with different anti-fouling strategies (Equatorial region)

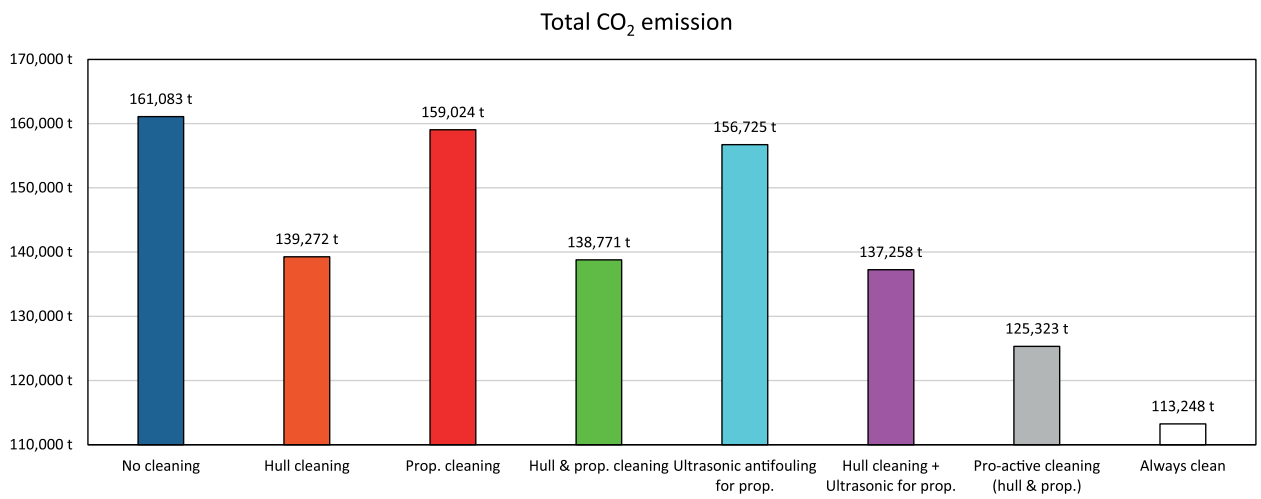

It is worth noting that the fouling level of the no cleaning scenario reaches to the *heavy calcareous fouling*. The propeller-only mitigation scenarios (i.e. *propeller cleaning and Ultrasonic anti-fouling for propeller*) do not show significant differences compared to the *no cleaning* scenario because no mitigation is used for the hull fouling other than the SPC AF coating as the case of *no cleaning* scenario. It is worth mentioning that the fuel cost differences between the scenarios listed in Table 12 (see page 35) are not as evident as the results of the prediction studies in the literature (see **ANNEX G**) and it can be attributed to the fact that the results in Table 14 (see page 40) are showing the cumulative differences between the scenarios that started from the same clean hull/propeller condition.

Based on the predicted fuel consumption, the total CO_2 emissions of the bulk carrier with different scenarios were estimated. Figure 13 (see page 40) shows the estimated total CO_2 emission of the bulk carrier over the 5-year operation under the different anti-fouling scenarios. The *no cleaning* scenario showed the largest CO_2 emission, 161,083 tonnes, while this can be reduced to 139,272, 159,024, and 138,771 tonnes under the *hull cleaning* and *propeller cleaning,* and *hull & propeller cleaning* scenarios, respectively. On the other hand, the *Ultrasonic anti-fouling for propeller* and *Hull cleaning + Ultrasonic anti-fouling for propeller* scenarios showed total CO_2 emissions of 156,725 and 137,258 tonnes, respectively. Finally, the total CO_2 emission can be reduced to 123,323 tonnes with the proactive cleaning strategy. Table 15 (see next page) compares the differences in the total CO_2 emissions between different anti-fouling scenarios.

2.2.4 RESULT: MEDITERRANEAN REGION

Figure 14 (see next page) shows the added frictional resistance coefficients, ΔC_F, of the bulk carrier with different anti-fouling strategies over the 5-year operation. The ΔC_F values were calculated using the similarity law scaling method of Granville (1958) based on the biofouling growth prediction with different anti-fouling strategies. As expected, the *No cleaning, Propeller cleaning* and *Ultrasonic anti-fouling for propeller* scenarios showed the largest ΔC_F values, while the *Hull cleaning, Hull & propeller cleaning, Hull cleaning + Ultrasonic anti-fouling for propeller,* and *Proactive cleaning (hull & propeller)* scenarios showed significant reductions in the ΔC_F after the hull cleanings compared to compared to the *No cleaning* scenario. The ΔC_F values of the *Proactive cleaning* scenario showed smaller increases compared to other hull cleaning scenarios owing to the frequent cleanings. It is of note that although there is no increase in the $\Delta C_F$of the *Always clean* scenario, there is small and constant ΔC_F due to the hull roughness of the applied AF coating.

Figure 15 (see page 43) shows the propeller efficiency loss of the bulk carrier with different anti-fouling strategies over the 5 year operation. The efficiency loss was estimated based on the time-based biofouling growth prediction and the findings of the CFD prediction study of Farkas et al. (2021). When no mitigating measure is used for the propeller, the efficiencies drop by 8%. The propeller efficiency recovers after a propeller cleaning is applied. The efficiencies under the *Propeller cleaning* and *Hull & Propeller cleaning* scenarios drop by 7.5% before the first cleaning is conducted and remained within 5% for the rest of the operation time. The propeller efficiency of the *Proactive cleaning* (*hull & propeller*) scenario drops by 3% before the first cleaning and the efficiency loss remained within 2.5% for the rest of the operation time owing to the frequent cleanings. On the other hand, the *Ultrasonic anti-fouling for propeller and Hull cleaning + Ultrasonic anti-fouling for propeller* scenarios showed no efficiency drop with the ultrasonic anti-fouling system activated for the 5-year operation time.

Figure 16 (see page 43) shows the % increases in the required engine power of the bulk carrier to maintain the design speed. As expected, the *No cleaning* scenario shows the most severe increase in the engine power up to 45%, while the *Propeller cleaning and Ultrasonic anti-fouling for propeller* scenarios show slightly milder increases. The *Hull cleaning, Hull & propeller cleaning* and *hull Cleaning + Ultrasonic anti-fouling for propeller* scenarios showed similar trends with the power increases up to around 20%. The *Proactive cleaning (hull & propeller)* scenario showed the best performances owing to the frequent hull and propeller cleanings.

Based on the predictions of the engine power, the daily fuel consumption of the bulk carrier was estimated as well as the cumulative fuel consumption over the 5-year operation. Figure 17 (see page 44) compares the cumulative fuel consumption of the bulk carrier with different anti-fouling scenarios. The differences in the cumulative fuel consumption between the different anti-fouling scenarios become more pronounced as the operation time is prolonged. The *no cleaning* scenario shows more than 46,000 tonnes of total fuel consumption over the 5-year operation. The fuel consumption can be reduced to below 42,000 tonnes if the hull is cleaned after 3 and 5 years of operations, while it can be further reduced below 38,000 tonnes with the proactive cleaning strategy.

Table 15 Difference in the total CO_2 emission with different anti-fouling scenarios (Equatorial region)

	Total CO_2 emission	Difference compared to *"No cleaning"*	%	Difference compared to *"Always clean"*	%
No cleaning	161083 t	N/A	N/A	47835 t	42%
Hull cleaning	139272 t	-21810 t	-14%	26025 t	23%
Propeller cleaning	159024 t	-2058 t	-1%	45777 t	40%
Hull & prop. cleaning	138771 t	-22312 t	-14%	25523 t	23%
Ultrasonic anti-fouling for prop.	156725 t	-4358 t	-3%	43477 t	38%
Hull cleaning + Ultrasonic anti-fouling for propeller	137258 t	-23825 t	-15%	24011 t	21%
Proactive cleaning (hull & propeller)	125323 t	-35760 t	-22%	12075 t	11%
Always clean	113248 t	-47835 t	-30%	N/A	N/A

Figure 14 added frictional resistance of the bulk carrier with different anti-fouling strategies over the 5-year operation (Mediterranean region)

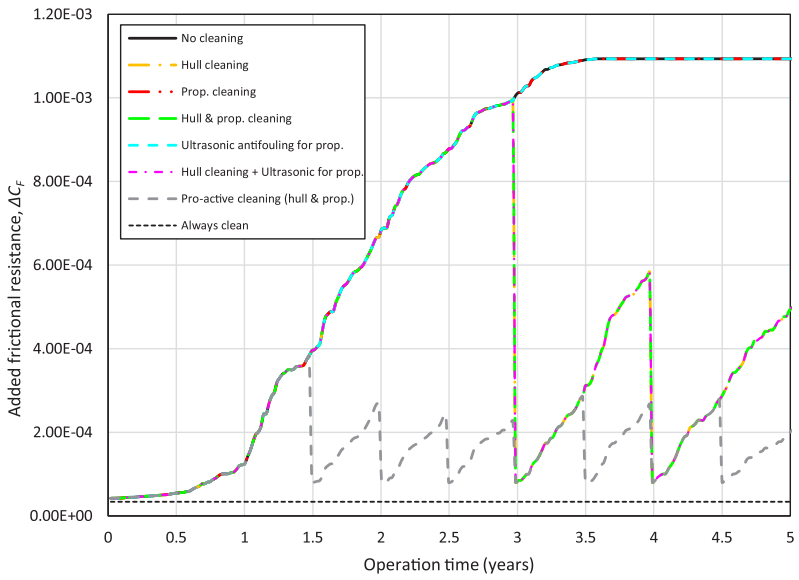

Figure 15 Propeller efficiency loss of the bulk carrier with different anti-fouling strategies over the 5-year operation (Mediterranean region)

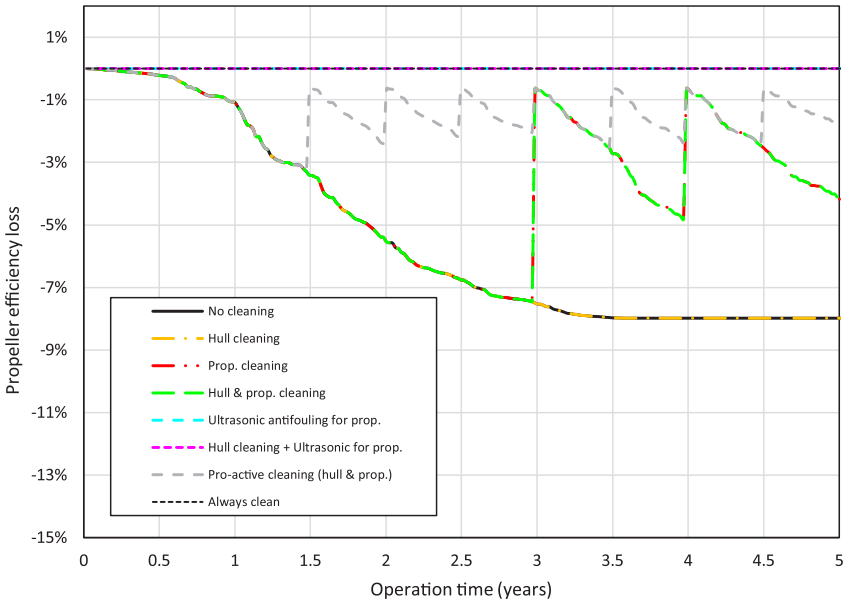

Figure 16 Required engine power increase of the bulk carrier at the design speed with different anti-fouling strategies over the 5-year operation (Mediterranean region)

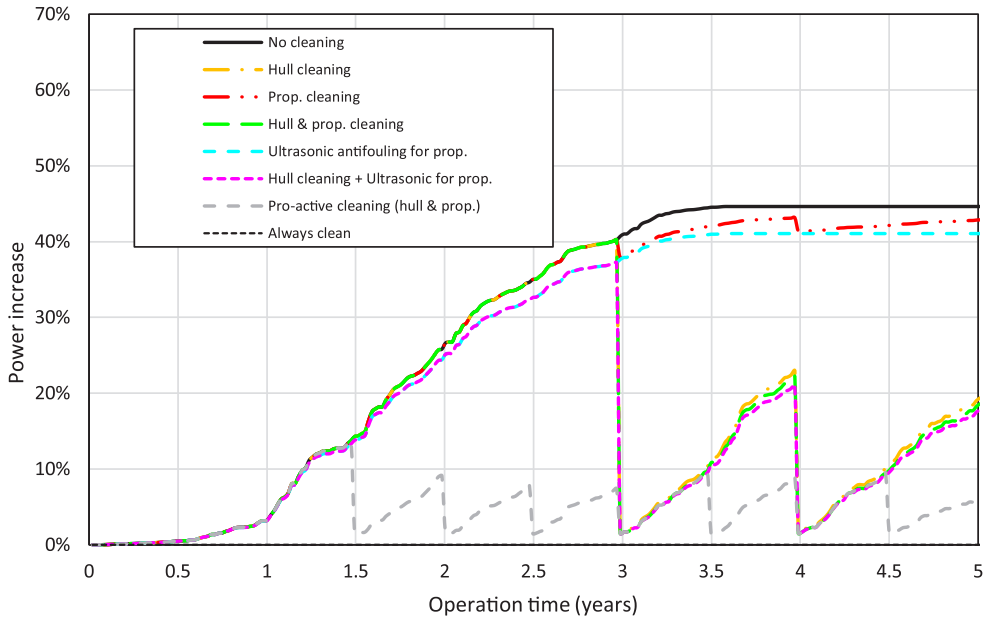

Figure 17 Cumulative fuel consumption of the bulk carrier at the design speed with different anti-fouling strategies over the 5-year operation (Mediterranean region)

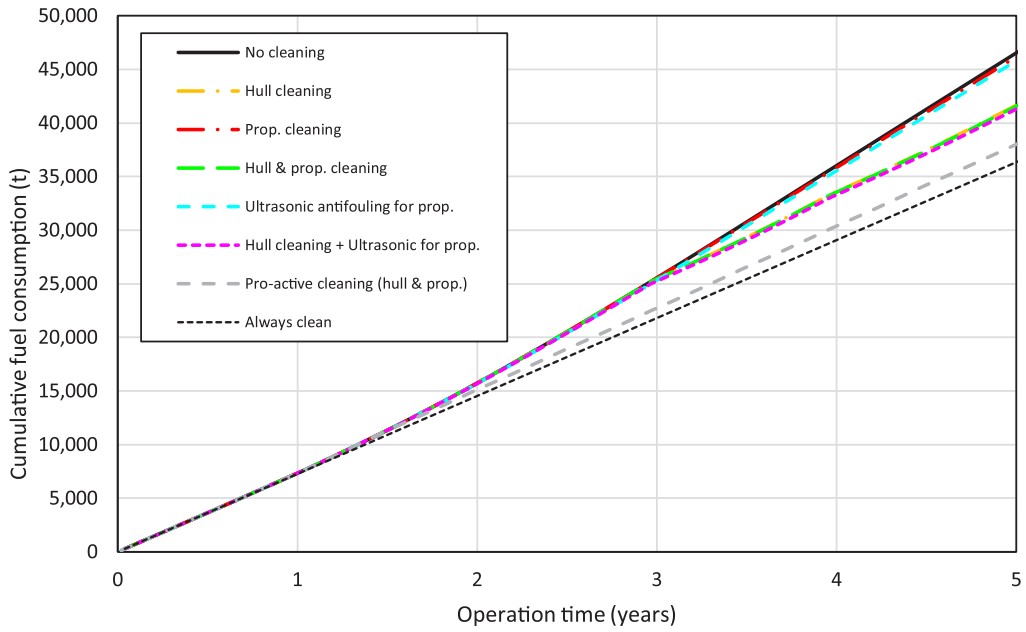

Based on the predicted fuel consumption of the bulk carrier for the 5-year operation, the total fuel costs with different scenarios were estimated. Figure 18 (see page 45) shows the total fuel cost of the bulk carrier under the different anti-fouling scenarios. Note that fuel price of 572.5 USD per metric ton of FO fuel was used for the calculation. It is worth noting that the fouling level of the *no cleaning* scenario reaches around k_s=1,000 which is equivalent to *small calcareous fouling or weed*. The propeller-only mitigation scenarios (i.e. *propeller cleaning and Ultrasonic anti-fouling for propeller*) do not show significant differences compared to the *no cleaning* scenario because no mitigation is used for the hull fouling other than the AF coating as the case of *no cleaning* scenario.

The result shows that the total fuel cost of the bulk carrier over the 5-year operation can be up to $26.70 million under the *no cleaning* scenario, and it is reduced to $23.89 million, $26.50 million and $23.85 million under the *hull cleaning, propeller cleaning*, and *hull & propeller cleaning* scenarios, respectively. On the other hand, the *Ultrasonic anti-fouling for propeller* and *Hull cleaning + Ultrasonic anti-fouling for propeller* scenarios showed total fuel costs of $26.28 million and $23.70 million, respectively. Finally, the total fuel cost can be reduced to $21.80 million under the *Proactive cleaning* (*hull & propeller*) scenario. Table 16 (see page 45) compares the differences in the total fuel cost between different anti-fouling scenarios.

Based on the predicted fuel consumption, the total CO_2 emissions of the bulk carrier with different scenarios were estimated. Figure 19 (see page 46) shows the estimated total CO_2 emission of the bulk carrier over the 5-year operation under the different anti-fouling scenarios. The *no cleaning* scenario showed the largest CO_2 emission, 145,043 tonnes, while this can be reduced to 119,798, 143,936, and 129,549 tonnes under the *hull cleaning* and *propeller cleaning,* and *hull & propeller cleaning* scenarios, respectively. On the other hand, the *Ultrasonic anti-fouling for propeller* and *Hull cleaning + Ultrasonic anti-fouling for propeller* scenarios showed total CO_2 emissions of 142,754 and 128,720 tonnes, respectively. Finally, the total CO_2 emission can be reduced to 113,248 tonnes with the proactive cleaning strategy. Table 17 (see page 46) compares the differences in the total CO_2 emissions between different anti-fouling scenarios.

Figure 18 Total fuel cost of the bulk carrier over the 5-year operation with different anti-fouling strategies (Mediterranean region)

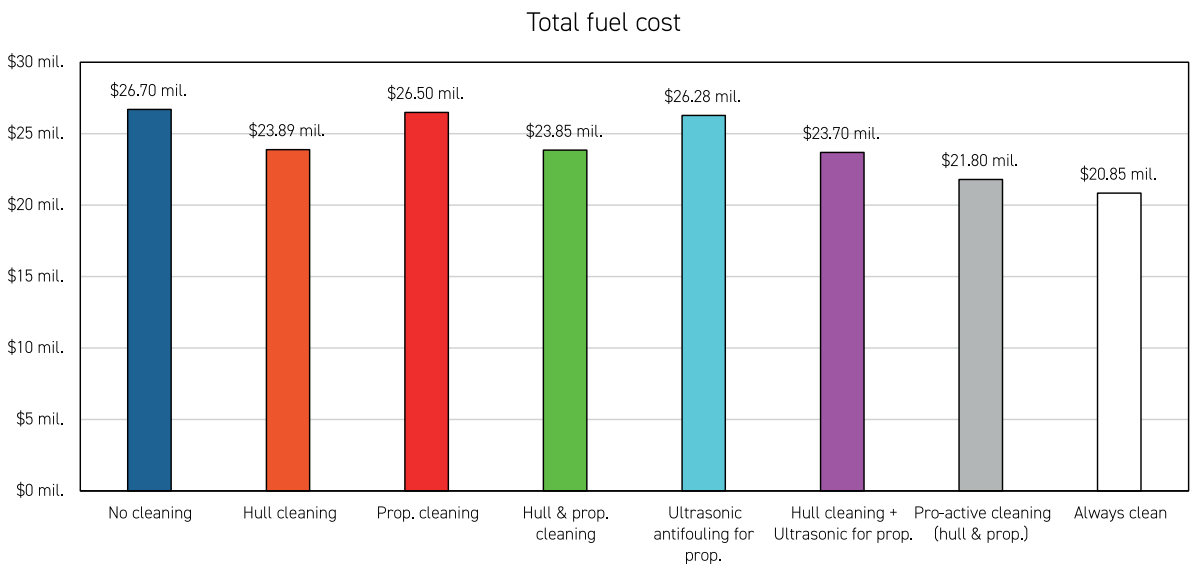

Table 16 Difference in the total fuel cost with different anti-fouling scenarios (Mediterranean region)

	Total fuel cost	Difference compared to *"No cleaning"*	%	Difference compared to *"Always clean"*	%
No cleaning	$26.70 mil.	N/A	N/A	$5.85 mil.	28%
Hull cleaning	$23.89 mil.	-$2.81 mil.	-11%	$3.05 mil.	15%
Propeller cleaning	$26.50 mil.	-$0.20 mil.	-1%	$5.65 mil.	27%
Hull & propeller cleaning	$23.85 mil.	-$2.85 mil.	-11%	$3.00 mil.	14%
Ultrasonic anti-fouling for propeller	$26.28 mil.	-$0.42 mil.	-2%	$5.43 mil.	26%
Hull cleaning + Ultrasonic anti-fouling for propeller	$23.70 mil.	-$3.00 mil.	-11%	$2.85 mil.	14%
Proactive cleaning (hull & propeller)	$21.80 mil.	-$4.90 mil.	-18%	$0.95 mil.	5%
Always clean	$20.85 mil.	-$5.85 mil.	-22%	N/A	N/A

Figure 19 Total CO_2 emission from the bulk carrier over the 5-year operation with different anti-fouling strategies (Mediterranean region)

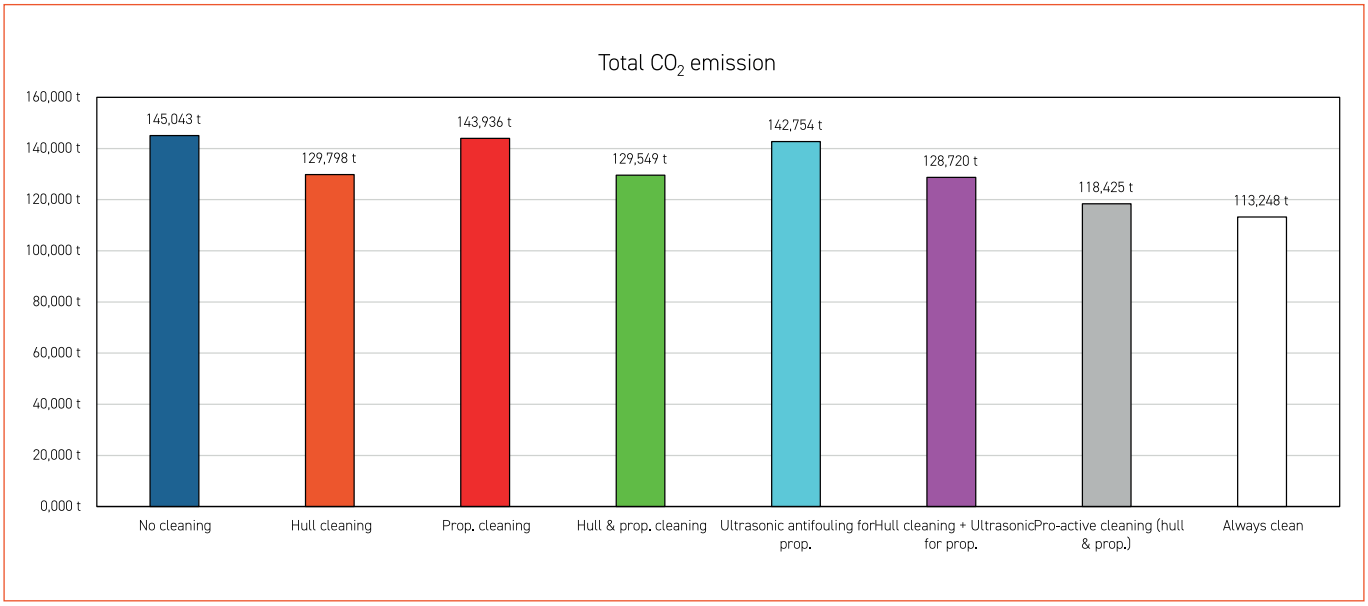

Table 17 Difference in the total CO_2 emission with different anti-fouling scenarios (Mediterranean region)

	Total CO_2 emission	Difference compared to *"No cleaning"*	%	Difference compared to *"Always clean"*	%
No cleaning	145,043 t	N/A	N/A	31,796 t	28%
Hull cleaning	129,798 t	-15,245 t	-11%	16,551 t	15%
Propeller cleaning	143,936 t	-1,107 t	-1%	30,688 t	27%
Hull & prop. cleaning	129,549 t	-15,494 t	-11%	16,301 t	14%
Ultrasonic anti-fouling for prop.	142,754 t	-2,289 t	-2%	29,506 t	26%
Hull cleaning + Ultrasonic anti-fouling for propeller	128,720 t	-16,323 t	-11%	15,473 t	14%
Proactive cleaning (hull & propeller)	118,425 t	-26,618 t	-18%	5,177 t	5%
Always clean	113,248 t	-31,796 t	-22%	N/A	N/A

CHAPTER 3

INFORMATION GAPS

3.1 INFORMATION GAPS AND RESEARCH RECOMMENDATIONS

This report made a summary of the reported impacts of biofouling on ships' energy efficiency either from full scale measurements, lab-scale experiments or numerical simulations. In addition, case studies were conducted to investigate the economic and environmental impacts of different anti-fouling scenarios applied to a commercial vessel with over an operation period of 5 years, using the prediction models in the literature. Most of the data in the literature that was analysed was based on simplified descriptions of the biofouling conditions, and therefore there are still difficulties in interpreting the findings for specific individual vessels operating under different conditions. In this context, there is a great need for comprehensive data collected from the industry, such as dry-dock and noon reports, photos, corresponding ship performance data (power requirements or speed loss), with the inclusion of parameters relevant to biofouling. Such data can be also used to validate the prediction methods and enable more precise and reasonable estimations of ship performances with different biofouling conditions and/or anti-fouling strategies.

Future work may simply involve data analysis based on ships' operation data without involving any prediction methods. Such data accumulation may help to define a useful formulation to correlate the ship resistance characteristics and different hull/propeller fouling conditions, which will enable users to estimate ship performance easily and robustly under different biofouling conditions.

On another note, the impacts of biofouling in niche areas or internal seawater systems and the mitigation options are not yet well established compared to the analysis of biofouling on ship hulls and propellers.

Finally, it is well-known that biofouling growth is highly affected by the flow over the surface. Thus, ship design can be made to induce the flow around the hull and propeller to disturb the biofouling growth on the surface. Therefore, further study should be conducted to investigate how ship design can reduce biofouling growth on hull and niche areas and influence the fuel consumption and GHG emissions from ships.

REFERENCES

Ballegooijen, E. v., & Muntean, T. (2016, 13-15 April). *Fuel Saving Potentials via Measuring Propeller Thrust and Hull Resistance at Full Scale:*

Industry standard on in-water cleaning with capture. BIMCO, 2021. Industry standard on in-water cleaning with capture (bimco.org)

Experience with Ships in Service 1st Hull Performance & Insight Conference (HullPIC'16), Castello di Pavone.

Bengough, G. D., & Shepheard, V. G. (1943). The corrosion and fouling of ships The Marin Corrosion Sub-committee of the Iron and Steel Institute and the British Iron and Steel Federation.

Cassé, F., & Swain, G. W. (2006). The development of microfouling on four commercial antifouling coatings under static and dynamic immersion. *International Biodeterioration & Biodegradation*, 57(3), 179-185. https://doi.org/10.1016/j.ibiod.2006.02.008

Cebeci, T., & Bradshaw, P. (1977). *Momentum Transfer in Boundary Layer (Vol. -1).*

Chung, D., Hutchins, N., Schultz, M. P., & Flack, K. A. (2021). Predicting the Drag of Rough Surfaces. *Annual Review of Fluid Mechanics*, 53(1), 439-471. https://doi.org/10.1146/annurev-fluid-062520-115127

Davis, H. F. D. (1930). The Increase in SHP and RPM due to Fouling. *Journal of the American Society of Naval Engineers, 42, 155-166.*

Demirel, Y. K., Song, S., Turan, O., & Incecik, A. (2019). Practical added resistance diagrams to predict fouling impact on ship performance. *Ocean Engineering,* 186, 106112. https://doi.org/10.1016/j.oceaneng.2019.106112

Demirel, Y. K., Turan, O., & Incecik, A. (2017a). Predicting the effect of biofouling on ship resistance using CFD. *Applied Ocean Research*, 62, 100-118. https://doi.org/10.1016/j.apor.2016.12.003

Demirel, Y. K., Uzun, D., Zhang, Y., Fang, H.-C., Day, A. H., & Turan, O. (2017b). Effect of barnacle fouling on ship resistance and powering. *Biofouling*, 33(10), 819-834. https://doi.org/10.1080/08927014.2017.1373279

Denny, M. E. (1951). BSRA Resistance Experiments on the Lucy Ashton: Part I: Full-scale Measurements. *Transactions of Royal Institution of Naval Architects*, 93, 21-31.

Farkas, A., Degiuli, N., & Martić, I. (2018). Towards the prediction of the effect of biofilm on the ship resistance using CFD. *Ocean Engineering,* 167, 169-186. https://doi.org/10.1016/j.oceaneng.2018.08.055

Farkas, A., Degiuli, N., & Martić, I. (2019). Impact of biofilm on the resistance characteristics and nominal wake. *Proceedings of the Institution of Mechanical Engineers, Part M: Journal of Engineering for the Maritime Environment,* 1475090219862897. https://doi.org/10.1177/1475090219862897

Farkas, A., Degiuli, N., & Martić, I. (2020a). An investigation into the effect of hard fouling on the ship resistance using CFD. *Applied Ocean Research*, 100, 102205. https://doi.org/10.1016/j.apor.2020.102205

Farkas, A., Degiuli, N., & Martić, I. (2021). The impact of biofouling on the propeller performance. *Ocean Engineering,* 219, 108376. https://doi.org/10.1016/j.oceaneng.2020.108376

Farkas, A., Song, S., Degiuli, N., Martić, I., & Demirel, Y. K. (2020b). Impact of biofilm on the ship propulsion characteristics and the speed reduction. *Ocean Engineering*, 199, 107033. https://doi.org/10.1016/j.oceaneng.2020.107033

Granville, P. S. (1958). The frictional resistance and turbulent boundary layer of rough surfaces. *J. Ship Res.,* 2(3), 52-74.

Granville, P. S. (1987). THREE INDIRECT METHODS FOR THE DRAG CHARACTERIZATION OF ARBITRARILY ROUGH SURFACES ON FLAT PLATES. *Journal of Ship Research*,

31(No.1), 8 p. https://trid.trb.org/view/395451

Grigson, C. (1992). Drag losses of new ships caused by hull finish. *Journal of Ship Research*, 36, 182-196.

Haslbeck, E. G., & Bohlander, G. S. (1992). Microbial biofilm effects on drag-lab and field. Ship Production Symposium Proceedings,

Hiraga, Y. (1934). Experimental investigations on the resistance of long planks and ships. *Zosen Kiokai*, 55, 159-199.

Hoffmann, M. (2021). Biofouling in Niche Areas: Addressing the Blind Spots. https://www.marinelink.com/news/biofouling-niche-areas-addressing-blind-484860

Holtrop, J., & Mennen, G. G. J. (1982). An approximate power prediction method. *International Shipbuilding Progress,* 29(335).

Hundley, H. L., & Tsai, S.-J. (1991, 22-23 October 1991). *The Use of Propulsion Shaft Torque and Speed Measurements to Improve the Life Cycle Performances of U.S. Naval Ships* Fleet Maintenance in the 21st Centurey, VA.

Hunsucker, K. Z., Koka, A., Lund, G., & Swain, G. (2014). Diatom community structure on in-service cruise ship hulls. *Biofouling*, 30(9), 1133-1140. https://doi.org/10.1080/08927014.2014.974576

ICCT. (2011). Reducing Greenhouse Gas Emissions from Ships - Cost

Effectiveness of Available Options. *International Council on Clean Transportation*, White Paper Number 11.

Izubuchi, T. (1934). Increase in hull resistance through shipbottom fouling. *Zosen Kiokai*, 55.

Kempf, G. (1937). On the effect of roughness on the resistance of ships. *Trans INA*, 79, 109-119.

Lewis, E. V. (1988). Principles of Naval Architecture : *Resistance, Propulsion and Vibration: 2*. The Society of Naval Architects and Marine Engineers.

Lewthwaite, J., Molland, A., & Thomas, K. (1985). An investigation into the variation of ship skin frictional resistance with fouling. *Transactions of Royal Institution of Naval Architects,* 127, 269-284.

Monty, J. P., Dogan, E., Hanson, R., Scardino, A. J., Ganapathisubramani, B., & Hutchins, N. (2016). An assessment of the ship drag penalty arising from light calcareous tubeworm fouling. *Biofouling*, 32(4), 451-464. https://doi.org/10.1080/08927014.2016.1148140

Mosaad, M. A. A.-R. (1986). *Marine propeller roughness penalties* Newcastle University]. Newcastle Upon Tyne.

Murrant, K., Kennedy, A., Pallard, R., & Montrose, M. (2019, 6-8 May 2019). *Effects of Hull and Propeller Cleaning on Propulsion Efficiency of an Offshore Patrol Vessel* 4th Hull Performance & Insight Conference (HullPIC'19), Gubbio.

NSTM. (2002). *NAVAL SHIPS' TECHNICAL MANUAL CHAPTER 081: WATERBORNE UNDERWATER HULL CLEANING OF NAVY SHIPS.*

Prandtl, L., & Schlichting, H. (1934). Das Widerstandsgesetz rauher Platten. *Werft Reeder: Hafen*, 15(1), 1-4.

Raupach, M. R., Antonia, R. A., & Rajagopalan, S. (1991). Rough-Wall Turbulent Boundary Layers. *Applied Mechanics Reviews*, 44(1), 1-25. https://doi.org/10.1115/1.3119492

Redfield, A. C., Hutchins, L. W., Redfield, A. C., E. S. Deevy, J., Ayers, J. C., Turner, H. J., Hutchins, L. W., Laidlaw, F. B., Ketchum, B. H., Ferry, J. D., & Todd, D. (1952). *Marine fouling and its prevention.*

Safinah. (2020). *Biofouling in Commercial Shipping: The Importance of Ship-Specific Functional Specifications.*

Schlichting, H. (1936). *Experimental investigation of the problem of surface roughness* (N.A.C.A. Technical Memorandum No. 823, Issue.

Schultz, M. P. (2004). Frictional Resistance of Antifouling

Coating Systems. *Journal of Fluids Engineering*, 126(6), 1039-1047. https://doi.org/10.1115/1.1845552

Schultz, M. P. (2007). Effects of coating roughness and biofouling on ship resistance and powering. Biofouling, 23(5), 331-341. https://doi.org/10.1080/08927010701461974

Schultz, M. P., Bendick, J. A., Holm, E. R., & Hertel, W. M. (2011). Economic impact of biofouling on a naval surface ship. *Biofouling*, 27(1), 87-98. https://doi.org/10.1080/08927014.2010.542809

Schultz, M. P., Walker, J. M., Steppe, C. N., & Flack, K. A. (2015). Impact of diatomaceous biofilms on the frictional drag of fouling-release coatings. *Biofouling*, 31(9-10), 759-773. https://doi.org/10.1080/08927014.2015.1108407

Song, C., & Cui, W. (2020a). Review of Underwater Ship Hull Cleaning Technologies. *Journal of Marine Science and Application,* 19(3), 415-429. https://doi.org/10.1007/s11804-020-00157-z

Song, S., Dai, S., Demirel, Y. K., Atlar, M., Day, S., & Turan, O. (2020b). Experimental and Theoretical Study of the Effect of Hull Roughness on Ship Resistance. *Journal of Ship Research, Preprint(Preprint),* 1-10. https://doi.org/

Song, S., Dai, S., Demirel, Y. K., Atlar, M., Day, S., & Turan, O. (2021a). Experimental and Theoretical Study of the Effect of Hull Roughness on Ship Resistance. *Journal of Ship Research,* 65(01), 62-71. https://doi.org/10.5957/JOSR.07190040

Song, S., Demirel, Y. K., & Atlar, M. (2019). An investigation into the effect of biofouling on the ship hydrodynamic characteristics using CFD. *Ocean Engineering*, 175, 122-137. https://doi.org/10.1016/j.oceaneng.2019.01.056

Song, S., Demirel, Y. K., & Atlar, M. (2020c). Penalty of hull and propeller fouling on ship self-propulsion performance. Applied *Ocean Research*, 94, 102006. https://doi.org/10.1016/j.apor.2019.102006

Song, S., Demirel, Y. K., & Atlar, M. (2020d). Propeller Performance Penalty of Biofouling: Computational Fluid Dynamics Prediction. Journal of Offshore *Mechanics and Arctic Engineering*, 142(6). https://doi.org/10.1115/1.4047201

Song, S., Demirel, Y. K., De Marco Muscat-Fenech, C., Tezdogan, T., & Atlar, M. (2020e). Fouling effect on the resistance of different ship types. *Ocean Engineering*, 216, 107736. https://doi.org/10.1016/j.oceaneng.2020.107736

Song, S., Ravenna, R., Dai, S., DeMarco Muscat-Fenech, C., Tani, G., Demirel, Y. K., Atlar, M., Day, S., & Incecik, A. (2021b). Experimental investigation on the effect of heterogeneous hull roughness on ship resistance. *Ocean Engineering,* 223, 108590. https://doi.org/10.1016/j.oceaneng.2021.108590

Swain, G., Erdogan, C., Foy, L., Gardner, H., Harper, M., Hearin, J., Hunsucker, K. Z., Hunsucker, J. T., Lieberman, K., Nanney, M., Ralston, E., Stephens, A., Tribou, M., Walker, B., & Wassick, A. (2022). Proactive In-Water Ship Hull Grooming as a Method to Reduce the Environmental Footprint of Ships [Original Research]. *Frontiers in Marine Science, 8.* https://doi.org/10.3389/fmars.2021.808549

Taylor, D. W. (1943). *The speed and power of ships: a manual of marine propulsion.* U.S. G.P.O.

Townsend, A. A. (1956). *The Structure of Turbulent Shear Flow. Cambridge Univ.* Press.

Townsin, R. L., Byrne, D., Svensen, T. E., & Milne, A. (1981). Estimating the technical and economic penalties of hull and propeller roughness. *Trans SNAME*, 295-318.

Townsin, R. L., & Dey, S. (1990). The correlation of roughness drag with surface characteristics. The RINA International Workshop on Marine Roughness and Drag,

Uzun, D., Demirel, Y. K., Coraddu, A., & Turan, O. (2019a). *Life cycle assessment of an antifouling coating based on time-dependent biofouling model* 18th Conference on Computer Applications and Information Technology in the Maritime Industries, Tullamore, Ireland.

Uzun, D., Demirel, Y. K., Coraddu, A., & Turan, O. (2019b). *Time-dependent biofouling growth model for predicting the effects of biofouling on ship resistance and powering. Ocean Engineering,* 191, 106432. https://doi.org/10.1016/j.oceaneng.2019.106432

Yeginbayeva, I. A., Granhag, L., & Chernoray, V. (2019). A multi-aspect study of commercial coatings under the effect of surface roughness and fouling. *Progress in Organic Coatings*, 135, 352-367. "https://doi.org/10.1016/j.porgcoat.2019.05.041

Safinah Group (2020). Biofouling in Commercial Shipping: The Importance of Ship-Specific Functional Specifications. Data Insights Paper Safinah Group.

Davidson I, Cahill P, Hinz A, Kluza D, Scianni C and Georgiades E (2021) A Review of Biofouling of Ships' Internal Seawater Systems. Front. Mar. Sci. 8:761531. doi: 10.3389/fmars.2021.761531

ANNEX A

SCIENTIFIC SYMBOLS AND UNITS

Symbol	ame	Dimension	Common unit
R_T	Total resistance	Force	[N]
R_F	Frictional resistance	Force	[N]
R_R	Residuary resistance	Force	[N]
R_{VP}	Viscous pressure resistance	Force	[N]
R_W	Wave-making resistance	Force	[N]
C_T	Total resistance coefficient	None	[-]
C_F	Frictional resistance coefficient	None	[-]
C_R	Residuary resistance coefficient	None	[-]
C_{VP}	Viscous pressure resistance coefficient	None	[-]
C_W	Wave-making resistance coefficient	None	[-]
Ra	Arithmetical mean roughness height (i.e. centre-line average height)	Length	[mm] or [µm]
Rt_{50}	Maximum peak-to-valley roughness height over a 50 mm sample length	Length	[mm] or [µm]
MHR	Mean hull roughness	Length	[mm] or [µm]
AHR	Average hull roughness	Length	[mm] or [µm]
k_s	Equivalent sand-grain roughness height	Length	[mm] or [µm]
k_G	Equivalent Grigson roughness height	Length	[mm] or [µm]
FR	Fouling rating	None	[-]
$h_{barnacle}$	Barnacle height	Length	[mm] or [µm]
h_{slime}	Slime thickness	Length	[mm] or [µm]
$\%SC_{barnacle}$	Barnacle percentage coverage	None	[%]
k_s	Biofilm thickness	Length	[mm] or [µm]
$\%SC_{biofilm}$	Biofilm percentage coverage	None	[%]
U^+	Non-dimensional velocity	None	[-]
y^+	Non-dimensional distance from wall	None	[-]
κ	Kármán constant	None	[-]
B	Log-law intercept	None	[-]
ΔU^+	Roughness function	None	[-]
k^+	Roughness Reynolds number	None	[-]
U_τ	Friction velocity	None	[-]
τ_w	Wall shear stress	None	[-]
ρ	Density of fluid	None	[-]
ν	Kinematic viscosity of the fluid	None	[-]

ANNEX B

GLOSSARY OF TERMS

Ablative anti-fouling coating – Also known as a self-polishing anti-fouling coating, this is a soft coating that wears off at a controlled rate.

AFS Convention – International Convention on the Control of Harmful Anti-fouling Systems on Ships

Anti-fouling system (AFS) – A coating, paint, surface treatment, surface or device that is used on a ship to control or prevent attachment of unwanted organisms.

Biocide – A chemical substance sometimes incorporated into anti-fouling systems to prevent settlement or survival of aquatic organisms.

Biofouling – The accumulation of aquatic organisms, such as microorganisms, plants and animals, on surfaces and structures immersed in, or exposed to, the aquatic environment. May include microfouling and macrofouling.

Contaminant – Any detrimental substance occurring in the environment as a result of human activities, even without adverse effects being observed.

IMO – A specialized agency of the United Nations, it is the global standard-setting authority for the safety, security and environmental performance of international shipping.

IMO Biofouling Guidelines – *Guidelines for the control and management of ships' biofouling to minimize the transfer of Invasive Aquatic Species* (resolution MEPC.207(62)), 15 July 2011.

IMO Biofouling Guidance for Recreational Craft – *Guidance for Minimizing the Transfer of Invasive Aquatic Species as Biofouling (Hull Fouling) for Recreational Craft (MEPC.1/Circ.792), 12 November 2012.*

In-water cleaning (IWC) – The physical removal of biofouling from a ship or other submerged structure while in the water.

Invasive Aquatic Species (IAS) – A non-indigenous species which may pose threats to human, animal and plant life, economic and cultural activities and the aquatic environment.

Macrofouling – Large, distinct multicellular organisms visible to the human eye, such as barnacles, tubeworms or fronds of algae.

Marine growth prevention system – An anti-fouling system used for the prevention of biofouling accumulation in niche areas.

Microfouling – Microscopic organisms including bacteria and diatoms and the slimy substances they produce. Biofouling comprised only of microfouling is commonly referred to as the slime layer.

Niche areas – Areas on a ship that may be more susceptible to biofouling due to different hydrodynamic forces, susceptibility to coating system wear or damage, or being inadequately painted or unpainted, e.g. sea chests, bow thrusters, propeller shafts, inlet gratings, dry-dock support strips.

Ship – For the purposes of this report, the definition of ship is consistent with the definition in the IMO Biofouling Guidelines: A vessel of any type whatsoever operating in the aquatic environment and includes hydrofoil boats, air-cushion vehicles, submersibles, floating craft, fixed or floating platforms, floating storage and production units (FSUs) and floating production storage and off-loading units (FPSOs).

ANNEX C

SHIP RESISTANCE COMPONENTS

The total resistance, R_T, of a ship can be divided into two main components: the frictional resistance, R_F, and the residuary resistance, R_R, given by

$$R_T = R_F + R_R \quad \text{(A1)}$$

The frictional resistance arises from the friction between the fluid and the hull surface while the residuary resistance is pressure-related resistance consisting of viscous pressure resistance, R_{VP}, and wave-making resistance, R_W, given by

$$R_T = R_F + R_{VP} + R_W \quad \text{(A2)}$$

The viscous pressure, also known as form drag, is broadly assumed to be proportional to the frictional resistance (Lewis, 1988), with the use of form factor, k, as given by

$$R_{VP} = kRF \quad \text{(A3)}$$

$$R_T = (1+k)\, R_F + R_W \quad \text{(A4)}$$

The resistance components can be non-dimensionalized by dividing each term by the dynamic pressure, $\frac{1}{2}\rho V^2$, and the wetted surface area of the ship hull, S. The resistance coefficients can be defined as

$$C_T = C_F + C_R \quad \text{(A5)}$$

$$C_T = C_F + C_{VP} + C_W \quad \text{(A6)}$$

$$C_T = (1+k)\, C_F + C_W \quad \text{(A7)}$$

where, C_T, C_F, and C_R are the coefficients of total, frictional and residuary resistance, respectively.

ANNEX D

ROUGHNESS HEIGHTS (*Ra*, Rt_{50}, *MHR* and *AHR*)

Arguably, the most widely used roughness parameters in the field of naval architecture are roughness heights such as "the arithmetical mean roughness height", *Ra* and "the peak-to-trough roughness height", *Rt*.

Ra is also often called "the centre-line average height". Figure D1 illustrates the definition of *Ra*, which can be calculated as,

$$Ra = \frac{1}{l}\int_0^l |z(x)|dx \quad \text{(A8)}$$

where l is the evaluation length of the roughness profile along with the x-axis, z is the deviation from the mean profile within the evaluation length.

Ra has been used to quantify the surface roughness of test samples mostly in lab-scale studies.

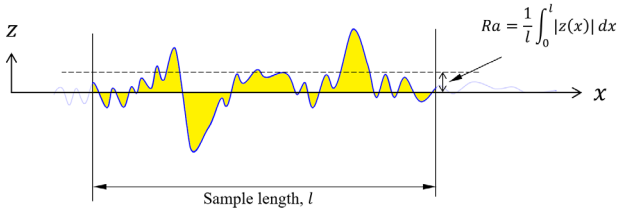

Figure D1 Definition of the arithmetical mean roughness height, *Ra*

On the other hand, the standard measure of hull roughness adopted in the marine industry is Rt_{50}, which is the maximum peak-to-valley height over a 50 mm sample length (Figure D2).

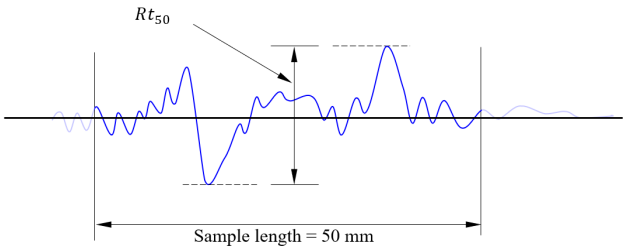

Figure D2 Definition of the peak-to-trough roughness height, Rt_{50}

The mean value of several Rt_{50} values determined in a particular location of the hull is defined as a mean hull roughness (MHR) as,

$$MHR = \frac{1}{n}\sum_{i=1}^{n} Rt_{50_i} \quad \text{(A9)}$$

where n is the total number of samples and Rt_{50i} is the Rt_{50} value measured on the i^{th} sample.

The average hull roughness (*AHR*), which represents the overall hull roughness of the vessel, is the average value of the *MHR* values obtained from different hull regions defined as

$$AHR = \frac{\sum_{j=1}^{m} w_j\, MHR_j}{\sum_{j=1}^{m} w_j} \quad \text{(A10)}$$

where m is the total number of hull regions, MHR_j is the *MHR* value of the j^{th} hull region, and w_j is the weight function of the hull region. Generally, w_j is put equal to unity; however, the w_j value can be adjusted as a means of weighting important areas of the hull.

ANNEX E

ROUGHNESS FUNCTION

One of the most accurate ways to predict the roughness effect on ship hydrodynamic performance is using the roughness function, ΔU^+, of the given rough (fouled) surface. Once the roughness function is known, it can be utilized for the full-scale resistance prediction through the similarity law scaling or computational fluid dynamics (CFD) as will be discussed in the following sections.

A rough surface in a turbulent boundary layer results in a downward shift in the velocity profile as shown in Figure E1. This downward shift is termed roughness function, ΔU^+.

The generalized velocity profile in the log-law region over a rough surface is given as,

$$U^+ = \frac{1}{\kappa}\ln y^+ + B - \Delta U^+ \quad (6)$$

The roughness function, ΔU^+ can be expressed as a function of the roughness Reynolds number, k^+, defined as

$$k^+ = \frac{kU_\tau}{\nu} \quad (7)$$

where k is the roughness height (e.g. R_{t50}, R_a, k_s, etc.), $U\tau$ is the friction velocity defined as $\sqrt{\tau_w/\rho}$. τ_w is the wall shear stress, ρ and ν are the density and the kinematic viscosity of the fluid.

The U^+ and corresponding k^+ values can be determined using experimental methods (Granville, 1987). However, there is still an unsolved issue: there is no universal model for roughness functions of different surfaces. In other words, different surfaces may show different roughness function behaviours even if they have the same roughness height value because of the effects of other surface properties (e.g. frontal solidity, effective slope, plan solidity, skewness). Therefore, the roughness functions need to be determined individually for different surfaces.

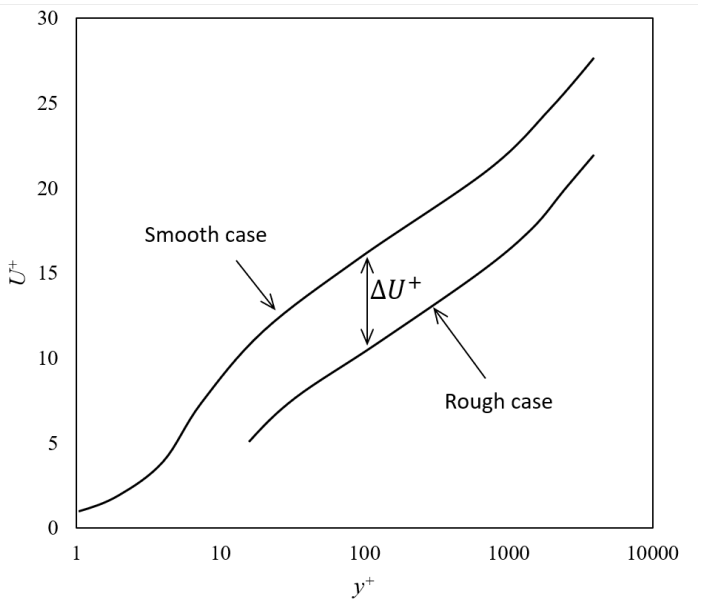

Figure E1 Velocity profile on smooth and rough walls

ANNEX F

EQUIVALENT SAND-GRAIN ROUGHNESS HEIGHT, K_S

Equivalent sand-grain roughness height, k_s, was introduced by Schlichting (1936), and it defines the grain size of uniform close-packed sand grains that would cause the same drag as the surface of interest. It should be noted that k_s does not measure a physical distance, but it is a hydraulic scale determined from experiments (or numerical simulations) for each rough surface.

A common method to determine the k_s values is finding the length scale which gives a good collapse of the roughness function values on top of a roughness function model for sand-grain (i.e. roughness function model of Cebeci et al. (1977)). For example, Figure F1 shows the roughness function values of the 60/80 grit aluminium oxide abrasive powder surface obtained by Song et al. (2021a). When the Rt_{50} value of the surface was directly used as a reference length scale, the roughness function values position in between the Colebrook-type and Nikuradse-type roughness function models. Song et al. (2021a) found that the roughness function values collapse on top of the Nikuradse-type roughness function model when 1.73 Rt_{50} is used as the reference length scale (Cyan rhombus in Figure F1). Therefore, this length scale (k= 1.73Rt_{50} = 610μm) is the equivalent sand-grain roughness height, k_s, of the rough surface of Song et al. (2021a).

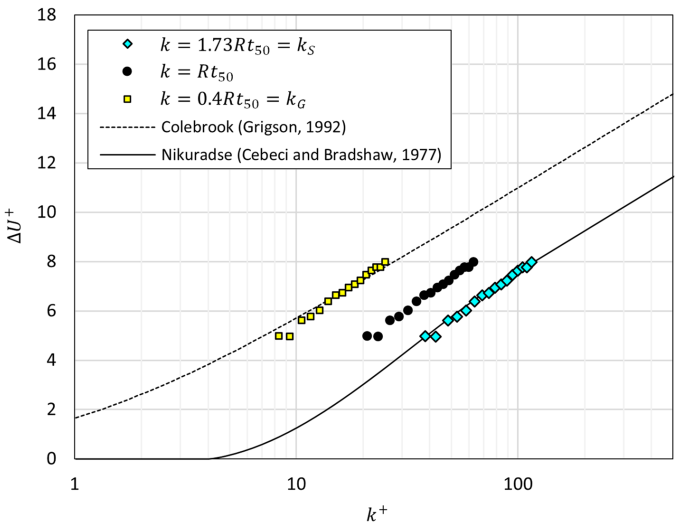

Figure F1 Roughness function of Song et al. (2021a)

In a similar manner, the roughness function values can be shifted on top of the Colebrook-type roughness function, as also shown in Figure F1. The Colebrook-type roughness function model of Grigson (1992) is mostly used for this roughness length scale, and in this report, it is termed as "equivalent Grigson roughness height, k_G". For example, the k_G of the test surface of Song et al. (2021a) is k_G = 0.4Rt_{50}=141μm (yellow squares in Figure F1).

It is of note that although different roughness length scales (e.g. k_s or k_G) can be derived from the same surface according to the choice of reference roughness function models (i.e. roughness function models of Cebeci et al. (1977) or Grigson (1992)), their effect in the boundary layer flow is the same. In other words, in the case of the study of Song et al. (2021a) for example, the different roughness length scales, k_s= 610 μm and k_G= 141 μm, will have the same effect.

Once the roughness length scale (k_s or k_G) of the surface of interest and the corresponding roughness model are given, the frictional resistance of the surface can be predicted using the similarity law scaling or computational fluid dynamics (CFD). Details regarding the resistance prediction are presented in Section 1.3.2.

ANNEX G

NSTM FOULING RATINGS

The most common quantification method for biofouling surfaces is the fouling rating used by the US Navy based on Naval Ships' Technical Manual (NSTM, 2002). *FR* is a fouling index ranging from 0 to 100, which represent a clean surface to a fully fouled surface, respectively. Descriptions of the fouling rating ranges defined by NSTM (2002) are given in Table G1.

Table G1 Difference in the total CO_2 emission with different anti-fouling scenarios (Mediterranean region)

Type	Description	*FR*
Soft	A clean, foul-free surface; red and/or black AF paint or a bare metal surface.	0
Soft	Light shades of red and green (incipient slime). Bare metal and painted surfaces are visible beneath the fouling.	10
Soft	Slime as dark green patches with yellow or brown coloured areas (advanced slime). Bare metal and painted surfaces may by obscured by the fouling.	20
Soft	Grass as filaments up to 3 inches (76 mm) in length, projections up to ¼ inch (6.4 mm) in height; or a flat network of filaments, green, yellow or brown in colour; or soft non-calcareous fouling such as sea cucumbers, sea grapes or sea squirts projecting up to ¼ inch (6.4 mm) in height. The fouling cannot be easily wiped off by hand.	30
Hard	Calcareous fouling in the form of tubeworms less than ¼ inch (6.4 mm) in diameter or height.	40
Hard	Calcareous fouling in the form of barnacles less than ¼ inch (6.4 mm) in diameter or height.	50
Hard	Combination of tubeworms and barnacles, less than 1.4 inch (6.4 mm) in diameter or height.	60
Hard	Combination of tubeworms and barnacles, greater than ¼ inch (6.4 mm) in diameter or height.	70
Hard	Tubeworms closely packed together and growing upright away from surface. Barnacles growing one on top of another, ¼ inch (6.4 mm) or less in height. Calcareous shells appear clean or white in colour.	80
Hard	Dense growth of tubeworms with barnacles, ¼ inch (6.4 mm) or greater in height; Calcareous shells brown in colour (oysters and mussels); or with slime or grass overlay.	90
Composite	All forms of fouling present, Soft and hard, particularly soft sedentary animals without calcareous covering (tunicates) growing over various forms of hard growth.	100

ANNEX H

STUDIES PREDICTING THE IMPACT OF BIOFOULING

Authors	Method	Ship/propeller	Speed/ operational condition	Surface condition	Surface parameters k_s: Equivalent sand-grain roughness height (see Annex F) k_G: Equivalent Grigson roughness height (see Annex F)	Results ΔC_F: increase in frictional resistance ΔC_T: increase in total resistance ΔP_E: increase in effective power ΔP_D: increase in delivered power ΔP_S: increase in shaft power $\Delta \eta_D$: efficiency loss at the operation condition
Schultz (2004)	Similarity law scaling (Granville, 1958)	150 m flat plate (representative of midsized merchant & naval ships)	12 knots	*Hull fouling* *Representative conditions of Schultz (2004)* 1. max. 6 mm barnacles with 60% coverage 2. max. 7 mm barnacles with 75% coverage 3. max. 5 mm barnacles with 1% coverage 4. max. 5 mm barnacles with 4% coverage 5. max. light layer of slime (1 mm thickness)	1. k_G= 2,742 µm 2. k_G= 3,577 µm 3. k_G= 295 µm 4. k_G= 590 µm 5. k_G= 110 µm	1. ΔC_F=195% 2. ΔC_F=205% 3. ΔC_F=75% 4. ΔC_F=95% 5. ΔC_F=50%
Schultz (2007)	Similarity law scaling (Granville, 1958)	FFG-7 Oliver Perry-class frigate (124 m)	a. 15 knots b. 30 knots	*Hull fouling* *Representative conditions of Schultz (2007)* 1. Typical as applied AF coating 2. Deteriorated coating or light slime 3. Heavy slime 4. Small calcareous fouling or weed 5. Medium calcareous fouling 6. Heavy calcareous fouling	1. k_s= 30 µm 2. k_s= 100 µm 3. k_s= 300 µm 4. k_s= 1,000 µm 5. k_s= 3,000 µm 6. k_s= 10,000 µm	a. 15 knots 1. ΔC_T=2%, ΔP_S=2% 2. ΔC_T=11%, ΔP_S=11% 3. ΔC_T=20%, ΔP_S=21% 4. ΔC_T=34%, ΔP_S=35% 5. ΔC_T=52%, ΔP_S=54% 6. ΔC_T=80%, ΔP_S=86% b. 30 knots 1. ΔC_T=4%, ΔP_S=4% 2. ΔC_T=10%, ΔP_S=10% 3. ΔC_T=16%, ΔP_S=16% 4. ΔC_T=25%, ΔP_S=26% 5. ΔC_T=36%, ΔP_S=38% 6. ΔC_T=55%, ΔP_S=59%
Schultz et al. (2011)	Similarity law scaling (Granville, 1958)	Arleigh Burke-class destroyer (DDG-51) (142 m)	a. 15 knots b. 30 knots	*Hull fouling* *Representative conditions of Schultz (2007)* 1. Typical as applied AF coating 2. Deteriorated coating or light slime 3. Heavy slime 4. Small calcareous fouling or weed 5. Medium calcareous fouling 6. Heavy calcareous fouling	1. k_s= 30 µm 2. k_s= 100 µm 3. k_s= 300 µm 4. k_s= 1,000 µm 5. k_s= 3,000 µm 6. k_s= 10,000 µm	a. 15 knots 1. ΔC_T=1%, ΔP_S=1% 2. ΔC_T=9%, ΔP_S=9% 3. ΔC_T=17%, ΔP_S=18% 4. ΔC_T=29%, ΔP_S=31% 5. ΔC_T=44%, ΔP_S=47% 6. ΔC_T=69%, ΔP_S=76% b. 30 knots 1. ΔC_T=3%, ΔP_S=3% 2. ΔC_T=7%, ΔP_S=7% 3. ΔC_T=12%, ΔP_S=12% 4. ΔC_T=19%, ΔP_S=20% 5. ΔC_T=28%, ΔP_S=30% 6. ΔC_T=43%, ΔP_S=47%

Authors	Method	Ship/propeller	Speed/ operational condition	Surface condition	Surface parameters k_s: Equivalent sand-grain roughness height (see Annex F) k_G: Equivalent Grigson roughness height (see Annex F)	Results ΔC_F: increase in frictional resistance ΔC_T: increase in total resistance ΔP_E: increase in effective power ΔP_D: increase in delivered power ΔP_S: increase in shaft power $\Delta \eta_0$: efficiency loss at the operation condition
Monty et al. (2016)	Similarity law scaling (Monty et al., 2016)	FFG-7 Oliver Perry-class frigate (124 m)	a. 15 knots b. 30 knots	*Hull fouling* *Representative condition of Monty et al. (2016)* 1. Tubeworm fouling	k_s= 325 µm	a. 15 knots ΔC_F=46%, ΔC_T=ΔP_E=23% b. 30 knots ΔC_F=59%, ΔC_T=ΔP_E=13%
Demirel et al. (2017b)	Similarity law scaling (Granville, 1958)	230 m container ship	24 knots	*Hull fouling* *Representative conditions of Demirel et al. (2017)* 1. 1.25 mm barnacles with 10% coverage 2. 1.25 mm barnacles with 20% coverage 3. 1.25 mm barnacles with 40% coverage 4. 1.25 mm barnacles with 50% coverage 5. 2.5 mm barnacles with 10% coverage 6. 2.5 mm barnacles with 20% coverage 7. 2.5 mm barnacles with 40% coverage 8. 2.5 mm barnacles with 50% coverage 9. 5 mm barnacles with 10% coverage 10. 5 mm barnacles with 20% coverage	1. k_G= 24 µm 2. k_G= 63 µm 3. k_G= 149 µm 4. k_G= 194 µm 5. k_G= 84 µm 6. k_G= 165 µm 7. k_G= 388 µm 8. k_G= 460 µm 9. k_G= 174 µm 10. k_G= 489 µm	1. ΔC_F=27%, ΔC_T=ΔP_E=17% 2. ΔC_F=42%, ΔC_T=ΔP_E=27% 3. ΔC_F=66%, ΔC_T=ΔP_E=43% 4. ΔC_F=70%, ΔC_T=ΔP_E=45% 5. ΔC_F=49%, ΔC_T=ΔP_E=32% 6. ΔC_F=67%, ΔC_T=ΔP_E=43% 7. ΔC_F=97%, ΔC_T=ΔP_E=63% 8. ΔC_F=103%, ΔC_T=ΔP_E=66% 9. ΔC_F=72%%, ΔC_T=ΔP_E=46% 10. ΔC_F=103%, ΔC_T=ΔP_E=66%
Demirel et al. (2019)	Similarity law scaling (Granville, 1958)	10 m to 400 m flat plates (10 m interval)	4- 26 m/s (8-50 knots)	*Hull fouling* *Representative conditions of Schultz (2007)* 1. Typical as applied AF coating 2. Deteriorated coating or light slime 3. Heavy slime 4. Small calcareous fouling or weed 5. Medium calcareous fouling 6. Heavy calcareous fouling	1. k_s= 30 µm 2. k_s= 100 µm 3. k_s= 300 µm 4. k_s= 1,000 µm 5. k_s= 3,000 µm 6. k_s= 10,000 µm	For 230 m containership (24 knots) 1. ΔC_F=9%, ΔC_T=ΔP_E=6% 2. ΔC_F=30%, ΔC_T=ΔP_E=19% 3. ΔC_F=51%, ΔC_T=ΔP_E=33% 4 ΔC_F=84%, ΔC_T=ΔP_E=54% 5. ΔC_F=124%, ΔC_T=ΔP_E=80% 6. ΔC_F=174%, ΔC_T=ΔP_E=113% For 320 m containership (15.5 knots) 1. ΔC_F=4%, ΔC_T=ΔP_E=2% 2. ΔC_F=20%, ΔC_T=ΔP_E=14% 3. ΔC_F=43%, ΔC_T=ΔP_E=29% 4. ΔC_F=72%, ΔC_T=ΔP_E=49% 5. ΔC_F=104%, ΔC_T=ΔP_E=71% 6. ΔC_F=153%, ΔC_T=ΔP_E=104%
Demirel et al. (2017 a)	CFD (modified wall-function)	230 m container ship	a. 24 knots b. 19 knots	*Hull fouling* *Representative conditions of Schultz (2007)* 1. Typical as applied AF coating 2. Deteriorated coating or light slime 3. Heavy slime 4. Small calcareous fouling or weed 5. Medium calcareous fouling 6. Heavy calcareous fouling	1. k_s= 30 µm 2. k_s= 100 µm 3. k_s= 300 µm 4. k_s= 1,000 µm 5. k_s= 3,000 µm 6. k_s= 10,000 µm	a. 24 knots 1. ΔC_F=10.9%, ΔC_T=ΔP_E=7.1% 2. ΔC_F=29.4%, ΔC_T=ΔP_E=18.1% 3. ΔC_F=49.2%, ΔC_T=ΔP_E=30.8% 4. ΔC_F=76.9%, ΔC_T=ΔP_E=49.1% 5. ΔC_F=112.1%, ΔC_T=ΔP_E=72.6% 6. ΔC_F=163.2%, ΔC_T=ΔP_E=107.5% b. 19 knots 1. ΔC_F=7.4%, ΔC_T=ΔP_E=5.9% 2. ΔC_F=26.3%, ΔC_T=ΔP_E=21.2% 3. ΔC_F=45.6%, ΔC_T=ΔP_E=37.0% 4. ΔC_F=72.8%, ΔC_T=ΔP_E=59.5% 5. ΔC_F=107.1%, ΔC_T=ΔP_E=88.2% 6. ΔC_F=157.1%, ΔC_T=ΔP_E=130.9%

Authors	Method	Ship/propeller	Speed/ operational condition	Surface condition	Surface parameters k_s: Equivalent sand-grain roughness height (see Annex F) k_G: Equivalent Grigson roughness height (see Annex F)	Results ΔC_F: increase in frictional resistance ΔC_T: increase in total resistance ΔP_E: increase in effective power ΔP_D: increase in delivered power ΔP_S: increase in shaft power $\Delta \eta_0$: efficiency loss at the operation condition
Farkas et al. (2018)	CFD (modified wall-function)	230 m container ship	24 knots	*Hull fouling* 1. 100 µm biofilm with 50% coverage 2. 500 µm biofilm with 50% coverage 3. 100 µm biofilm with 25% coverage 4. 500 µm biofilm with 25% coverage 5. 100 µm biofilm with 15% coverage 6. 500 µm biofilm with 15% coverage 7. 100 µm biofilm with 5% coverage 8. 500 µm biofilm with 5% coverage	1. k_s= 39 µm 2. k_s= 195 µm 3. k_s= 27.5 µm 4. k_s= 137.5 µm 5. k_s= 21.3 µm 6. k_s= 106.5 µm 7. k_s= 12.3 µm 8. k_s= 61.5 µm	1. ΔC_F=13.9% 2. ΔC_F=39.5% 3. ΔC_F=9.2% 4. ΔC_F=33.3% 5. ΔC_F=6.4% 6. ΔC_F=17.8% 7. ΔC_F=0.11% 8. ΔC_F=8.1%
Farkas et al. (2019)	CFD (modified wall-function)	a. 230 m container ship b. 175 m bulk carrier	a. 24 knots b. 16.3 knots	*Hull fouling* 1. 100 µm biofilm with 50% coverage 2. 500 µm biofilm with 50% coverage 3. 100 µm biofilm with 25% coverage 4. 500 µm biofilm with 25% coverage 5. 100 µm biofilm with 15% coverage 6. 500 µm biofilm with 15% coverage 7. 100 µm biofilm with 5% coverage 8. 500 µm biofilm with 5% coverage	1. k_s= 39 µm 2. k_s= 195 µm 3. k_s= 27.5 µm 4. k_s= 137.5 µm 5. k_s= 21.3 µm 6. k_s= 106.5 µm 7. k_s= 12.3 µm 8. k_s= 61.5 µm	a. 230 m container ship 1. ΔC_F=14.3%, ΔC_T=ΔP_E=9.5% 2. ΔC_F=40.1%, ΔC_T=ΔP_E=28.9% 3. ΔC_F=9.7%, ΔC_T=ΔP_E=5.5% 4. ΔC_F=33.8%, ΔC_T=ΔP_E=23.0% 5. ΔC_F=6.5%, ΔC_T=ΔP_E=3.9% 6. ΔC_F=18.1%, ΔC_T=ΔP_E=11.5% 7. ΔC_F=0.079%, ΔC_T=ΔP_E=0.0% 8. ΔC_F=8.3%, ΔC_T=ΔP_E=4.6% b. 175 m bulk carrier 1. ΔC_F=10.0%, ΔC_T=ΔP_E=8.1% 2. ΔC_F=35.1%, ΔC_T=ΔP_E=29.0% 3. ΔC_F=5.4%, ΔC_T=ΔP_E=4.4% 4. ΔC_F=29.0%, ΔC_T=ΔP_E=24.3% 5. ΔC_F=1.8%, ΔC_T=ΔP_E=1.6% 6. ΔC_F=15.2%, ΔC_T=ΔP_E=12.7% 7. ΔC_F=0.0%, ΔC_T=ΔP_E=0.015% 8. ΔC_F=6.6%, ΔC_T=ΔP_E=5.4%
Song et al. (2019)	CFD (modified wall-function)	230 m container ship	a. 24 knots b. 19 knots	*Hull fouling* *Representative conditions of Demirel et al. (2017)* 1. 1.25 mm barnacles with 10% coverage 2. 1.25 mm barnacles with 20% coverage 3. 1.25 mm barnacles with 40% coverage 4. 1.25 mm barnacles with 50% coverage 5. 2.5 mm barnacles with 10% coverage 6. 2.5 mm barnacles with 20% coverage 7. 2.5 mm barnacles with 40% coverage 8. 2.5 mm barnacles with 50% coverage 9. 5 mm barnacles with 10% coverage 10. 5 mm barnacles with 20% coverage	1. k_G= 24 µm 2. k_G= 63 µm 3. k_G= 149 µm 4. k_G= 194 µm 5. k_G= 84 µm 6. k_G= 165 µm 7. k_G= 388 µm 8. k_G= 460 µm 9. k_G= 174 µm 10. k_G= 489 µm	a. 24 knots 1. ΔC_F=29%, ΔC_T=ΔP_E=18% 2. ΔC_F=45%, ΔC_T=ΔP_E=28% 3. ΔC_F=62%, ΔC_T=ΔP_E=40% 4. ΔC_F=68%, ΔC_T=ΔP_E=44% 5. ΔC_F=50%, ΔC_T=ΔP_E=32% 6. ΔC_F=65%, ΔC_T=ΔP_E=42% 7. ΔC_F=86%, ΔC_T=ΔP_E=56% 8. ΔC_F=91%, ΔC_T=ΔP_E=59% 9. ΔC_F=66%, ΔC_T=ΔP_E=42% 10. ΔC_F=93%, ΔC_T=ΔP_E=60% b. 19 knots 1. ΔC_F=26%, ΔC_T=ΔP_E=22% 2. ΔC_F=42%, ΔC_T=ΔP_E=34% 3. ΔC_F=59%, ΔC_T=ΔP_E=48% 4. ΔC_F=65%, ΔC_T=ΔP_E=53% 5. ΔC_F=47%, ΔC_T=ΔP_E=39% 6. ΔC_F=61%, Δ=ΔP_E=50% 7. ΔC_F=82%, ΔC_T=ΔP_E=67% 8. ΔC_F=86%, ΔC_T=ΔP_E=71% 9. ΔC_F=62%, ΔC_T=ΔP_E=51% 10. ΔC_F=88%, ΔC_T=ΔP_E=73%

Authors	Method	Ship/propeller	Speed/ operational condition	Surface condition	Surface parameters k_s: Equivalent sand-grain roughness height (see Annex F) k_G: Equivalent Grigson roughness height (see Annex F)	Results ΔC_F: increase in frictional resistance ΔC_T: increase in total resistance ΔP_E: increase in effective power ΔP_D: increase in delivered power ΔP_S: increase in shaft power $\Delta \eta_0$: efficiency loss at the operation condition
Song et al. (2020b)	CFD (modified wall-function)	a. 230 m container ship b. 320 m tanker	a. 12–26 knots b. 9 – 17 knots	*Hull fouling* *Representative conditions of Demirel et al. (2017)* 1. 1.25 mm barnacles with 20% coverage 2. 2.5 mm barnacles with 20% coverage 3. 5 mm barnacles with 20% coverage	1. k_G= 63 µm 2. k_G= 165 µm 3. k_G= 489 µm	a. 230 m container ship 1. ΔC_T=ΔP_E=29 - 19% (for 12-26 knots) 2. ΔC_T=ΔP_E=44 - 28% (for 12-26 knots) 3. ΔC_T=ΔP_E=66 - 40% (for 12-26 knots) b. 320 m tanker 1. ΔC_T=ΔP_E=27 - 36% (for 9-17 knots) 2. ΔC_T=ΔP_E=42 - 53% (for 9-17 knots) 3. ΔC_T=ΔP_E=65 - 78% (for 9-17 knots)
Farkas et al. (2020 a)	CFD (modified wall-function)	a. 230 m container ship b. 320 m tanker	a. 24 knots b. 15.5 knots	*Hull fouling* 1. 7 mm barnacles with 25% coverage 2. 5 mm barnacles with 25% coverage 3. 7 mm barnacles with 5% coverage 4. 5 mm barnacles with 5% coverage 5. 7 mm barnacles with 1% coverage 6. 5 mm barnacles with 1% coverage	1. k_G= 2,007 µm 2. k_G= 1,475 µm 3. k_G= 924 µm 4. k_G= 660 µm 5. k_G= 413 µm 6. k_G= 295 µm	a. 230 m container ship 1. ΔC_F= %, ΔC_T=ΔP_E=86% 2. ΔC_F= %, ΔC_T=ΔP_E=80% 3. ΔC_F= %, ΔC_T=ΔP_E=74% 4. ΔC_F= %, ΔC_T=ΔP_E=61% 5. ΔC_F= %, ΔC_T=ΔP_E=49% 6. ΔC_F= %, ΔC_T=ΔP_E=45% b. 320 m tanker 1. ΔC_F= %, ΔC_T=ΔP_E=117% 2. ΔC_F= %,ΔC_T=ΔP_E=105% 3. ΔC_F= %,ΔC_T=ΔP_E=92% 4. ΔC_F= %,ΔC_T=ΔP_E=84% 5. ΔC_F= %,ΔC_T=ΔP_E=71% 6. ΔC_F= %,ΔC_T=ΔP_E=61%
Song et al. (2020 d)	CFD (modified wall-function)	7.9 m propeller (for 230 m containership)	J=0.7 (operation condition at 24 knots)	*Propeller fouling* *Representative conditions of Demirel et al. (2017)* 1. 1.25 mm barnacles with 10% coverage 2. 1.25 mm barnacles with 20% coverage 3. 1.25 mm barnacles with 40% coverage 4. 1.25 mm barnacles with 50% coverage 5. 2.5 mm barnacles with 10% coverage 6. 2.5 mm barnacles with 20% coverage 7. 2.5 mm barnacles with 40% coverage 8. 2.5 mm barnacles with 50% coverage 9. 5 mm barnacles with 10% coverage 10. 5 mm barnacles with 20% coverage	1. k_G= 24 µm 2. k_G= 63 µm 3. k_G= 149 µm 4. k_G= 194 µm 5. k_G= 84 µm 6. k_G= 165 µm 7. k_G= 388 µm 8. k_G= 460 µm 9. k_G= 174 µm 10. k_G= 489 µm	1. $\Delta \eta_0$= -5%, ΔP_D=6% 2. $\Delta \eta_0$= -7%, ΔP_D=9% 3. $\Delta \eta_0$= -10%, ΔP_D=13% 4. $\Delta \eta_0$= -11%, ΔP_D=14% 5. $\Delta \eta_0$= -8%, ΔP_D=10% 6. $\Delta \eta_0$= -10%, ΔP_D=13% 7. $\Delta \eta_0$= -13%, ΔP_D=18% 8. $\Delta \eta_0$= -14%, ΔP_D=19% 9. $\Delta \eta_0$= -10%, ΔP_D=14% 10. $\Delta \eta_0$= -14%, ΔP_D=20%

Authors	Method	Ship/propeller	Speed/ operational condition	Surface condition	Surface parameters k_s: Equivalent sand-grain roughness height (see Annex F) k_G: Equivalent Grigson roughness height (see Annex F)	Results ΔC_F: increase in frictional resistance ΔC_T: increase in total resistance ΔP_E: increase in effective power ΔP_D: increase in delivered power ΔP_S: increase in shaft power $\Delta \eta_0$: efficiency loss at the operation condition
Farkas et al. (2021)	CFD (modified wall-function)	a. 6.2 m propeller (for 175 m bulk carrier) b. 7.9 m propeller (for 230 m containership) c. 9.9 m propeller (for 320 m tanker)	a. J=0.56 (operation condition at 16.3 knots) b. J=0.7 (operation condition at 24 knots) c. J=0.5 (operation condition at 15.5 knots)	*Propeller fouling – biofilm* 1. 100 µm biofilm with 50% coverage 2. 500 µm biofilm with 50% coverage 3. 100 µm biofilm with 25% coverage 4. 500 µm biofilm with 25% coverage 5. 100 µm biofilm with 15% coverage 6. 500 µm biofilm with 15% coverage 7. 100 µm biofilm with 5% coverage 8. 500 µm biofilm with 5% coverage *Propeller fouling - hard fouling* 9. 7 mm barnacles with 25% coverage 10. 5 mm barnacles with 25% coverage 11. 7 mm barnacles with 5% coverage 12. 5 mm barnacles with 5% coverage 13. 7 mm barnacles with 1% coverage 14. 5 mm barnacles with 1% coverage	*Biofilm* 1. k_s= 39 µm 2. k_s= 195 µm 3. k_s= 27.5 µm 4. k_s= 137.5 µm 5. k_s= 21.3 µm 6. k_s= 106.5 µm 7. k_s= 12.3 µm 8. k_s= 61.5 µm *Hard fouling* 9. k_G= 2,007 µm 10. k_G= 1,475 µm 11. k_G= 924 µm 12. k_G= 660 µm 13. k_G= 413 µm 14. k_G= 295 µm	a. 6.2 m propeller (for 175 m bulk carrier) *Biofilm* 1. $\Delta\eta_0$=-3% 2. $\Delta\eta_0$=-5% 3. $\Delta\eta_0$=-2% 4. $\Delta\eta_0$=-5% 5. $\Delta\eta_0$=-1% 6. $\Delta\eta_0$=-3% 7. $\Delta\eta_0$=0% 8. $\Delta\eta_0$=-1% *Hard fouling* 9. $\Delta\eta_0$=-29% 10. $\Delta\eta_0$=-27% 11. $\Delta\eta_0$=-25% 12. $\Delta\eta_0$=-23% 13. $\Delta\eta_0$=-21% 14. $\Delta\eta_0$=-20% b. 7.9 m propeller (for 230 m containership) *Biofilm* 1. $\Delta\eta_0$=-3% 2. $\Delta\eta_0$=-7% 3. $\Delta\eta_0$=-2% 4. $\Delta\eta_0$=-6% 5. $\Delta\eta_0$=-1% 6. $\Delta\eta_0$=-3% 7. $\Delta\eta_0$=0% 8. $\Delta\eta_0$=-2% *Hard fouling* 9. $\Delta\eta_0$=-28% 10. $\Delta\eta_0$=-26% 11. $\Delta\eta_0$=-23% 12. $\Delta\eta_0$=-22% 13. $\Delta\eta_0$=-20% 14. $\Delta\eta_0$=-19% c. 9.9 m propeller (for 320 m tanker) *Biofilm* 1. $\Delta\eta_0$=-3% 2. $\Delta\eta_0$=-7% 3. $\Delta\eta_0$=-3% 4. $\Delta\eta_0$=-6% 5. $\Delta\eta_0$=-1% 6. $\Delta\eta_0$=-3% 7. $\Delta\eta_0$=-1% 8. $\Delta\eta_0$=-2% Hard fouling 9. $\Delta\eta_0$=-32% 10. $\Delta\eta_0$=-30% 11. $\Delta\eta_0$=-28% 12. $\Delta\eta_0$=-26% 13. $\Delta\eta_0$=-24% 14. $\Delta\eta_0$=-23%

Authors	Method	Ship/propeller	Speed/ operational condition	Surface condition	Surface parameters k_s: Equivalent sand-grain roughness height (see Annex F) k_G: Equivalent Grigson roughness height (see Annex F)	Results ΔC_F: increase in frictional resistance ΔC_T: increase in total resistance ΔP_E: increase in effective power ΔP_D: increase in delivered power ΔP_S: increase in shaft power $\Delta \eta_O$: efficiency loss at the operation condition
Song et al. (2020c)	CFD (modified wall-function)	230 m container ship	24 knots	*Hull and/or Propeller fouling* *Representative conditions of Demirel et al. (2017)* 1. 1.25 mm barnacles with 10% coverage 2. 1.25 mm barnacles with 20% coverage 3. 1.25 mm barnacles with 40% coverage 4. 1.25 mm barnacles with 50% coverage 5. 2.5 mm barnacles with 10% coverage 6. 2.5 mm barnacles with 20% coverage 7. 2.5 mm barnacles with 40% coverage 8. 2.5 mm barnacles with 50% coverage 9. 5 mm barnacles with 10% coverage 10. 5 mm barnacles with 20% coverage	1. k_G= 24 µm 2. k_G= 63 µm 3. k_G= 149 µm 4. k_G= 194 µm 5. k_G= 84 µm 6. k_G= 165 µm 7. k_G= 388 µm 8. k_G= 460 µm 9. k_G= 174 µm 10. k_G= 489 µm	*Fouled-hull/clean-propeller* 1. ΔP_D=16% 2. ΔP_D=26% 3. ΔP_D=37% 4. ΔP_D=41% 5. ΔP_D=29% 6. ΔP_D=39% 7. ΔP_D=53% 8. ΔP_D=57% 9. ΔP_D=40% 10. ΔP_D=58% *Clean-hull/fouled-propeller* 1. ΔP_D=6% 2. ΔP_D=9% 3. ΔP_D=13% 4. ΔP_D=14% 5. ΔP_D=10% 6. ΔP_D=13% 7. ΔP_D=18% 8. ΔP_D=19% 9. ΔP_D=13% 10. ΔP_D=19% *Fouled-hull/fouled-propeller* 1. ΔP_D=23% 2. ΔP_D=36% 3. ΔP_D=52% 4. ΔP_D=57% 5. ΔP_D=41% 6. ΔP_D=54% 7. ΔP_D=75% 8. ΔP_D=80% 9. ΔP_D=55% 10. ΔP_D=82%
Farkas et al. (2020b)	CFD (modified wall-function)	230 m container ship	24 knots	*Hull & propeller fouling* 1. 100 µm biofilm with 50% coverage 2. 500 µm biofilm with 50% coverage 3. 100 µm biofilm with 25% coverage 4. 500 µm biofilm with 25% coverage 5. 100 µm biofilm with 15% coverage 6. 500 µm biofilm with 15% coverage 7. 100 µm biofilm with 5% coverage 8. 500 µm biofilm with 5% coverage	1. k_s= 39 µm 2. k_s= 195 µm 3. k_s= 27.5 µm 4. k_s= 137.5 µm 5. k_s= 21.3 µm 6. k_s= 106.5 µm 7. k_s= 12.3 µm 8. k_s= 61.5 µm	1. ΔP_D=9.0% 2. ΔP_D=25.8% 3. ΔP_D=6.4% 4. ΔP_D=22.1% 5. ΔP_D=4.0% 6. ΔP_D=11.9% 7. ΔP_D=0.48% 8. ΔP_D=5.3%

ANNEX I

ECONOMIC AND ENVIRONMENTAL IMPACTS OF BIOFOULING INTERPRETED FROM THE LITERATURE

Ship/propeller	Speed/ operational condition	Surface condition/ exposure time	Interpretations ΔFC: increase in fuel consumption ΔGE: increase in GHG emission
23 m fleet tender	Unknown	Thin slime (too thin to measure)/ 240 days	$\Delta FC = \Delta GE$=19-21%
23 m fleet tender	Unknown	Thick slime (~1 mm)/ 500 days	$\Delta FC = \Delta GE$=62-69%
58 m Passenger carrier	5-15 knots	Slime/ 40 days	$\Delta FC = \Delta GE$=4-5%
62 m offshore patrol ship	13.5-16 knots	Light slime/ 2 years	$\Delta FC = \Delta GE$=5%
120 m cargo vessel	9 knots	Barnacles and slime	$\Delta FC = \Delta GE$=270-320%
150 m flat plate (representative of midsized merchant & naval ships)	12 knots	1. max. 6 mm barnacles with 60% coverage 2. max. 7 mm barnacles with 75% coverage 3. max. 5 mm barnacles with 1% coverage 4. max. 5 mm barnacles with 4% coverage 5. max. light layer of slime (1 mm thickness)	*for 150 m bulk carrier 1. $\Delta FC = \Delta GE$=140-160% 2. $\Delta FC = \Delta GE$=150-170% 3. $\Delta FC = \Delta GE$=50-60% 4. $\Delta FC = \Delta GE$=70-80% 5. $\Delta FC = \Delta GE$=35-40%
96 m destroyer	24 knots	Barnacles and slime	$\Delta FC = \Delta GE$=130-145%
111 m destroyer	10-20 knots	12 months	$\Delta FC = \Delta GE$=100%
115 m destroyer	28 knots	8 months	$\Delta FC = \Delta GE$=32%
124 m frigate	15 knots	1. Typical as applied AF coating 2. Deteriorated coating or light slime 3. Heavy slime 4. Small calcareous fouling or weed 5. Medium calcareous fouling 6. Heavy calcareous fouling	1. $\Delta FC = \Delta GE$=2% 2. $\Delta FC = \Delta GE$=11% 3. $\Delta FC = \Delta GE$=21% 4. $\Delta FC = \Delta GE$35% 5. $\Delta FC = \Delta GE$=54% 6. $\Delta FC = \Delta GE$=86%

Ship/propeller	Speed/ operational condition	Surface condition/ exposure time	Interpretations ΔFC: increase in fuel consumption ΔGE: increase in GHG emission
124 m frigate	30 knots	1. Typical as applied AF coating 2. Deteriorated coating or light slime 3. Heavy slime 4. Small calcareous fouling or weed 5. Medium calcareous fouling 6. Heavy calcareous fouling	1. $\Delta FC = \Delta GE$=4% 2. $\Delta FC = \Delta GE$=10% 3. $\Delta FC = \Delta GE$=16% 4. $\Delta FC = \Delta GE$=26% 5. $\Delta FC = \Delta GE$=38% 6. $\Delta FC = \Delta GE$=59%
124 m frigate	15 knots	Tubeworm fouling	$\Delta FC = \Delta GE$=23%
124 m frigate	30 knots	Tubeworm fouling	$\Delta FC = \Delta GE$=13%
142 m destroyer	15 knots	1. Typical as applied AF coating 2. Deteriorated coating or light slime 3. Heavy slime 4. Small calcareous fouling or weed 5. Medium calcareous fouling 6. Heavy calcareous fouling	1. $\Delta FC = \Delta GE$=1% 2. $\Delta FC = \Delta GE$=9% 3. $\Delta FC = \Delta GE$=18% 4. $\Delta FC = \Delta GE$=31% 5. $\Delta FC = \Delta GE$=47% 6. $\Delta FC = \Delta GE$=76%
142 m destroyer	30 knots	1. Typical as applied AF coating 2. Deteriorated coating or light slime 3. Heavy slime 4. Small calcareous fouling or weed 5. Medium calcareous fouling 6. Heavy calcareous fouling	b1. $\Delta FC = \Delta GE$=3% b2. $\Delta FC = \Delta GE$=7% b3. $\Delta FC = \Delta GE$=12% b4. $\Delta FC = \Delta GE$=20% b5. $\Delta FC = \Delta GE$=30% b6. $\Delta FC = \Delta GE$=47%
183 m battleship	21 knots	10 months	$\Delta FC = \Delta GE$=37%
13,000 TEU container	Unknown	1.5 years	$\Delta FC = \Delta GE$=9.2%
230 m container ship	24 knots	1. Typical as applied AF coating 2. Deteriorated coating or light slime 3. Heavy slime 4. Small calcareous fouling or weed 5. Medium calcareous fouling 6. Heavy calcareous fouling	1. $\Delta FC = \Delta GE$=7.1% 2. $\Delta FC = \Delta GE$=18.1% 3. $\Delta FC = \Delta GE$=30.8% 4. $\Delta FC = \Delta GE$=49.1% 5. $\Delta FC = \Delta GE$=72.6% 6. $\Delta FC = \Delta GE$=107.5%
230 m container ship	24 knots	1. 1.25 mm barnacles with 10% coverage 2. 1.25 mm barnacles with 20% coverage 3. 1.25 mm barnacles with 40% coverage 4. 1.25 mm barnacles with 50% coverage 5. 2.5 mm barnacles with 10% coverage 6. 2.5 mm barnacles with 20% coverage 7. 2.5 mm barnacles with 40% coverage 8. 2.5 mm barnacles with 50% coverage 9. 5 mm barnacles with 10% coverage 10. 5 mm barnacles with 20% coverage	1. $\Delta FC = \Delta GE$=17% 2. $\Delta FC = \Delta GE$=27% 3. $\Delta FC = \Delta GE$=43% 4. $\Delta FC = \Delta GE$=45% 5. $\Delta FC = \Delta GE$=32% 6. $\Delta FC = \Delta GE$=43% 7. $\Delta FC = \Delta GE$=63% 8. $\Delta FC = \Delta GE$=66% 9. $\Delta FC = \Delta GE$=46% 10. $\Delta FC = \Delta GE$=66%

Ship/propeller	Speed/ operational condition	Surface condition/ exposure time	Interpretations *ΔFC*: increase in fuel consumption *ΔGE*: increase in GHG emission
230 m container ship	24 knots	1. 100 µm biofilm with 50% coverage 2. 500 µm biofilm with 50% coverage 3. 100 µm biofilm with 25% coverage 4. 500 µm biofilm with 25% coverage 5. 100 µm biofilm with 15% coverage 6. 500 µm biofilm with 15% coverage 7. 100 µm biofilm with 5% coverage 8. 500 µm biofilm with 5% coverage	1. *ΔFC* = *ΔGE*=9-10% 2. *ΔFC* = *ΔGE*=26-29% 3. *ΔFC* = *ΔGE*=6-7% 4. *ΔFC* = *ΔGE*=22-24% 5. *ΔFC* = *ΔGE*=4-5% 6. *ΔFC* = *ΔGE*=12-13% 7. *ΔC*= *ΔGE*=0.1% 8. *ΔFC* = *ΔGE*=5-6%
230 m container ship	24 knots	1. 100 µm biofilm with 50% coverage 2. 500 µm biofilm with 50% coverage 3. 100 µm biofilm with 25% coverage 4. 500 µm biofilm with 25% coverage 5. 100 µm biofilm with 15% coverage 6. 500 µm biofilm with 15% coverage 7. 100 µm biofilm with 5% coverage 8. 500 µm biofilm with 5% coverage	1. *ΔFC* = *ΔGE*=9.5% 2. *ΔFC* = *ΔGE*=28.9% 3. *ΔFC* = *ΔGE*=5.5% 4. *ΔFC* = *ΔGE*=23.0% 5. *ΔFC* = *ΔGE*=3.9% 6. *ΔFC* = *ΔGE*=11.5% 7. *ΔFC* = *ΔGE*=0.0% 8. *ΔFC* = *ΔGE*=4.6%
230 m container ship	24 knots	1. 1.25 mm barnacles with 10% coverage 2. 1.25 mm barnacles with 20% coverage 3. 1.25 mm barnacles with 40% coverage 4. 1.25 mm barnacles with 50% coverage 5. 2.5 mm barnacles with 10% coverage 6. 2.5 mm barnacles with 20% coverage 7. 2.5 mm barnacles with 40% coverage 8. 2.5 mm barnacles with 50% coverage 9. 5 mm barnacles with 10% coverage 10. 5 mm barnacles with 20% coverage	1. *ΔFC* = *ΔGE*=18% 2. *ΔFC* = *ΔGE*=28% 3. *ΔFC* = *ΔGE*=40% 4. *ΔFC* = *ΔGE*=44% 5. *ΔFC* = *ΔGE*=32% 6. *ΔFC* = *ΔGE*=42% 7. *ΔFC* = *ΔGE*=56% 8. *ΔFC* = *ΔGE*=59% 9. *ΔFC* = *ΔGE*=42% 10. *ΔFC* = *ΔGE*=60%
230 m container ship	24 knots	1. 7 mm barnacles with 25% coverage 2. 5 mm barnacles with 25% coverage 3. 7 mm barnacles with 5% coverage 4. 5 mm barnacles with 5% coverage 5. 7 mm barnacles with 1% coverage 6. 5 mm barnacles with 1% coverage	1. *ΔFC* = *ΔGE*=86% 2. *ΔFC* = *ΔGE*=80% 3. *ΔFC* = *ΔGE*=74% 4. *ΔFC* = *ΔGE*=61% 5. *ΔFC* = *ΔGE*=49% 6. *ΔFC* = *ΔGE*=45%
230 m container ship	24 knots	*Hull fouling* 1. 1.25 mm barnacles with 10% coverage 2. 1.25 mm barnacles with 20% coverage 3. 1.25 mm barnacles with 40% coverage 4. 1.25 mm barnacles with 50% coverage 5. 2.5 mm barnacles with 10% coverage 6. 2.5 mm barnacles with 20% coverage 7. 2.5 mm barnacles with 40% coverage 8. 2.5 mm barnacles with 50% coverage 9. 5 mm barnacles with 10% coverage 10. 5 mm barnacles with 20% coverage	1. *ΔFC* = *ΔGE*=16% 2. *ΔFC* = *ΔGE*=26% 3. *ΔFC* = *ΔGE*=37% 4. *ΔFC* = *ΔGE*=41% 5. *ΔFC* = *ΔGE*=29% 6. *ΔFC* = *ΔGE*=39% 7. *ΔFC* = *ΔGE*=53% 8. *ΔFC* = *ΔGE*=57% 9. *ΔFC* = *ΔGE*=40% 10. *ΔFC* = *ΔGE*=58%
230 m container ship	19 knots	1. Typical as applied AF coating 2. Deteriorated coating or light slime 3. Heavy slime 4. Small calcareous fouling or weed 5. Medium calcareous fouling 6. Heavy calcareous fouling	1. *ΔFC* = *ΔGE*=5.9% 2. *ΔFC* = *ΔGE*=21.2% 3. *ΔFC* = *ΔGE*=37.0% 4. *ΔFC* = *ΔGE*=59.5% 5. *ΔFC* = *ΔGE*=88.2% 6. *ΔFC* = *ΔGE*=130.9%

Ship/propeller	Speed/ operational condition	Surface condition/ exposure time	Interpretations ΔFC: increase in fuel consumption ΔGE: increase in GHG emission
230 m container ship	19 knots	1. 1.25 mm barnacles with 10% coverage 2. 1.25 mm barnacles with 20% coverage 3. 1.25 mm barnacles with 40% coverage 4. 1.25 mm barnacles with 50% coverage 5. 2.5 mm barnacles with 10% coverage 6. 2.5 mm barnacles with 20% coverage 7. 2.5 mm barnacles with 40% coverage 8. 2.5 mm barnacles with 50% coverage 9. 5 mm barnacles with 10% coverage 10. 5 mm barnacles with 20% coverage	1. $\Delta FC = \Delta GE$=22% 2. $\Delta FC = \Delta GE$=34% 3. $\Delta FC = \Delta GE$=48% 4. $\Delta FC = \Delta GE$=53% 5. $\Delta FC = \Delta GE$=39% 6. $\Delta FC = \Delta GE$=50% 7. $\Delta FC = \Delta GE$=67% 8. $\Delta FC = \Delta GE$=71% 9. $\Delta FC = \Delta GE$=51% 10. $\Delta FC = \Delta GE$=73%
230 m container ship	12-26 knots	1. 1.25 mm barnacles with 20% coverage 2. 2.5 mm barnacles with 20% coverage 3. 5 mm barnacles with 20% coverage	1. $\Delta FC = \Delta GE$=29 - 19% (for 12-26 knots) 2. $\Delta FC = \Delta GE$=44 - 28% (for 12-26 knots) 3. $\Delta FC = \Delta GE$=66 - 40% (for 12-26 knots
230 m container ship with 7.9 m propeller	24 knots	*Hull & propeller fouling* 1. 1.25 mm barnacles with 10% coverage 2. 1.25 mm barnacles with 20% coverage 3. 1.25 mm barnacles with 40% coverage 4. 1.25 mm barnacles with 50% coverage 5. 2.5 mm barnacles with 10% coverage 6. 2.5 mm barnacles with 20% coverage 7. 2.5 mm barnacles with 40% coverage 8. 2.5 mm barnacles with 50% coverage 9. 5 mm barnacles with 10% coverage 10. 5 mm barnacles with 20% coverage	1. $\Delta FC = \Delta GE$=23% 2. $\Delta FC = \Delta GE$=36% 3. $\Delta FC = \Delta GE$=52% 4. $\Delta FC = \Delta GE$=57% 5. $\Delta FC = \Delta GE$=41% 6. $\Delta FC = \Delta GE$=54% 7. $\Delta FC = \Delta GE$=75% 8. $\Delta FC = \Delta GE$=80% 9. $\Delta FC = \Delta GE$=55% 10. $\Delta FC = \Delta GE$=82%
230 m container ship	24 knots	*Hull & propeller fouling* 1. 100 µm biofilm with 50% coverage 2. 500 µm biofilm with 50% coverage 3. 100 µm biofilm with 25% coverage 4. 500 µm biofilm with 25% coverage 5. 100 µm biofilm with 15% coverage 6. 500 µm biofilm with 15% coverage 7. 100 µm biofilm with 5% coverage 8. 500 µm biofilm with 5% coverage	1. $\Delta FC = \Delta GE$=9.0% 2. $\Delta FC = \Delta GE$=25.8% 3. $\Delta FC = \Delta GE$=6.4% 4. $\Delta FC = \Delta GE$=22.1% 5. $\Delta FC = \Delta GE$=4.0% 6. $\Delta C = \Delta GE$=11.9% 7. $\Delta FC = \Delta GE$=0.48% 8. $\Delta FC = \Delta GE$=5.3%
320 m tanker	15.5 knots	1. 7 mm barnacles with 25% coverage 2. 5 mm barnacles with 25% coverage 3. 7 mm barnacles with 5% coverage 4. 5 mm barnacles with 5% coverage 5. 7 mm barnacles with 1% coverage 6. 5 mm barnacles with 1% coverage	1. $\Delta FC = \Delta GE$=117% 2. $\Delta FC = \Delta GE$=105% 3. $\Delta FC = \Delta GE$=92% 4. $\Delta FC = \Delta GE$=84% 5. $\Delta FC = \Delta GE$=71% 6. $\Delta FC = \Delta GE$=61%
320 m tanker	9-17 knots	1. 1.25 mm barnacles with 20% coverage 2. 2.5 mm barnacles with 20% coverage 3. 5 mm barnacles with 20% coverage	1. $\Delta FC = \Delta GE$=27 - 36% (for 9-17 knots) 2. $\Delta FC = \Delta GE$=42 - 53% (for 9-17 knots) 3. $\Delta FC = \Delta GE$=65 - 78% (for 9-17 knots)
175 m bulk carrier	16.3 knots	1. 100 µm biofilm with 50% coverage 2. 500 µm biofilm with 50% coverage 3. 100 µm biofilm with 25% coverage 4. 500 µm biofilm with 25% coverage 5. 100 µm biofilm with 15% coverage 6. 500 µm biofilm with 15% coverage 7. 100 µm biofilm with 5% coverage 8. 500 µm biofilm with 5% coverage	1. $\Delta FC = \Delta GE$=8.1% 2. $\Delta FC = \Delta GE$=29.0% 3. $\Delta FC = \Delta GE$=4.4% 4. $\Delta FC = \Delta GE$=24.3% 5. $\Delta FC = \Delta GE$=1.6% 6. $\Delta FC = \Delta GE$=12.7% 7. $\Delta FC = \Delta GE$=0.015% 8. $\Delta FC = \Delta GE$=5.4%

Ship/propeller	Speed/ operational condition	Surface condition/ exposure time	Interpretations ΔFC: increase in fuel consumption ΔGE: increase in GHG emission
7.9 m propeller (for 230 m containership)	J=0.7 (operation condition at 24 knots)	*Propeller fouling* 1. 1.25 mm barnacles with 10% coverage 2. 1.25 mm barnacles with 20% coverage 3. 1.25 mm barnacles with 40% coverage 4. 1.25 mm barnacles with 50% coverage 5. 2.5 mm barnacles with 10% coverage 6. 2.5 mm barnacles with 20% coverage 7. 2.5 mm barnacles with 40% coverage 8. 2.5 mm barnacles with 50% coverage 9. 5 mm barnacles with 10% coverage 10. 5 mm barnacles with 20% coverage	1. $\Delta FC = \Delta GE$=6% 2. $\Delta FC = \Delta GE$=9% 3. $\Delta FC = \Delta GE$=13% 4. $\Delta FC = \Delta GE$=14% 5. $\Delta FC = \Delta GE$=10% 6. $\Delta FC = \Delta GE$=13% 7. $\Delta FC = \Delta GE$=18% 8. $\Delta FC = \Delta GE$=19% 9. $\Delta FC = \Delta GE$=14% 10. $\Delta FC = \Delta GE$=20%
7.9 m propeller (for 230 m containership)	J=0.7 (operation condition at 24 knots)	*Propeller fouling* 1. 100 µm biofilm with 50% coverage 2. 500 µm biofilm with 50% coverage 3. 100 µm biofilm with 25% coverage 4. 500 µm biofilm with 25% coverage 5. 100 µm biofilm with 15% coverage 6. 500 µm biofilm with 15% coverage 7. 100 µm biofilm with 5% coverage 8. 500 µm biofilm with 5% coverage	1. $\Delta FC = \Delta GE$=3% 2. $\Delta FC = \Delta GE$=8% 3. $\Delta FC = \Delta GE$=2% 4. $\Delta FC = \Delta GE$=6% 5. $\Delta FC = \Delta GE$=1% 6. $\Delta FC = \Delta GE$=3% 7. $\Delta FC = \Delta GE$=0% 8. $\Delta FC = \Delta GE$=2%
7.9 m propeller (for 230 m containership)	J=0.7 (operation condition at 24 knots)	*Propeller fouling* 1. 7 mm barnacles with 25% coverage 2. 5 mm barnacles with 25% coverage 3. 7 mm barnacles with 5% coverage 4. 5 mm barnacles with 5% coverage 5. 7 mm barnacles with 1% coverage 6. 5 mm barnacles with 1% coverage	1. $\Delta FC = \Delta GE$=39% 2. $\Delta FC = \Delta GE$=35% 3. $\Delta FC = \Delta GE$=30% 4. $\Delta FC = \Delta GE$=28% 5. $\Delta FC = \Delta GE$=25% 6. $\Delta FC = \Delta GE$=23%
9.9 m propeller (for 320m tanker)	J=0.5 (operation condition at 15.5 knots)	*Propeller fouling* 1. 7 mm barnacles with 25% coverage 2. 5 mm barnacles with 25% coverage 3. 7 mm barnacles with 5% coverage 4. 5 mm barnacles with 5% coverage 5. 7 mm barnacles with 1% coverage 6. 5 mm barnacles with 1% coverage	1. $\Delta FC = \Delta GE$=47% 2. $\Delta FC = \Delta GE$=43% 3. $\Delta FC = \Delta GE$=39% 4. $\Delta FC = \Delta GE$=35% 5. $\Delta FC = \Delta GE$=32% 6. $\Delta FC = \Delta GE$=30%
9.9 m propeller (for 320m tanker)	J=0.5 (operation condition at 15.5 knots)	*Propeller fouling* 1. 100 µm biofilm with 50% coverage 2. 500 µm biofilm with 50% coverage 3. 100 µm biofilm with 25% coverage 4. 500 µm biofilm with 25% coverage 5. 100 µm biofilm with 15% coverage 6. 500 µm biofilm with 15% coverage 7. 100 µm biofilm with 5% coverage 8. 500 µm biofilm with 5% coverage	1. $\Delta FC = \Delta GE$=3% 2. $\Delta FC = \Delta GE$=8% 3. $\Delta FC = \Delta GE$=3% 4. $\Delta FC = \Delta GE$=6% 5. $\Delta FC = \Delta GE$=1% 6. $\Delta FC = \Delta GE$=3% 7. $\Delta FC = \Delta GE$=1% 8. $\Delta FC = \Delta GE$=2%

More information:
GloFouling Partnerships Project Coordination Unit
Department of Partnerships and Projects
International Maritime Organization
4 Albert Embankment
London SE1 7SR
United Kingdom
www.glofouling.imo.org